ผลของกรดสองโปรตอนต่อประสิทธิภาพการกราฟต์และการดูดซึมน้ำ ของแป้งมันสำปะหลัง-พอลิอะคริลาไมด์โดยการฉายรังสีแกมมา

นางสาวกัลยา มงคลสวัสดิ์

วิทยานิพนธ์นี้เป็นส่วนหนึ่งของการศึกษาตามหลักสูตรปริญญาวิทยาศาสตรมหาบัณฑิต
สาขาวิชาปิโตรเคมีและวิทยาศาสตร์พอลิเมอร์
หลักสูตรปิโตรเคมีและวิทยาศาสตร์พอลิเมอร์
คณะวิทยาศาสตร์ จุฬาลงกรณ์มหาวิทยาลัย
ปีการศึกษา 2543

ISBN 974-13-0812-4

EFFECT OF DIPROTIC ACIDS ON GRAFTING EFFICIENCY AND WATER ABSORPTION OF CASSAVA STARCH-POLYACRYLAMIDE VIA γ-IRRADIATION

Miss Kanlaya Mongkolsawat

A Thesis Submitted in Partial Fulfillment of the Requirements
for the Degree of Master of Science in Petrochemistry and Polymer Science
Program of Petrochemistry and Polymer Science
Faculty of Science
Chulalongkorn University
Academic Year 2000

ISBN 974-13-0812-4

Thesis Title EFFECT OF DIPROTIC ACIDS ON GRAFTING
EFFICIENCY AND WATER ABSORPTION OF CASSAVA
STARCH-POLYACRYLAMIDE VIA γ-IRRADIATION
By Miss Kanlaya Mongkolsawat
Field of Study Petrochemistry and Polymer Science
Thesis Advisor Professor Suda Kiatkamjornwong, Ph. D.
Thesis Co-advisor Manit Sonsuk, M.S.

Accepted by the Faculty of Science, Chulalongkorn University in Partial Fulfillment of the Requirements for the Master's Degree

……………………………………………….. Dean of Faculty of Science
(Associate Professor Wanchai Phothiphichitr, Ph. D.)

Thesis Committee

……………………………………………….. Chairman
(Professor Pattarapan Prasassarakich, Ph.D.)

……………………………………………….. Thesis Advisor
(Professor Suda Kiatkamjornwong, Ph.D.)

……………………………………………….. Thesis Co-advisor
(Manit Sonsuk, M.S.)

……………………………………………….. Member
(Associate Professor Wimonrat Trakarnpruk, Ph.D.)

……………………………………………….. Member
(Jindarom Chvajarernpun, M.S.)

กัลยา มงคลสวัสดิ์: ผลของกรดสองโปรตอนต่อประสิทธิภาพการกราฟต์และการดูดซึมน้ำของแป้งมันสำปะหลัง-พอลิอะคริลาไมด์โดยการฉายรังสีแกมมา (EFFECT OF DIPROTIC ACIDS ON GRAFTING EFFICIENCY AND WATER ABSORPTION OF CASSAVA STARCH-POLYACRYLAMIDE VIA γ-IRRADIATION) อ. ที่ปรึกษาวิทยานิพนธ์: ศาสตราจารย์ ดร. สุดา เกียรติกำจรวงศ์, อ. ที่ปรึกษาวิทยานิพนธ์ร่วม: นายมานิตย์ ซ้อนสุข, 184 หน้า. ISBN 974-13-0812-4.

งานวิจัยนี้ได้ศึกษาปฏิกิริยากราฟต์โคพอลิเมอไรเซชันของอะคริลาไมด์บนแป้งมันสำปะหลัง โดยริเริ่มปฏิกิริยาด้วยวิธีการฉายรังสีแกมมาพร้อมกับศึกษาตัวแปรที่สำคัญ ได้แก่ ปริมาณรังสี อัตราการเปล่งรังสี อัตราส่วนของมอนอเมอร์ต่อแป้งมันสำปะหลัง ปริมาณของกรดมาเลอิก และศึกษาผลของสารเติมแต่งต่างๆ ได้แก่ กรดซัลฟิวริกและกรดมาเลอิกที่มีต่อปฏิกิริยากราฟต์โคพอลิเมอไรเซชันของอะคริลาไมด์ และ/หรือ กรดอะคริลิกบนแป้งมันสำปะหลัง โดยใช้อัตราส่วนของมอนอเมอร์ต่อแป้งมันสำปะหลังเท่ากับ 2:1 อัตราส่วนของอะคริลาไมด์ต่อกรดอะคริลิกเท่ากับ 1:1 ปริมาณรังสี 6.0 กิโลเกรย์ และอัตราการเปล่งรังสี 1.71 กิโลเกรย์ต่อชั่วโมง ผลพลอยได้จากปฏิกิริยากราฟต์โคพอลิเมอไรเซชัน คือ โฮโมพอลิเมอร์และโคพอลิเมอร์อิสระ สามารถแยกจากแป้งที่กราฟต์แล้วโดยการสกัดด้วยน้ำหรือเมทานอล นำกราฟต์โคพอลิเมอร์ที่ได้มาทำปฏิกิริยาสะพอนิฟิเคชันด้วยสารละลายโพแทสเซียมไฮดรอกไซด์ความเข้มข้นร้อยละ 5 ที่อุณหภูมิห้องเพื่อเปลี่ยนหมู่เอไมด์ หรือหมู่คาร์บอกซิลิกแอซิดให้เป็นหมู่คาร์บอกซิเลต หาตัวแปรการกราฟต์ที่เป็นตัวบ่งชี้ระดับการเกิดปฏิกิริยากราฟต์โคพอลิเมอไรเซชัน อันได้แก่ ร้อยละของการเกิดเจล ร้อยละของการเกิดโฮโมพอลิเมอร์ ร้อยละของประสิทธิภาพการเกิดกราฟต์โคพอลิเมอร์ ซึ่งมีความสัมพันธ์กับความสามารถในการดูดซึมน้ำ

กราฟต์โคพอลิเมอร์ของแป้งมันสำปะหลัง-พอลิอะคริลาไมด์ที่สังเคราะห์ได้จากภาวะที่ปริมาณรังสีเท่ากับ 4.0 กิโลเกรย์ ปริมาณอัตราการเปล่งรังสี 1.71 กิโลเกรย์ต่อชั่วโมง อัตราส่วนของมอนอเมอร์ต่อแป้งมันสำปะหลัง 2.5:1 และปริมาณของกรดมาเลอิกเท่ากับ 2 เปอร์เซ็นต์โดยน้ำหนักของมอนอเมอร์ มีความสามารถในการดูดซึมน้ำกลั่นสูงถึง 2,256 กรัมต่อกรัมของน้ำหนักแห้ง เมื่อทดสอบการดูดซึมน้ำของพอลิเมอร์ในสารละลายเกลือและสารละลายบัฟเฟอร์ พบว่าความสามารถในการดูดซึมน้ำขึ้นอยู่กับชนิดและความเข้มข้นของลารละลายเกลือและค่าความเป็นกรด-เบสของสารละลายบัฟเฟอร์ และเมื่อทดสอบความสามารถในการดูดซึมน้ำภายใต้แรงดัน พบว่าค่าการดูดซึมน้ำลดลงตามแรงดัน เมื่อเติมกรดซัลฟิวริกและกรดมาเลอิกในกราฟต์โคพอลิเมอร์ของแป้งมันสำปะหลัง-พอลิอะคริลาไมด์/กรดอะคริลิก พบว่าปริมาณโฮโมพอลิเมอร์เพิ่มขึ้น ประสิทธิภาพในการกราฟต์ลดลงและความสามารถในการดูดซึมน้ำลดลง งานวิจัยนี้ได้อธิบายกลไกที่เป็นไปได้ของการเกิดปฏิกิริยาของกรดมาเลอิกและอะคริลาไมด์บนแป้งมันสำปะหลัง และอธิบายเหตุผลของความสามารถในการดูดซึมน้ำของกราฟต์โคพอลิเมอร์ที่ได้สังเคราะห์ขึ้นใหม่

สาขาวิชา ปิโตรเคมีและวิทยาศาสตร์พอลิเมอร์ ลายมือชื่อนิสิต ....
หลักสูตร ปิโตรเคมีและวิทยาศาสตร์พอลิเมอร์ ลายมือชื่ออาจารย์ที่ปรึกษา ....
ปีการศึกษา 2543 ลายมือชื่ออาจารย์ที่ปรึกษาร่วม..

4172216323 : MAJOR PETROCHEMISTRY AND POLYMER SCIENCE
KEY WORD: GRAFT COPOLYMERIZATION / GAMMA IRRADIATION / CASSAVA STARCH / ACRYLAMIDE / MALEIC ACID

KANLAYA MONGKOLSAWAT: EFFECT OF DIPROTIC ACIDS ON GRAFTING EFFICIENCY AND WATER ABSORPTION OF CASSAVA STARCH-POLYACRYLAMIDE VIA γ-IRRADIATION. THESIS ADVISOR: PROF. SUDA KIATKAMJORNWONG, Ph.D. THESIS CO-ADVISOR: MANIT SONSUK, M.S. 184 pp. ISBN 974-13-0812-4.

Graft copolymerization of acrylamide onto cassava starch by a simultaneous irradiation technique using gamma-rays as initiator were studied via various important parameters: total dose (kGy), dose rate (kGy h^{-1}), monomer-to-cassava starch ratio and maleic acid content. Graft copolymerization of acrylamide and/or acrylic acid onto cassava starch was also studied with the addition of sulfuric acid and maleic acid as acid additives. The graft copolymer was produced with the monomer-to-cassava starch ratio 2:1, acrylamide-to-acrylic acid ratio 1:1, total dose 6.0 kGy and dose rate 1.71 kGy h^{-1}. Homopolymer and their free copolymer, which were the by-products of graft copolymerization, were removed by water or methanol extraction. The purified graft copolymer was subsequently saponified with a 5% aqueous solution of potassium hydroxide at room temperature to convert the amide groups or carboxylic groups to carboxylate groups. Grafting parameters denoting the degree of graft copolymerization were determined in terms of the percentage of gel content, homopolymer, grafting efficiency, add-on in relation to the water absorption.

The graft copolymer produced with the total dose 4.0 kGy, dose rate 1.71 kGy h^{-1}, the monomer-to-cassava starch ratio 2.5:1 and maleic acid content 2% w w^{-1} of monomer gave the saponified graft copolymer having the water absorption in distilled water as high as 2,256 g g^{-1} of its dried weight. The water absorptions of this saponified graft copolymer in salt solutions and buffer solutions were also carried out. The water absorption depends largely on type and concentration of salt solutions (Ionic strength) and pH of buffer solutions. The presence of sulfuric acid or maleic acid in graft copolymerization of acrylamide and/or acrylic acid onto cassava starch increased the homopolymer, but decreased the grafting yield and the water absorption. This research explains the possible mechanism of polymerization reaction of maleic acid and acrylamide onto cassava starch. It also describes the influences that affect water absorption of graft copolymer newly synthesized.

Department Petrochemistry and Polymer Science Student's signature…………………………………..
Program Petrochemistry and Polymer Science Advisor's signature…………………………………..
Academic year 2000 Co-advisor's signature………………………………

ACKNOWLEDGEMENT

I would like to express my deep gratitude to my advisor, Professor Suda Kiatkamjornwong, Ph.D. and co-advisor, Mr. Manit Sonsuk, M.S., for their tireless assistance, suggestion of valuable points of the experiments and encouragement throughout this research. In addition, I wish to show my gratitude to Mrs. Jindarom Chvajarernpun, M.S. for her kind assistance; Professor Pattarapan Prasassarakich, Ph.D., Associate Professor Wimonrat Trakarnpruk, Ph.D. for serving as chairman and on members of this thesis committee, respectively.

Appreciations are also extended to Thai Wah Co.,Ltd., for kind support of cassava starch; to Siam Resin Co., Ltd., for kind support of acrylamide and acrylic acid; to the Office of Atomic Energy for Peace and the Department of Photographic Science and Printing Technology of Faculty of Science, Chulalongkorn University, for providing the facilities in laboratory, equipment as well as some chemicals.

Finally, I would like to extend my appreciation to my family, and friends whose names are not mentioned here for their encouragement and love throughout the long year research for the Master's degree.

CONTENTS

PAGE

PAGE

Part I: Effect of Diprotic Acids on Grafting Efficiency and Water Absorption of Cassava Starch-Polyacrylamide via γ-Irradiation

Part II: Effect of Acid Additives on Grafting Efficiency and Water Absorption of Cassava Starch-Polyacrylamide/acrylic acid via γ-Irradiation

PAGE

PAGE

PAGE

Part II: Effect of Acid Additives on Grafting Efficiency and Water Absorption of Cassava Starch-Polyacrylamide/acrylic acid via γ-Irradiation

PAGE

LIST OF TABLES

TABLE **PAGE**

TABLE **PAGE**

LIST OF FIGURES

FIGURE **PAGE**

FIGURE **PAGE**

FIGURE **PAGE**

FIGURE **PAGE**

LIST OF ABBREVIATIONS

kGy	kilogray
kGy h^{-1}	kilogray per hour
Co^{60}	Cobalt-60
γ	gamma rays
^{O}C	degree Celsius
g	gram
M	molarity
w w^{-1}	weight by weight
w v^{-1}	weight by volume
rpm	round per minute
cm^{-1}	unit of wave number
DP	degree of polymerization
M_c	molecular weight between cross-link
AM	acrylamide
AA	acrylic acid
MA	maleic acid
FTIR	Fourier Transform Infrared Spectroscopy
EA	Elemental Analyzer
SEM	Scanning Electron Microscope
J. Appl. Polym. Sci.	Journal of Applied Polymer Science
Radiat. Phys. Chem.	Radiation Physics and Chemistry
Polym. Adv. Technol.	Polymers for Advanced Technologies

J. Polym. Sci., Polym, Lett. Ed.	Journal of Polymer Science, Polymer Letters Edition
Sep. Sci. Technol.	Separation Science and Technology

CHAPTER 1

INTRODUCTION

1.1 Introduction.

During the last decade hydrogel research has made remarkable progress owing to the strenuous efforts by researchers from many different fields. Since ancient times hydrogels have been closely affiliated with our daily life. From the early 1940's numerous synthethic hydrogels have been designed and developed for various usages. Disposable diapers and sanitary napkins use hydrogels as super water absorbents. Sheets of hydrogels are developed that tightly wrap fishes and meats. The gels keep them moist but absorb unnecessary excess water and are useful for efficient transportations and storages. Hydrogels are used for agricultural purposes as retainers of water and solutes. Soft contact lenses, artificial lenses, artificial vitreous, and materials used in plastic surgeries are made of hydrogels. Hydrogels are also used as control delivery systems for drugs and perfumes [1].

To function as an absorbent for aqueous fluids, a polymer must have the following certain properties:

1) It must be hydrophilic, for example, many if not most of the superabsorbents contain polymerized acrylamide, acrylic acid, or acrylic acid salts.

2) The polymer must swell in aqueous fluids but must not dissolve. In most instances, this requirement dictates that some crosslinking takes place either

during polymerization or after the polymer is prepared. With totally synthetic polymers, a crosslinking agent may be conveniently included in the polymerization recipe, however, in the preparation of polysaccharide graft copolymers, crosslinker can in many cases be excluded because:

a) Some crosslinking often occurs naturally during the graft copolymerization process.
b) Hydrogen bonding between polysaccharide chains (particularly cellulose) prevents the graft copolymer from dissolving.

Crosslink density is a critical factor in determining properties of the absorbent. Too little a crosslinking density will produce a soft, loose gel and excessive water solubility, whereas too much crosslinking reduces polymer swelling to the point where little fluid is absorbed.

3) Although not a strict requirement, absorbents should have some ionic character, since charge repulsion is an important factor in promoting polymer swelling in aqueous fluids.

The production of cassava starch in Thailand exceeds the export and consumption scale which cause too much surplus and unused cassava. This situation forces the cassava starch go to into vain and is usually destroyed in order to keep the stable pricing of the product. Moreover, about 90% of all superabsorbent materials are imported and used in disposable articles, most of which are disposed of landfills or by inceneration, there is a perceived environmental problem with superabsorbent polymers. Use of starch as an extender and replacement for synthetic polymers is currently an active research area. Incoporation of starch into other polymers not only reduces our dependence on petrochemical-derived monomers but also provides materials in which the starch portion can biodegrade rapidly in the environment.

1.2 Objectives

The objectives of this research are the following.

1. To develop a suitable synthetic technique of high water absorbing polymer of acrylamide and diprotic acid onto cassava starch via γ-irradiation.
2. To study the effects of reaction parameters on radiation grafting.
3. To study the effects of particle size and selected solution on absorption capacity.
4. To study the absorption under pressure of the graft copolymer.

1.3 Expected Benefits Obtainable for Future Development of the Research

The benefits for the development can be

1. To develop a technology of producing high water absorbing polymer for the local industry at a large scale production.
2. To decrease the import of this type of materials and reduce our dependence on petrochemical-derived monomers.
3. To add more values to this crop.

1.4 Scope of the Investigation

In this research, the necessary procedures of graft copolymerization of acrylamide and diprotic acid (maleic acid) onto cassava starch via gamma radiation to achieve the best product are as follows:

1. Intensive literature survey and in-depth study of this research work.
2. Preparing the graft copolymers of acrylamide and maleic acid onto cassava starch via gamma-ray radiation by a simultaneous irradiation method.

The following parameters for a proper selection of the preparation technique through the appropriate reaction conditions are studied:

a) The optimum dose rate (kGy h^{-1}).
b) The optimum total dose (kGy).
c) The optimum ratio of mixed monomers (g) to cassava starch (g).
d) The optimum quantity of the maleic acid.

3. Extracting the homopolymer (polyacrylamide) and the free copolymer of the crude product.

4. Bringing the graft copolymer obtained from Section 3 to further characterization steps:

a) Determination of percentage conversion of the monomer.
b) Determination of gel content.
c) Determination of the homopolymer and free copolymer formation.
d) Determination of the percentage add-on of graft copolymer.
e) Determination of the grafting efficiency of the grafted polymer.

5. Saponification of starch graft copolymer at the optimum reaction time and temperature that give the maximum water absorption.

6. Studying the absorption capacity of the saponified starch grafted copolymer in distilled water, sodium chloride, magnesium chloride, calcium chloride, and pH buffered solutions.

7. Studying the effects of particle size on water absorption capacity.

8. Studying the absorption under pressure of the starch grafted copolymer.

9. Summarizing the result and preparing the report.

CHAPTER 2

THEORY AND LITERATURE REVIEW

2.1 Superabsorbent Polymers or Hydrogels

Hydrogels are three-dimensional polymer networks that swell in aqueous solutions while maintaining their structural integrity. A hydrogel's water content is usually more than 20% of its total weight. If the water content is more than 95% of the total weight (i.e.. if a dried hydrogel swells in water to absorb more than 20 times its weight), the hydrogel is called superabsorbent. Dried hydrogels (often called xerogels) swell in the presence of water to regain their shape before drying. Hydrogels swell in water for the same reason that hydrophilic polymer molecules dissolve in water. The polymer chains that make up the network do not dissolve in water because they are connected to each other through either covalent or noncovalent bonds. The hydrogels with covalently bonded polymer chains are known as chemical gels, and the other types of hydrogels are known as physical gels. Swelling in water is one of the inherent properties of hydrogels [2].

2.1.1 Classification of Superabsorptive Polymer

Classification of superabsorptive polymers from composition and preparation methods (network formation, introduction of hydrophilic groups and product form) is indicated in Table 2.1. In general, superabsorptive polymer has been made insoluble by some process, typically by means of crosslinking agents, resulting in polymers that have the capacity to absorb several hundred times their weight in pure water. To make superabsorptive polymers, various raw materials and preparation methods can be used.

Table 2.1. Four Classifications of Superabsorbent Polymers

A. Polymer composition	
a) Starch	Graft polymerization Carboxymethylation
b) Cellulose	Graft polymerization Carboxymethylation
c) Synthetic polymer	Poly(acrylic acid) Poly(vinyl alcohol) Polyacrylamide Polyoxyethylene
B. Network formation	
a) Graft polymerization	
b) Crosslinked copolymerization	
c) Network forming reaction of water-soluble polymers	
d) Self-crosslinked polymerization	
e) Radiation crosslinking	
f) Introduction of crystal structure	

Table 2.1. Four Classifications of Superabsorbent Polymers (continued)

C. Hydrophilic groups	
a) Polymerization of hydrophilic monomers	
b) Carboxymethylation of hydrophilic monomers	
c) Graft polymerization of hydrophobic polymers with hydrophilic monomers	
d) Hydrolysis of nitrile or ester group	
D. Product form	
a) Powder	Globular
	Amorphous
b) Film	
c) Fiber	Short fiber
	Long fiber
	Nonwoven fiber

2.1.2 Water Absorption Mechanism

Figures 2.1 and 2.2 show the absorption mechanism of an example of a superabsorptive resin, in this case a crosslinking polymer contains sodium carboxylate groups. Before absorption, long chains of polymers are interwoven and polymers make a three-dimensional structure by crosslinking between the chains to make a dense phase. These superabsorptive polymers instantaneously absorb water and swell with dissolution of Na^+, owing to the hydrophilic ionic groups, and thus become a gel [3].

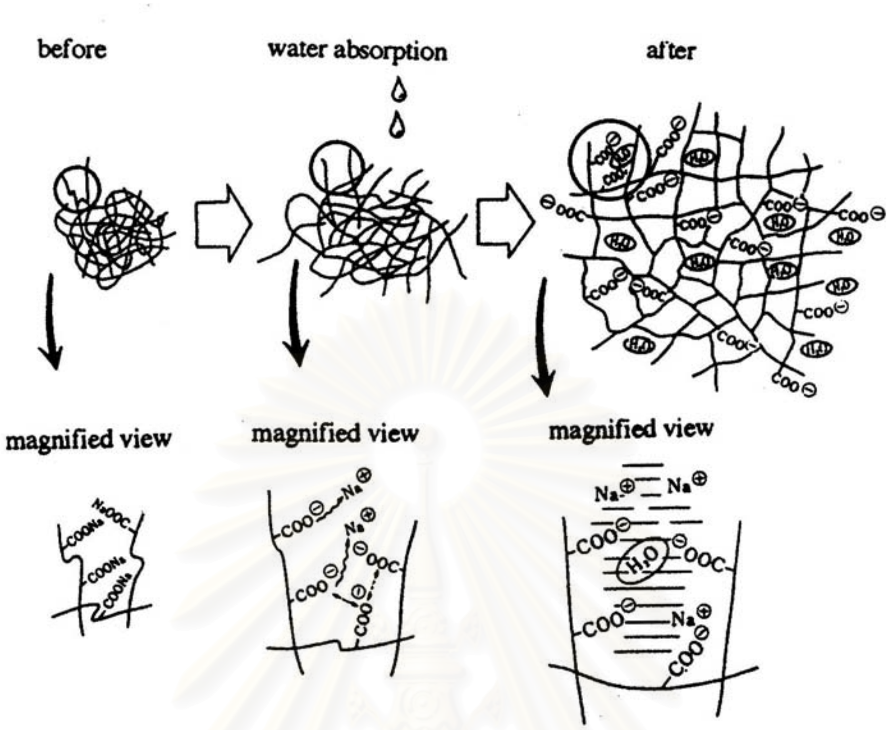

Figure 2.1 Water absorption in polymer network.

Figure 2.2 shows the mechanism of swelling of superabsorbent polymers caused by several features. In contact with water the hydrophilic polymer backbone, containing hydrophilic functional groups, interacts with the solvent accompanied by energy decrease and entropy increase. Hydration and the formation of hydrogen bonds are two sources for such polymer/solvent interactions. The polymer chains also tend to disperse in the given volume of solvent. This leads to a higher number of allowed configurations for the system, which is equivalent to a higher degree of entropy.

Due to the presence of the cross-links the polymer chains are restricted in swelling by elastic retraction forces of the network. The more the chains separate from each other, the more stiffened the originally coiled polymer chains become. This decreases the entropy of the chains. Finally there is a balance between the trend toward infinite dilution of the chains and the reactive forces. Higher cross-link densities give networks with stronger retractive forces and SAPs with lower degrees of swelling at equilibrium.

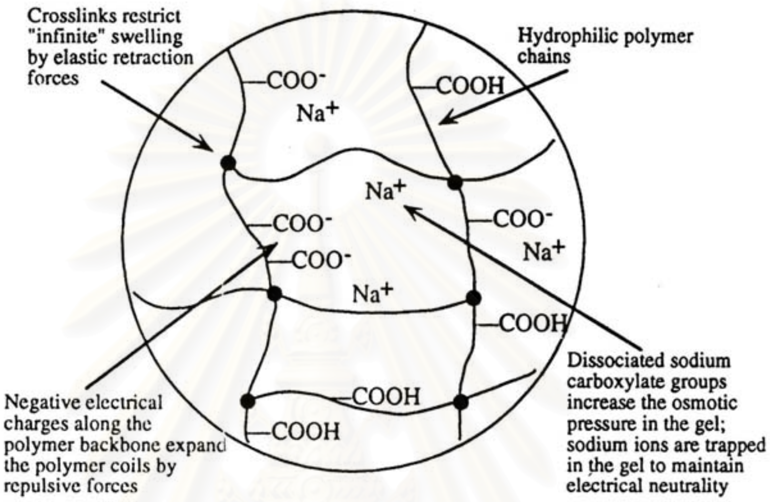

Figure 2.2 Mechanisms of swelling of superabsorbent polymers

For ionic polymers the solvent/polymer interactions include more than a simple mixing term. These gels bear electrical charges along the polymer chains. The negative charges of the carboxyl groups repel one another and are compensated for by the positive charges of the sodium ions, in order to maintain electrical neutrality. When the polymer comes into contact with water, the solvent diffuses into the polymer network and solvates the sodium ions. Water with its high dielectric constant lowers the attractive forces between the sodium ions and the negatively charged carboxylate groups. As in solutions of simple salts, the sodium ions are released and become freely moveable within the gel. Hence they contribute to the osmotic pressure. But for them it is impossible to leave the gel region due to the attraction forces of the negative charges, which are fixed along the polymer backbones. The sodium ions therefore behave as if they were trapped by an invisible, semi-permeable membrane. The driving force for swelling is then the difference between the osmotic pressure inside and outside of the gel. Based on this phenomenon, increasing the salinity causes the osmotic pressure of any external aqueous solution to reduce the absorption capacity of the gel for that fluid [4].

The water absorbency and the strength of superabsorptive polymers can be expressed by Equation 2.1 (Flory's equation) and Equation 2.2, respectively.

$$Q^{5/3} \quad = \quad [(i/2 \ * \ \nu_u S^{*1/2})^2 + (1/2 - \chi_1/\nu_1] / \nu_e/V_o) \qquad (2.1)$$

$$G \quad = \quad RT * \nu_e/V_o \qquad (2.2)$$

Where Q is the degree of swelling, i/ν_u is the charge density of polymer, S^* is the ionic strength of solution, $(1/2 - \chi_1)\nu_1$ is polymer-solvent affinity, ν_e/V_o is crosslinking density, and G is rigidity.

The water absorbency, therefore, increases with increasing number of hydrophilic and ionic functional groups, and decreases when increasing the crosslinking density of the polymer network and in the concentrated ionic solutions (NaCl solution, urine, etc.).

2.1.3 Water Absorption Capacity

Water absorption capacity is generally a term employed to indicate a capacity to retain as much absorbed fluid as possible (retention). In addition, this term also has two other meanings. One is the capacity to swell by absorbing fluid (absorption), and the other is the capacity to gel and decrease flowability by absorbing fluid (gelation). These three types of water absorption capacity can be influenced by modifying the composition and the product form.

Table 2.2 shows the methods for measuring water absorption capacity according to each definition. The water absorption rate is more influenced by the product form than by the composition of the superabsorptive polymer. Fundamentally, the larger the surface area the higher the water absorption rate. However, lumps are produced in the case of fine powders, and tend to obstruct absorption. A way to eliminate this obstacle is to have coarse particles and to increase the surface area by making the resin with more porosity.

Table 2.2 Measurement of the Water Absorbing Capacity

Required performance	Measurement method	Outline of the method
Absorption power	Capillary method (Demand wetability method)	The resin is placed on a porous sheet or on a sheet with small holes, and put in contact with the fluid.
Water retention	Filtration method	After making the resin sufficiently swell in an excessive amount of fluid, the excess fluid is filtrated by a screen.
	Centrifugal dehydration method	After making the resin sufficiently swell in an excessive amount of fluid, it is placed in a bag, and centrifugal dehydration is performed.

Table 2.2 Measurement of the Water Absorbing Capacity (continued)

Required performance	**Measurement method**	**Outline of the method**
Water retention	Tea-bag method	The resin inclosed in a nonwoven bag, and after dipping it in the fluid for a certain time, it is weighed after draining water.
	Sheet method	The polymer is inserted between two layers of tissue paper in order to obtain a sheet, and is then immersed in the liquid.
	UV absorbance	The polymer swells in an aqueous Blue Dextrin solution, and UV absorbance is measured in comparison to a blank.
Gelation	Vortex method	A fixed volume of liquid is put in a beaker, the polymer is introduced while stirring, and time is measured until the disappearance of the vortex.
	Flow method	The polymer is put in a beaker, liquid is added to make it swell, and the point at which the gel starts to flow constitutes the end point.

2.1.4 Application

Table 2.3 indicates the application of these polymers classified from the market fields and the properties of polymers. Materials with high absorbing capacity for water or other aqueous fluids were used in a large number of sanitary products in the early years, and then uses as agricultural-gardening agents and in civil engineering. Further applications in cosmetic-toiletries, medical, and other fields also have been developed recently. These applications are based on the materials ability to soak up liquid and so immobilize it.

Although hard contact lenses with 10% moisture content were used in the past, lenses containing 70 to 80% moisture, superior in properties such as transparency, strength, oxygen permeability, and low irritation to eyes, have been developed using such polymers as silicone acrylate, fumaric acid diester, and alkylene glycol monoacrylate.

Drug-release-control agents using appropriate superabsorptive polymers have been devised to facilitate gradual drug dissolution at specific sites within the patient's body. Crosslinked polymer-materials composed of poly(*N*-vinyl-pyrrolidone) are particularly suitable with regard to biocompatibility and safety. The *N*-substituted acrylamide, cellulose ether, and poly(vinyl alcohol) derivatives are also used for the same application.

Wound dressings and artifical skins as cure supporters for burns of external wounds are made from the crosslinking of alcoholic soluble nylon with gelatin, sodium polyacrylate, and from porous films of chitin as polysaccharide coated with hydrophilic polymer. In food materials for preservation of freshness as well as the medical applications just mentioned above, triple-layer laminated films consisting of a porous sheet, superabsorptive polymer, and heat-sealed base material are in common use.

The layer of superabsorptive polymers in the above films is useful to absorb evaporated vapor and drips from vegetables and fruits, and to prevent decay and mold growth. Dehydrating agent sheets have also been developed, which contain highly concentrated solutions of superabsorptive polymer or sucrose between the base film and semipermeable membranes.

When in contact with fresh meat of fish, excess free water can be absorbed in concentrated sucrose solution through the semipermeable membrane and further absorbed in superabsorptive polymers. Then, the concentrated sucrose solution can again absorb excess free water in meat by the effect of osmotic pressure. By repeating these processes, the properties of meat can be well preserved.

Superasorbent polymers possess specific functions that are not found in other polymer products, and so comprise a class of promising materials for a range of uses. Further interesting applications will be developed in the future. Water is indispensable to our daily life. Consequently, many superabsorptive polymers of natural origin will be developed for various applications concerned with water [3].

Table 2.3 Possible Applications of Superabsorbent Polymers

Properties/ fields	**Water absorption and retention**	**Swelling in volume**	**Gelling ability**	**Increase in viscosity**
Sanitary products	*Sanitary napkins *Diapers *Breast pads			
Agriculture gardening	*Water-retaining agents in soil *Seed coatings *Drying preventives for samplings *Artificial moss		*Cultivation plot for mushrooms *Seed beds in fluid	
Civil engineering architecture	*Dew preventing agents in walls *Water-retaining agents in concrete	*Water sealing agents *Substitutes for sandbags	*Sludge *solidification agents *Lubricants in drilling works *Slurry explosives	*Mud shielding works
Cosmetics, Toiletries	*Sweat absorbing and kitchen papers		*Gelaromatics *Pocket warmers *Disposable chamber pots	
Medical	*Wound dressings *Sheets for surgical operation	*Control release agents for drug *Disintegrators in tablets	*Gelation of blood wastes	*Wet plasters

Table 2.3 Possible Applications of Superabsorbent Polymers (continued)

Properties/ fields	**Water absorption and retention**	**Swelling in volume**	**Gelling ability**	**Increase in viscosity**
Food industry	*Agents for preservation for *freshness *Drip absorbents *Dehydrating agents		*Gelling agents *Cold keeping hydrogels	*Viscosity enhancing additives
Others	*Fog preventing film *Dehydrating agents in oil *Moisture sensor *Ink jet resin for printer	*Toys swelling when soaked in water	*Hydrogel for fire fighting *Artficial snow *Water bed	*Emulsion paints

2.2 Starch

Starch is a reserve carbohydrate found principally in the seeds, roots, tubers, fruits and sometime in the pith of plants. It occurs as very small water-insoluble granules, usually associated with proteins, fats, and inorganic salts. The granules vary in shape and size ranging from about 1 to 100 μm in diameter depending on the source.

2.2.1 Chemical Composition of Starch Granules

Starch granules contain usually 10-20% (w/w) moisture and small amounts of proteins, fatty materials, phosphorus, and traces of inorganic materials. Table 2.4 gives the average chemical composition of various commercial starches.

1) Moisture

The moisture content of starch products depends on the relative humidity (RH) of the atmosphere in which they have been stored. If this humidity decreases, the starches give up moisture. If the RH increases, they absorb moisture. The equilibrium moisture content of starch is also dependent on the type of starch product. Under normal atmospheric conditions, most commercial native starches contain 10-20% (w/w) moisture.

2) Fatty Substances (Lipids, Fats)

The tuber (potato) and root (tapioca) starches contain only a very small percentage of fatty substances (0.1% w/w or lower), compared with the common cereal starches (corn, wheat, rice, and sorghum), which contain 0.6-0.8% (w/w) fatty substances. Cornstarch contains 0.5% (w/w) fatty acids (mainly palmitic, linoleic, and oleic acid) and 0.1% (w/w) phospholipids. Wheat starch contains 0.4% (w/w) free fatty acids (mainly palmitic, linoleic, and oleic acid) and 0.4% (w/w) phospholipids.

The presence of lipids in the common cereal starches has a profound effect on the physical properties of these starches.

3) Proteins

The amount of proteins, as shown in Table 2.4 includes the real proteins, but also the peptides, amides, amino acids, nucleic acids, and enzymes, that may be present in the starch granules. The tuber (potato) and root (tapioca) starches contain only a small amount of proteins (0.1% w/w or lower), compared with the common cereal starches (corn and wheat), which contain 0.3-0.5% (w/w) proteins.

4) Phosphorus

The phosphorus in the cereal starches is mainly present as phospholipids. The root starches (tapioca) contain a very low amount of phosphorus compounds. Potato starch is the only commercial starch that contains an appreciable amount of chemically bound phosphate ester groups. The amount of phosphate groups in potato starch ranges from 1 phosphate group per 200 to 400 glucose units. The phosphate substituent confers on potato starch amylopectin the properties of a polyelectrolyte, when dispersed into aqueous solutions. The mutual repulsion of the charged groups forces the molecules to expand. The phosphate groups can be considered ion-exchanging groups.

5) Ash

All commercial starches contain minor or trace quantities of inorganic materials. The approximate concentration of these materials is determined as the residue after complete combustion at a specified temperature (ash). Potato starch contains phosphate groups in a salt form, the cation that contained in the potatoes or in the processing water. The ash content of potato starch corresponds with the amount of phosphate groups. The ash content of the cereal starches corresponds partly with the amount of phospholipids. The ash of the commercial starches contains mainly sodium, potassium, magnesium, and calcium as metal compounds .

6) Flavor

The common cereal starches (corn, wheat, sorghum, and rice) have a pronounced and persistent raw cereal flavor. Waxy maize starch has less cereal flavor than cornstarch. Potato and tapioca starches are relatively free from starchy flavors. The flavors of the cereal starches appear to be due to the oxidation of lipids. The less pronounced starchy flavor of the tuber, root, and waxy starches may result from their lower lipid content [5].

Table 2.4 Average Chemical Composition of Starch Granules

Starch	Moisture at 65% RH^2 and 20 ^{o}C	Lipids, % on DS^b	Proteins % on DS, N^c x 6.25	Ash, % on DS	Phosphorus, % on DS
Corn	13	0.6	0.35	0.1	0.015
Potato	19	0.05	0.06	0.4	0.08
Wheat	14	0.8	0.4	0.15	0.06
Topioca	13	0.1	0.1	0.2	0.01
Waxy maize	13	0.2	0.25	0.07	0.007
Sorghum	13	0.7	0.3	0.08	-
Rice	-	0.8	0.45	0.5	0.1

Table 2.4 Average Chemical Composition of Starch Granules (continued)

Starch	Moisture at 65% RH^2 and 20 ^{o}C	Lipids, % on DS^b	Proteins % on DS, N^c x 6.25	Ash, % on DS	Phosphorus, % on DS
Sago	-	0.1	0.1	0.2	0.02
Amylomaize	13	0.4	-	0.2	0.07
Sweet potato	13	-	-	0.1	-

^{a}RH = relative humidity.

^{b}DS = dry substance.

^{c}N = nitrogen content.

2.2.2 Molecular Structure

Starch is a carbohydrate, composed of carbon, hydrogen, and oxygen atoms in the ratio 6:10:5, $(C_6H_{10}O_5)_n$. Starch can be considered as a condensation polymer of glucose, consisting of anhydroglucose units. The glucose units are linked to one another through the C1-C4 oxygen, known as glucoside bond. The glucoside linkage is stable under alkaline conditions and hydrolyzable under acid conditions. The glucose unit at the end of the polymeric chain has a latent aldehyde group and is known as the reducing end group.

Most starches are a mixture of amylose and amylopectin, each, with a wide range of molecular sizes. Starches of different origins have different amylose-amylopectin ratios as shown in Table 2.5. Table 2.5 shows the average degree of polymerization (DP) of both fractions in various starches [5].

1) Amylose

Amylose is essentially a linear polymer in which the anhydroglucose units are predominantly linked through α-D-(1→ 4) glucosidic bonds. The amylose polymer fraction of a starch will show a distribution of molecular sizes, and the average degree of polymerization (DP) will vary with the plant variety from which the starch is obtained. Depending upon the type of starch, the DP will range from about 250 to 4000 AGU per amylose molecule, corresponding to a molecular weight of approximately 40,000 to 650,000. The amylose from potato and tapioca starches has a higher molecular weight than that from corn starch. The relative severity of the treatment used to isolate the starch from its plant source and to fractionate the amylose from the starch will affect the molecular size of the amylose and the amylopectin.

Amylose forms inclusion complexes with iodine and polar organic compounds, such as butanol, fatty acids, nitroparaffins, and phenols, as well as with nonpolar compounds such as aliphatic and cyclic hydrocarbons. These complexes are essentially insoluble in water. The iodine complex is formed by interaction with iodine in the presence of iodide ions to give a blue color. The color is related to chain length, with a chain length in excess of 40 AGU needed to give the blue color. Shorter chains give purple, red, brown, or yellow complexes [6].

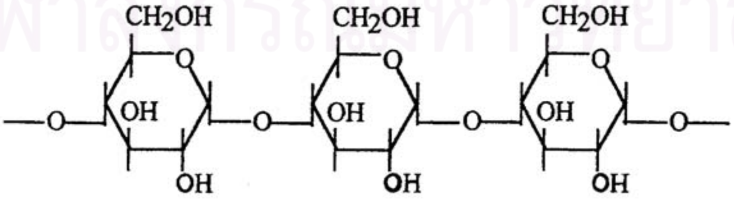

Figure 2.3 Chemical structure of amylose

2) Amylopectin

Amylopectin is a branched polymer containing, in addition to anhydroglucose units linked together as in amylose through α-D-(1→ 4) glucosidic bonds. Periodic branches at the carbon-6 position. These branches are linked to the 6 carbon by α-D-(1→ 6) glucosidic bonds. Each branch contains about 20 to 30 anhydroglucose units. A schematic diagram of the amylopectin molecule is shown in Figure 2.4.

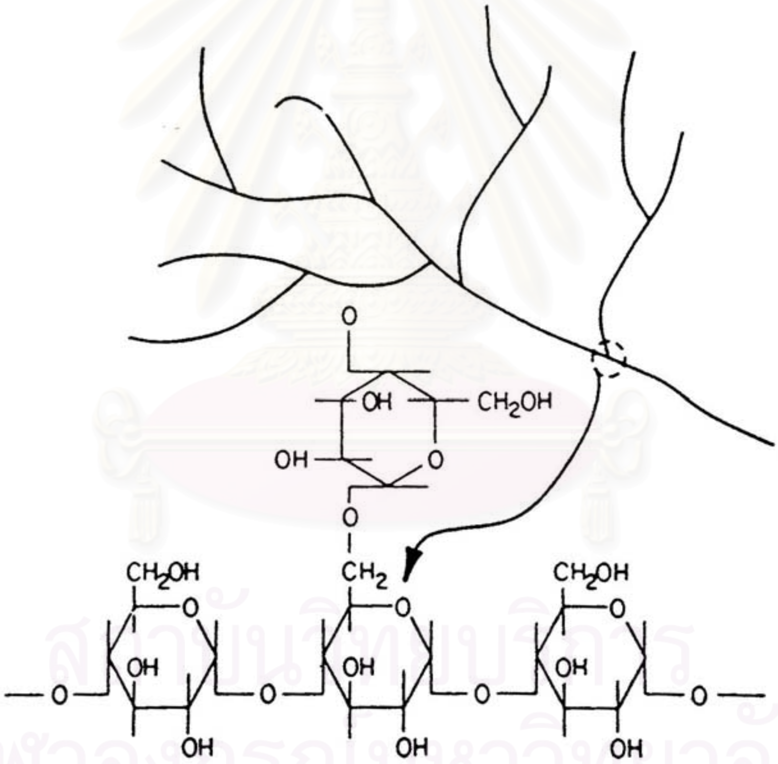

Figure 2.4 Schematic structure of amylopectin

The large size and branched nature of amylopectin reduce the mobility of the polymers and interfere with any tendency for them to become oriented closely enough to permit significant levels of hydrogen bonding. As a result, aqueous sols of amylopectin are characterized by clarity and stability as measured by resistance to gelling on aging. Amylopectin sols do not form as strong and flexible films as the linear amylose. They do not form an iodine complex with its associated deep blue coloration [7].

Table 2.5 Amylose and Amylopectin Contents and Degree of Polymerization of Various Starches

Starch	Amylose % (w/w)	Amylopectin % (w/w)	Average DP, amylose	Average DP, amylopectin
Corn	28	72	800	2,000,000
Potato	21	79	3000	2,000,000
Wheat	28	72	800	2,000,000
Tapioca	17	83	-	2,000,000
Waxy maize	0	100	-	2,000,000
Sorghum	28	72	-	-
Rice	17	83	-	-
Sago	27	73	-	-
Arrowroot	20	80	-	-
Amylomaize	50-80	20-50	-	-

2.2.3 Swelling and Gelatinization

Native starches are insoluble in water below their gelatinization temperature. This is a very important property, which enables the starch granules to be easily extracted from the plant source in aqueous systems. In addition, the native starches can be chemically modified in suspension or in water and recovered in purified form by filtration, washing with water, and drying.

Starch granules are insoluble in cold water due to the hydrogen bonds, formed either directly via neighboring alcoholic OH groups of the individual starch molecules or indirectly via water bridges. The hydrogen bonding forces are weak, but there are so many hydrogen bonds in starch granule that it does not dissolve in cold water. Starch granules swell slightly in cold water (10-15% increase in diameter), but this swelling is reversible. The granules shrink back to their original dimensions on drying.

When starch granules are heated in water to progressively higher temperatures, a point is reached where the polarization cross starts to fade at the hilum, and this rapidly extends to the periphery of the granule. Simultaneously, the granule starts to swell irreversibly. The term "*gelatinization*" is applied to this loss of polarization and concurrent initiation of swelling [5].

The critical temperture at which this occurs is known as the *pasting or gelatinization temperature*. The granules take up the water, swelling to many times their original volume, rupturing and collapsing as the heating and agitation of the mixture continues, and releasing concurrently some of the starch molecules, particularly amylose, into solution. The viscosity increases to a maximum that corresponds to the largest hydrated, swollen granules disintegrate. The result is a viscous colloidal dispersion which is a complex mixture of residual, swollen granule masses, hydrated molecular aggregates, and dissolved molecules.

Table 2.6 Gelatinization Temperature of Starch Granules

Starch	Gelatinization temperature, ^{o}C
Corn	62-72
Waxy corn (waxy maize)	63-72
Tapioca (Thailand)	62-73
Patoto	59-68
Sorghum	68-78
Wheat	58-64
Rice	68-78
Sago	-
Amylomaize (high-amylose corn)	63-92

The initial swelling during gelatinization takes place in the amorphous regions of the granule, disrupting the weak hydrogen bonding between the molecules and hydrating them. As the temperature of the aqueous starch mixture rises, more hydration occurs in the amorphous region and the hydrogen bonding in the crystalline regions begins to be disrupted. The granule swells to give an expanded network hydrated amylopectin molecules (and some amylose molecules) held together by residual organized micellular areas which have not been disrupted (figure 2.5) [6].

Figure 2.5 Structure of molecules in a cooked starch paste.

2.3 Gamma Rays

Gamma rays are high-energy photons and as such carry no charge or mass. X-rays and gamma rays are the same except for their source. X-rays are the result of an extranuclear process, i.e., the energy released when an electron falls into an unfilled orbital of an atom. Gamma rays are the result of nuclear processes: they are released in the fission process and also in the decay process of radioactive isotopes.

2.3.1 Radiation-Induced Synthesis

When electromagnetic radiation passes through matter its intensity decreases, primarily as a result of scattering and energy absorption by some of the irradiated molecules. Three major processes are operative.

a) Photoelectric Process

In the photoelectric process a photon is completely absorbed in a collision with an orbital electron and the electron is ejected from the atom. This can happen whenever the energy of the photon is greater than the binding energy of the electron. The difference between the electron binding energy and the photon energy is carried away by the electron.

The photoelectric effect is greatest for the radiation of low energy and for material of high atomic numbers.

b) Compton Process

The Compton process is the result of an elastic collision between a photon and an orbital electron in which part of the photon energy is transferred to the electron. The electron causes further ionization and excitation, while the photon is scattered with reduced energy.

The Compton scattering process is often the principal effect for γ-rays in radiation chemistry for example, it is the only important process occurring when Co^{60} γ-rays (1.17 and 1.33 MeV) interact with water or other substances of low atomic number.

c) Pair Production

If a photon has an energy greater than twice that equivalent to the rest mass of an electron then the pair-production process can occur. Since the rest mass of an electron is 0.51 MeV, the minimum energy for a pair production is 1.02 MeV. In this process the photon interacts with a nucleus and disappears with the production of two particles, a positive electron and a negative electron. The energy of photon in excess of the minimum 1.02 MeV appears primarily as kinetic energy of the particle pair.

The positron so formed usually is annihilated by an electron. When this occurs, two annihilation photons occur travelling in opposite directions and carrying one-half of the energy, 1.02/2 MeV, or 0.51 MeV [8].

For gamma rays from the Co^{60} source the predominant effect in organic materials is Compton scattering. In the Compton effect the incident, gamma ray interacts with an orbital electron ejecting the electron from its orbit and producing another photon of lower energy. Both the electron and photon subsequently interact with the material of the surroundings giving rise to essentially two processes, one of ionization and the other of excitation. In the case of ionization the Compton electron transfers sufficient energy to the orbital electron of another atom to overcome the forces binding it to the nucleus. The electron is therefore ejected, leaving behind a positive ion. If the energy transferred is insufficient to cause ejection of an electron, the energy level of the atom is raised and the atom is said to be in an excited state. The ions and excited molecules are very reactive; they either react with other materials present in the system or decompose into radicals and atoms or molecules. The free radicals produced upon irradiation of polymeric systems may be used to initiate graft polymerization.

The growth in popularity of radiation as an initiating system stems from the improvement in availability and cost of the ionizing radiation as a result of the introduction over recent years of more powerful nuclear reactors. Apart from its cheapness, radiation is a very convenient method for graft initiation as it allows a considerable degree of control to be exercised over structural factors, such as the number and length of the grafted chains by careful selection of the dose and dose rate. Radiation is also unique in its ability to enable grafting to be carried out on “prefabricated” or “shaped” articles [9].

2.3.2 *G*-value

the “*G* value” for a given irradiated system is the absolute chemical yield expressed as the number of individual chemical events occurring per 100 eV of absorbed energy. Thus $G(H_2)$ or G_{H2} are symbols for the “absolute number of hydrogen molecules produced per 100 eV” in a certain reaction, $G(CH_3^{\bullet})$ means the number of methyl radicals per 100 eV. and $G(R^{\bullet})$, G_R or G (free radicals) the total number of free radicals per 100 eV [9].

2.3.3 Interaction of Radiation with water

The overall process of producing chemical changes by the use of ionizing radiation starts with the bombardment of water or aqueous solution by the radiation and terminates with the reestablishment of chemical equilibrium. This process is usually divided into three stages.

1) The physical stage consists of energy transfer to the system. Its duration is of the order of 10^{-15} sec or less. The incident radiation produces, indirectly, ionization of water,

$$H_2O \quad \wedge\wedge\wedge\!\rightarrow \quad e^- + H_2O^+ \qquad (2.3)$$

as well as directly excitation,

$$H_2O \quad \wedge\wedge\wedge\!\rightarrow \quad H_2O^* \qquad (2.4)$$

2) The physicochemical stage consists of processes which lead to the establishment of thermal equilibrium in the system. Its duration is usually taken to be

of the order of 10^{-11} sec or less. Electrons ejected in the ionization process become thermalized and hydrated:

$$e^{-} \rightarrow e^{-}_{\text{therm}} \rightarrow e^{-}_{aq} \tag{2.5}$$

The H_2O^+ ions undergo a proton transfer reaction with neighboring water molecules,

$$H_2O^{+} + H_2O \rightarrow H_3O^{+} + OH \tag{2.6}$$

and the H_3O^+ becomes hydrated; hence, the point of formation and the initial spatial distribution of $H_3O^+_{aq}$ and OH are essentially the same and different from those for e^{-}_{aq}. If the volume in which they arose is considered to be spherical, then the radius for the initial distribution of the hydroxyl radicals and $H_3O^+_{aq}$ is about three times smaller than that of the hydrated electrons.

The dissociation of excited water molecules gives the hydrogen atom and hydroxyl radical as main products,

$$H_2O^{*} \rightarrow H + OH^{\bullet} \tag{2.7}$$

it also gives a low yield of hydrated electrons and, eventually, molecular hydrogen. It seems, however, that the contribution of excited water molecules to the formation of primary free-radical products in water radiolysis is of minor importance in comparison with that of the ionization processes.

3) The chemical stage consists of diffusion away from the point of origin and chemical reaction of primary species (e^{-}_{aq}, $OH^{\bullet}$, $H_3O^{+}_{aq}$, and H), and leads to the establishment of chemical equilibrium. It begins in the spur about 10^{-11} sec after

the passage of the radiation and about 10^{-10} sec in the bulk of the solution. Table 2.7 summarizes important chemical reactions of the primary species.

The expression for radiation-induced water decomposition,

$$H_2O \quad \text{^^^}\!\rightarrow \quad H_3O^+_{aq},\ OH^{\bullet},\ e^-_{aq},\ H,\ H_2O_2,\ H_2 \qquad (2.8)$$

represents the state in irradiated water about 10^{-9} sec after the passage of high energy radiation, when the reactions in the spurs, blobs, and short tracks are practically terminated. These products are found in irradiated water irrespective of the type and energy of radiation.

When dilute aqueous solutions are irradiated practically all the energy absorbed is deposited in water molecules and the observed chemical changes are brought about *indirectly* via the molecular and, particularly, the radical products. *Direct* action due to energy deposited directly in the solute is generally unimportant in dilute solutions. At higher solute concentrations direct action may be significant, and there is some evidence that excited water molecules may transfer energy directly to the solute [11].

Table 2.7 Reactions of Free Radicals in Irradiated Water

Reaction	Rate Constant, $M^{-1}\ s^{-1}$	pH
$e^-_{eq} + e^-_{eq} \xrightarrow{2H_2O} H_2 + 2OH^-$	5.5×10^9	13.3
	5×10^9	10-13
	6×10^9	11
$e^-_{eq} + H \quad H_2O \quad H_2 + OH^-$	2.5×10^9	10.5
	3×10^9	10.9
$e^-_{eq} + OH \rightarrow OH^-$	3×10^9	11
$e^-_{eq} + O^- \rightarrow 2OH^-$	2.2×10^{10}	13
$e^-_{eq} + H_3O^+ \rightarrow H + H_2O$	2.06×10^{10}	2.1-4.3
	2.36×10^{10}	4-5
	2.2×10^{10}	-
	2.26×10^{10}	4.1-4.7
$e^-_{eq} + H_2O_2 \rightarrow OH + OH^-$	1.23×10^{10}	7
	1.36×10^{10}	11
	1.1×10^{10}	-
	1.3×10^{10}	11
$e^-_{eq} + HO_2^- \rightarrow O + OH^-$	3.5×10^9	13
$e^-_{eq} + H_2O \rightarrow H + OH^-$	16	8.3-9.0
$H + H \rightarrow H_2$	1.5×10^{10}	0.2-0.8 N H_2SO_4
	1.0×10^{10}	2.1
	7.75×10^9	3
	1.3×10^{10}	0.4-3
	1.25×10^{10}	2-3
$H + OH \rightarrow H_2O$	3.2×10^{10}	0.4-3

Table 2.7 Reactions of Free Radicals in Irradiated Water (continutded)

Reaction	Rate Constant, $M^{-1} s^{-1}$	pH
$H + OH^- \rightarrow e^-_{eq}$	1.8×10^7	11.5
	2.2×10^7	11-13
$H + H_2O_2 \rightarrow H_2O + OH$	5×10^7	acid
	1.6×10^8	0.4-3
	9×10^7	2
	4×10^7	-
$OH + OH \rightarrow H_2O_2$	6×10^9	0.4-3
	4×10^9	7
	5×10^9	-
$O^- + O^- \rightarrow O_2^{-2}$		
$\xrightarrow{H_2O} HO_2^- + OH^-$	1×10^9	13
$OH + OH^- \rightarrow O^- + H_2O$	3.6×10^8	-
$OH + H_2O_2 \rightarrow HO_2 + H_2O$	4.5×10^7	7
	1.2×10^7	0.4-3
$O^- + H_2O \rightarrow O^-_2 + HO^-$	7×10^8	13
	2.74×10^8	13
$OH + H_2 \rightarrow O^- + H_2O$	6×10^7	7
$O^- + H_2 \rightarrow H + OH^-$	4.5×10^7	7
	8×10^7	13
$H_2O^+ + OH^- \rightarrow 2H_2O$	14.3×10^{10}	-
	4.4×10^{10a}	-

2.4 Graft Copylymerization

A graft copolymer consists of a polymeric backbone with covalently linked polymeric side chains. In principle, both the backbone and side chains could be homopolymers or copolymers. Graft copolymers are of great interest in the field of absorbency in a number of aspects. Grafting can be carried out in such a way that the properties of the side chains can be added to those of the substrate polymer without greatly chaging the latter.

2.4.1 Method of Graft Copolymerization

In principle, there are two general methods for the synthesis of graft copolymers.

1) Side chain polymer A could be linked directly by a suitable chemical reaction to the backbone polymer B.

2) The backbone polymer B could have active sites such as free radicals or ions formed upon it. These can then be used to polymerize a suitable monomer to produce the side chains of polymer A.

The former method is difficult except in solution and perhaps the most successful has been by treating “living” polymers to a suitably reactive backbone. There are many advantages to this approach which is, in principle, a simple synthetic method. There could be fewer problems of homopolymer formation. More importantly, the length and number of side chains could be readily controlled. This could lead to superior properties, including absorbency because of the higher degrees of substitution and shorter side chains. However, the difficulty of inducing polymer reactions presents a real problem and little promise can be seen at present with this approach.

The second general method has been much successful and a large number of techniques have been developed [12].

2.4.2 Radical Graft Polymerization

1) Chain Transfer and copolymerization

The radical polymerization of a momomer, in the presence of a dissolved polymer, by thermal decomposition of an initiator, results in a mixture of homopolymerization and graft polymerization. Polymer radicals formed by chain transfer between the propagating radical and polymer initiate graft polymerization.

Polymer radicals are also formed by attack on polymer by primary radicals from the initiator attacking on the polymer chains. For polymers containing double bonds, graft polymerization also involves copolymerization between the polymerizing monomer and the double bonds of polymer.

In addition to grafting initiated by chain transfer, the relative amounts of the two processes depend on the identity of the double bond.

2) Ionizing Radiation

Polymer radicals can also be produced by the irradiation of a polymer-monomer mixture with ionizing radiation. Most graft polymerization, irrespective of the initiation process, yields mixtures of the graft copolymer, ungrafted backbone polymer, and homopolymer of the monomer. The relative amounts of the three species depend on the monomer-polymer combination and the initiation process. The grafting efficiency of the irradiation process is often discussed in terms of the relative extents of radical formation in the polymer and monomer.

Graft copolymerization can also be achieved by irradiation with ultraviolet radiation, often in the presence of a photosensitizer. Photolytic grafting is similar to radiation grafting, except that the depth of penetration by uv is far less than by ionizing radiation.

3) Redox Initiation

Redox initiation is often an efficient method for graft polymerization. Redox initiation usually results in grafting with a minimum of homopolymerization since only the polymer radical is formed. It is, however, limited to polymers containing the necessary functional groups [13].

2.4.3 The Different Methods of Radiation Grafting

1) The direct Grafting Method

In its simplest form the direct grafting method involves the irradiation of a polymeric substrate in the presence of a monomer and in the absence of oxygen. Graft copolymerization of the monomer to the polymer is then initiated through the free radicals generated in the latter.

A number of important factors must be considered, however, before applying the direct radiation method to a given polymer-monomer system. Ionizing radiation as such is unselective. One must therefore consider not only the effect of radiation on the polymeric substrate but also the effect on the monomer, the solvent, or any other substance present in the system.

The radiation sensitivity of a substrate is measured in terms of its G_r value or free radical yield which is the number of free radicals formed per 100 eV energy absorbed per gram. The highest, grafting yields will occur for polymer-monomer combinations in which the free radical yield of the polymer is much greater than for the monomer.

Together with the radiation sensitivity of the polymer-monomer combination, one must, also consider the effect of the radiation on the actual polymeric substrate. In general, polymers either degrade or crosslink under irradiation. If the polymer degrades then irradiation in the presence of a monomer will lead predominantly to block-type copolymers; if the polymer crosslinks, graft structures will result. This may be represented as equation 2.9 and 2.10.

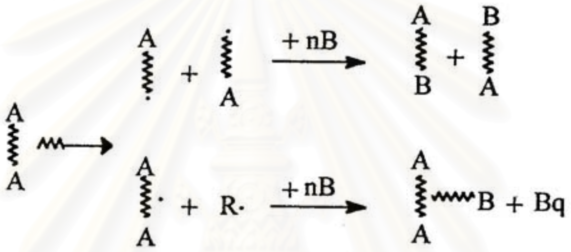

(2.9)

(2.10)

Here A$\sim\sim\bullet$ and A$\overset{\bullet}{\sim\sim}$A represent polymeric free radicals derived from Ap and R$^\bullet$ represents a low molecular weight radical or hydrogen atom.

As a general empirical rule it may be stated that when the structure of a vinyl polymer is such that each carbon atom of the main chain carries at least one hydrogen atom, the polymer crosslinks (case I),

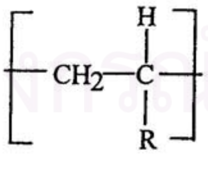

(I)

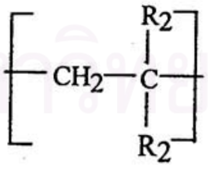

(II)

whereas if a tetrasubstituted carbon atom is present in the monomer unit, the polymer degrades (case II).

The dose and dose rate of irradiation are important factors in any radiation grafting system. In the direct method the total dose determines the number of grafting sites while the dose rate determines the length of the grafted branches. The length of the branches is also controlled by other factors, such as the presence of chain transfer, the concentration of monomers, the reaction temperature, the viscosity of the reacting medium, diffusion phenomonon, etc.

Diffusion of the monomer into the polymer plays an important role in the direct radiation method as it is by this means that the monomer reaches the active sites within the polymer. It would be expected that the rate of graft polymerization would be directly proportional to the radiation dose rate. In some cases, however, the diffusion of monomer cannot satisfy the increased rate of initiation within the polymer.

The effect of temperature on the kinetics of the direct radiation method is quite complex. Increase in temperature increases the monomer diffusion rate but also increases transfer and termination reaction rates of the growing chains, reducing the importance of the gel effect. Solubilities and radical mobilities may also change as the temperature is varied.

It will be appreciated that in the direct radiation method a certain amount of homopolymer will always be formed both because of the effect of the rediation on the monomer and as a normal consequence of the grafting reaction (see Eq. 2.10). Contamination of the grafted product with homopolymer can be quite inconvenient as by at large most polymers are incompatible and due to a segregative tendency, the presence of physically mixed polymer impurity can yield a product with poor physical, optical, and electrical properties. The direct radiation method is, on the other hand, by far the most efficient technique since it, involves rapid utilization of the accessible backbone polymer radicals as they are formed. It is not surprising then that, numerous techniques have been developed in an effort to reduce the amount of homopolymerization formed during the reaction.

2) Preirradiation in Air

In this method the polymeric substrate is irradiated in air or oxygen to produce peroxide bonds. Those peroxide groups are reasonably stable and the polymer can be stored in the cold without loss of activity. If heated subsequently in the presence of monomer (as liquid or vapor) to about 150 °C in the absence of air, the peroxide groups decompose liberating free radicals which can then initiate graft polymerization.

In principle the preirradiation method should not yield homopolymer because the monomer is never directly exposed to radiation. In some cases, however, there is evidence that irradiation in air leads to the formation of hydroperoxides on the polymer backbone. These, on heating, decompose giving a hydroxyl radical which can initiate the homopolymerization of the added monomer. Homopolymer formation can, however, be reduced considerably by the incorporation of a redox system during irradiation to convert the hydroxyl radicals to hydroxyl ions.

$$P_x \xrightarrow{O_2} P_xO_2\cdot \longrightarrow P_xOOH \xrightarrow[UV]{heat} P_xO\cdot + \cdot OH \qquad (2.11)$$

$$P_xO\cdot + M \longrightarrow P_xOM\cdot \text{ graft copolymer} \qquad (2.12)$$

$$\cdot OH + M \longrightarrow HOM\cdot \text{ homopolymer} \qquad (2.13)$$

$$POOH + Fe^{2+} \longrightarrow PO\cdot + OH^- + Fe^{3+} \qquad (2.14)$$

The efficiency of the grafting reaction will depend directly on the kinetics of the radiation peroxidation process. The peroxide yield will necessarily depend on both the G_r value of the irradiated substance and the stability of the resulting peroxide at the irradiation temperature.

3) Grafting Initiated by Trapped Radicals

One of the primary effects of ionizing radiation on polymers is the formation of free radicals. Although free radicals are highly reactive it has been demonstrated that they can become trapped for extremely long periods (several days or even months) in a viscous medium such as that encountered in a polymer at a temperature below its glass transition point. If the polymer is partly crystalline, the free radicals formed within the crystalline regions upon irradiation are still more firmly trapped, since the mobility of polymeric segments is much lower if those are involved in an organized structure. Although the free radicals are trapped they are still highly reactive and provided the monomer can diffuse through the polymer to reach the reactive sites, the trapped radicals can be used to initiate graft copolymerization.

The grafting yield obtained by this method will depend directly on the efficiency of radical trapping. Radical mobility is a function of temperature and the physical state of the system; it follows therefore that the most efficient radical trapping will occur for crystalline polymers irradiated at low temperature. The concentration of free radicals in an irradiated polymer has been shown to increase linearly with dose but tends to reach a limiting value for a certain dose. This limiting dose is apparently a function of the particular polymer system and has to be determined experimentally.

As with the peroxidation technique, homopolymer formation should not occur in this process as the monomer is not exposed to radiation. Moreover, low molecular weight radicals, which would also initiate homopolymerization, are not expected to remain trapped at ordinary temperatures.

4) Irradiation of Polymer Mixture

If an intimate mixture of two or more polymers is irradiated, it is possible that a crosslinking type of reaction will occur with the formation of some graft copolymers. The efficiency of this process depends on obtaining close physical contact between the different components and, as most polymers are incompatible this technique, has found only limited use. The type of polymer present and the respective reactions under irradiation are another important factor. Thus if the mixture contains two polymers of the crosslinking type, the reactions in Equations 2.15-2.17 are expected to occur.

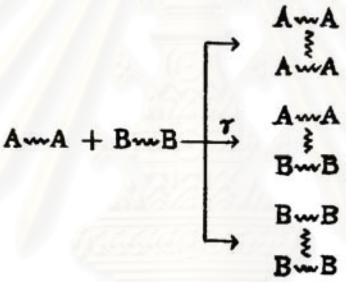

(2.15)

(2.16)

(2.17)

If one of the polymers, say B, is of the degrading type, one can still expect the formation of grafted structures such as

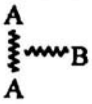

(III)

However, if both polymers are of the degrading type, the yield of graft (or block) copolymers is very small.

Little work has been reported in this field and the majority of graft copolymers prepared by this method appear in the patent literature.

5) Radiation Grafting in Emulsion Systems

If the irradiation of a polymer-monomer combination is carried out in emulsion the reaction medium does not become unduly viscous at high conversions and the system remains homogeneous throughout the duration of the reaction. Homogeneous grafting in emulsion results in high grafting efficiencies with less homopolymer formation and it is therefore a very attractive method of grafting. The copolymerization can be initiated by free radical sites formed on the backbone as a result of several reactions: (a) direct reaction of the irradiation on the polymer, (b) removal of a hydrogen atom from the polymer by hydroxyl radicals produced by the irradiation of the aqueous phase, and to a lesser extent by chain transfer and the formation of buried polymer radicals.

It is not surprising that the majority of grafting work using this technique has been done on natural rubber latices.

2.4.4 Kinetic Features of Radiation Grafting

Accurate kinetic data is necessary for the optimum design of graft polymerization processes as the rate of grafting and the location of the grafted branches within the polymeric substrate can affect the properties of the copolymer formed. In principle, the conventional free radical polymerization scheme should be applicable to radiation grafting systems as, in general, the reaction involves the polymerization of a vinyl monomer initiated by a polymeric radical. In practice, however, the situation is not quite as straight forward as this because of the number of specific featured systems. The gel effect, chain transfer, phase separation, and diffusion effects are but, a few of the many factors, which can seriously affect the reaction kinetics.

1) The Direct Radiation Technique

If one assumes that the graft polymerization occurs by a radical chain process then the overall reaction scheme can be divided into three main steps: initiation, propagation, and termination. This may be represented as follows.

Initiation:

$$P \xrightarrow{k} P^{\bullet} \tag{2.18}$$

$$r = kI \tag{2.19}$$

Propagation of initial radical:

$$P^{\bullet} + M \xrightarrow{k_i} PM^{\bullet} \tag{2.20}$$

$$r_i = k_i[P^{\bullet}][M] \tag{2.21}$$

Propagation:

$$PM_n^{\bullet} + M \xrightarrow{k_p} PM_{n+1}^{\bullet} \tag{2.22}$$

$$r_p = k_p[PM_n^{\bullet}][M] \tag{2.23}$$

Termination by two growing radicals:

$$PM_m^{\bullet} + PM_n^{\bullet} \xrightarrow{k_t} PM_{m+n} \text{ or } PM_m + PM_n \tag{2.24}$$

$$r_t = 2k_t[PM^{\bullet}]^2 \tag{2.25}$$

If one makes the normal assumption that the length of the polymer chains is long, then Reaction 2.20 can be neglected with respect to Reaction 2.22, and one obtains the following relation for the rate of graft polymerization :

$$r_p = k_p[\mathrm{PM_n}^\bullet][\mathrm{M}] \qquad (2.26)$$

Introducing the conventional steady-state assumption that the rate of change of the radical concentration is small compared to its rates of formation and disappearance, then

$$k_i\,[\mathrm{P}^\bullet][\mathrm{M}] = 2\,k_t[\mathrm{PM}^\bullet]^2 \qquad (2.27)$$

i.e.,

$$r_i = 2\,k_t[\mathrm{PM}^\bullet]^2 \qquad (2.28)$$

then

$$[\mathrm{PM}^\bullet] = (r_i\,/\,2\,k_t)^{1/2} \qquad (2.29)$$

On combining Equation 2.26 and 2.29 one obtains the rate of graft polymerization:

$$r_p = k_p\,[\mathrm{M}]\,(r_i/2\,k_t)^{1/2} \qquad (2.30)$$

Where

I = intensity of radiation

P = backbone polymer

$\mathrm{P}^\bullet$ = polymer radical

$\mathrm{PM_m}$, $\mathrm{PM_n}$, or $\mathrm{PM_{m+n}}$ = graft copolymer

M = grafting monomer

r = rate of initiation of polymer radicals

r_i = rate of initiation of graft reaction

r_p, r_t = rates of propagation and termination, respectively

k = rate constant for initiation of polymer radicals

k_i = rate constant for initiation of graft reaction

k_p , k_t = propagation and termination rate constants, respectively

2) Grafting with More than One Monomer

Deviations from normal copolymerization kinetics have also been noted in cases of the direct radiation grafting of more than one monomer to a polymeric substrate. On the basis of the normal copolymer composition equation, one obtains:

$$\frac{dM_1}{dM_2} = \frac{M_1}{M_2} \frac{r_1M_1 + M_2}{r_2M_2 + M_1} \tag{2.31}$$

Where

dM_1/dM_2 = ratio of monomer 1 to monomer 2 in the copolymer formed at any instant

M_1, M_2 = concentrations of monomer 1 and 2, respectively, in the comonomer solution

r_1, r_2 = relative reactivities of monomers 1 and 2, respectively

One should be able to predict the composition of the grafted copolymer provided the values of r_1 and r_2 are known [9].

2.5 Terminology and Definition

Before proceeding to the experimental part, several technical terms need to be clarified for the better understanding of readers.

1) Percentage Add-on

It is referred to as the weight percentage of synthetic polymer in the graft copolymer and is determined as follows:

$$\%\text{add-on} = \frac{\text{weight of polymer grafted} \times 100}{\text{weight of the grafted copolymer}} \tag{2.32}$$

It is calculated by the acid hydrolysis method. The grafted polymers are separated from the starch backbone by heating the graft copolymer under reflux in dilute acid solution.

2) Grafting Efficiency

It is a term often used to describe graft copolymerization reactions and is defined as the percentage of the total synthetic polymer formed that has been grafted to starch. High grafting efficiencies are desirable since a polymerization of the low grafting effciency would afford mainly a physical mixture of starch and homopolymer. It can be calculated as follows:

$$\%\text{grafting efficiency} = \frac{\text{weight of polymer grafted} \times 100}{\text{weight of homopolymer} + \text{weight of polymer grafted}} \tag{2.33}$$

3) Percentage Conversion

It is used to describe the degree of the monomer polymerization, which undergoes graft copolymerization and homopolymerization. It can be evaluated by the following expression.

$$\%\text{conversion of monomer} = \frac{\text{weight of polymer formed}}{\text{weight of monomer charged}} \times 100 \qquad (2.34)$$

4) Percentage Gel Content

It is used to describe the degree of crosslink densities, which is related to the amount of soluble fraction. It can be calculated by the following equation [4].

$$\%\text{gel content} = \frac{\text{weight of sample after extraction}}{\text{weight of sample before extraction}} \times 100 \qquad (2.35)$$

The soluble polymer fraction can readily be extracted from the gel by extracting the graft copolymer under reflux in distilled water

2.6 Literature Survey

Ranby et al., [14] prepared the starch copolymers with polyacrylonitrile using the Mn^{3+} initiation method and different amounts of acrylonitile. The product was hydrolyzed in aqueous alkali (to convert nitrile groups to amide and carboxyl groups) to enhance the hydrophilic character of the copolymer and achieve “superabsorbent properties”. At relative humidities (RH) up to 95-97% the modified starch showed “normal” water vapor absorption like cellulose and other polysaccharides. When in contact with liquid or distilled water, the modified starch formed a “superabsorbent” gel which retained very large amounts of water (up to 800 g g^{-1}). At low and high pH and in aqueous salt solutions (NaCl, $CaCl_2$ and synthetic urine) the water retention was strongly reduced. This was interpreted as due to the ionic strength (salt effect) and for Ca^{2+} ions probably also crosslinking by salt formation with carboxyl groups on adjacent chains or chain segments.

Iyer et al., [15] prepared superabsorbent polymers using acrylonitrile grafted to corn starch employing low levels of gamma ray radiation as initiator. Various grafting parameters had been studied at these low dosages. Absorbency values for the final products were reported. Use of the above superabsorbent as a desiccant had been evaluated. The product would find application where dispersions of low viscosity and high water absorbencies were desired.

Hongfei et al., [16] investigated the acid effect in mutual radiation grafting of acrylic acid (AA), 4-vinyl-pyridine (4-VP) and N-2-vinylpyrrolidone (2-NVP) in methanol on silicone rubber . Measurements of grafting yields as a function of dose were carried out. In addition, the effects of Cu^{2+} and monomer concentrations in solvent were observed. It was found that acid in grafting system of 4-VP had an enhancement effect; in NVP system had an inhibition effect with a wide absorbed dose range. But in the case of AA the relationship was more complex: below 6 kGy of total dose irradiation, acid enhanced the grafting yield; while total dose was up to 13 kGy the opposite results were obtained. The mechanisms of acid effects in the methanol systems were discussed.

Kiatkamjornwong et al., [17] studied radiation modification on liquid retention properties of native cassava starch, gelatinized at 85°C. Graft copolymerization with acrylonitrile was carried out by mutual irradiation to gamma – rays. A thin aluminum foil was used to cover the inner wall of the reaction vessel, so that the homopolymer concentration was reduced to be less than 1.0% with a distilled water retention value of 665 g/g of the dry weight of the saponified grafted product. Confirmation of graft copolymerization and saponification reactions was made by the infrared spectrophotometric technique. The combined effect of radiation parameters in terms of an irradiation time and a dose rate to the total dose on the extent of the grafting reaction expressed in terms of grafting parameters which directly influenced liquid retention values evaluated in conjunction with statistical analysis was studied.

Yao et al., [18] prepared a series of novel copolymer superabsorbents based on acrylamide, sodium allylsulfonate, sodium acrylate, and *N,N'*–methylenebisacrylamide by copolymerization. The resulting superabsorbents had a fast swelling rate. The experimental results showed that absorbency increased to a maximum as the cross-linking density increased, but an excessive of cross-linking density led to a decreased swelling. Their water retention was also observed at pressures of 1-10 kg cm^{-2} and temperatures of 60 and 100°C, respectively. The water retention of soil had been enhanced using the poly(acrylamide-sodium allylsulfonate-sodium acrylate) superabsorbent; its use for bean growth was also investigated.

Huyen et al., [19] studied the grafting of acrylamide onto starch by radiation method. The urease was immobilized on the grafted starch. Some experiments to observe the quantitative relationships between the percent graft and the activity of immobilized enzyme were determined. The enzyme activity was maintained by more than seven batch enzyme reactions.

Saraydin et al., [20] investigated the biocompatibility of acrylamide and acrylamide-maleic acid hydrogels prepared using γ-rays against some biochemical parameters of human serum. First, the swelling kinetics of acrylamide and acrylamide-maleic acid hydrogels were investigated in distilled water and physiological saline solution and some swelling and diffusion parameters had been calculated. For the analysis of biocompatibility, acrylamide and acrylamide/maleic acid hydrogels were incubated in 10 different human sera for 24 h and their biocompatibility with some biochemical parameters had been investigated. No significant difference in biocompatibility values before and after the test procedures had been found. It was therefore concluded that acrylamide and acrylamide/maleic acid hydrogels were biocompatible.

Saraydin et al., [21] prepared acrylamide/maleic acid hydrogels in the form of rods by γ-irradiating ternary mixtures of acrylamide-maleic acid-water with 2.00-5.71 kGy γ-rays. The influence of dose and relative content of maleic acid on the spectroscopic, thermal and mechanical properties, swelling properties, diffusional behavior of water and diffusion coefficients of hydrogels systems were examined. Acrylamide-maleic acid hydrogels were swelled in the range of 1000-2800%, while polyacrylamide hydrogels were swelled in the range of 650-700%. Water diffusion to hydrogels was non-Fickian type diffusion. The diffusion coefficients varied from 4.5×10^{-7} to 12.2×10^{-7} cm^2 s^{-1}.

Saraydin et al., [22] prepared acrylamide-maleic acid (AAm/MA) hydrogels containing different quantities of maleic acid by γ-irradiation. They had been used in experiments on swelling, diffusion, and the adsorption of basic dyes such as methylene blue, methyl violet, and nile blue. Acrylamide-maleic acid hydrogel containing 40 mg maleic acid irradiated at 3.73 kGy had been used for swelling and diffusion studies in water and solutions of basic dyes. For this hydrogel, maximum and minimum swellings had been observed with solutions of nile blue (2000% swelling) and water (1480% swelling). Diffusions of water and dyes within hydrogels had been found to be non-Fickian in character. In experiments on the adsorption of dyes, Type III adsorption had been found. One gram of AAm/MA hydrogel adsorbed 0.3-2.2 mg of methylene blue, 0.3-3.4 mg of methyl violet, and 1.6-3.9 mg of nile blue, while acrylamide hydrogel had not adsorbed any basic dye. This result showed that AAm/MA hydrogel could be used as a sorbent for water pollutants such as dyes, and immobilization of these organic contaminants in the hydrogels from wastewater could solve one of the most important environmental problems of the textile industry.

Saraydin et al., [23] prepared acrylamide-maleic acid (AAm/MA) hydrogels by irradiating with γ-radiation and investigated on swelling, diffusion, and uptake of some cationic dyes such as basic red 9 (BR-9), basic green 4 (BG-4), cresyl violet (CV), and basic blue 20 (BB-20). AAm/MA hydrogel containing 60 mg maleic acid and irradiated at 5.71 kGy had been used for swelling and diffusion studies in water and solutions of basic dyes. For this hydrogel, swelling studies indicated that swelling increased in the following order: BR-9 > BG-4 > CV > BB-20 > water. Diffusion of water and the dyes within hydrogels was found to be of a non-Fickian character. The uptake of the cationic dyes to

AAm/MA hydrogels was studied by the batch adsorption technique at 25°C. In the adsorption experiments, Langmuir-type adsorption in the Giles classification system was found. Some binding and thermodynamic parameters for AAm/MA hydrogel-dye systems were calculated using the Klotz method. Adsorption studies indicated that monolayer coverages of AAm/MA hydrogel by these dyes increased in the following order : BB-20 > CV > BG-4 > BR-9.

Liu et al., [24] prepared high water-absorbent copolymers comprising acrylic acid (AA) and acrylamide (AM) in the presence of a crosslinking agent, monofunctional aldehyde, by a solution polymerization technique using a redox initiation system. Such copolymers had very high water absorbency and absorbing kinetics to the distilled water. The copolymer formed which absorbed about 900 g water/g dry copolymer was used to study the influence of sodium chloride on the absorption capacity at 24°C. The swelling of this copolymer was studied in alcohol/water mixtures of increasing alcohol content at 294, 304, and 314 K. The main transition for ethanol/water and methanol/water mixtures was a rapid decrease of the retention capacity of the copolymer at 50-60 vol% ethanol and 55-65 vol% methanol, respectively. Swelling in distilled water at different temperatures (T) and the effect of solvent composition were also studied. Among the variables examined were initiator concentration, polymerization temperature, and amount of AM in the copolymer.

Kiatkamjornwong and Suwanmala [25] prepared partially hydrolyzed polyacrylamide-*co*-poly(*n*-vinyl pyrrolidone) superabsorbent from acrylamide monomers exposed to γ-rays to become polyacrylamide that was subsequently partially hydrolyzed and was then copolymerized with *n*-vinylpyrrolidone to obtain a terpolymeric superabsorbent with a water retention value of 1100 times its dried weight. The total dose and dose rate along with the appropriate degree of hydrolysis were investigated for percentage conversion in each polymerization and the extent of water absorption.

Kiatkamjornwong and Meechai [26] studied the enhancement of the gamma radiation grafting of acrylonitrile onto gelatinized cassava starch. Infrared spectrometry was used to follow the chemical changes in the grafting reaction and from saponification. The saponified starch-*g*-PAN (HSPAN) was then characterized in terms of grafting parameters to provide a guide for the optimum total dose (kGy) and the appropriate ratio of starch/acrylonitrile for a fixed dose rate of 2.5 x 10^{-1} kGy min^{-1}. Other dose rates were also carried out to obtain the appropriate result of grafting copolymerization and of water absorption. A thin aluminium foil, covering the inner wall of the reaction vessel, was found to be far more effective than any other metal films in the enhancement of the grafting reaction and the water absorption as well. Nitric acid in the medium increased the grafting yield and the water absorption. Methyl ether hydroquinone inhibitor was evaluated for its ability to increase homopolymerization and decrease graft reaction. When styrene was used as a comonomer, it hampered the grafting of acrylonitrile onto starch backbone. The water absorption capacity was improved by freeze-drying the HSPAN. The treatment of the HSPAN with aluminium trichloride hexahydrate was found to enhance the degree of wicking, but to decrease the water absorbency.

Saraydin et al., [27] studied the influence of some aromatic amino acids (histidine, phenylalanine and tryptophan) on the swelling behavior of acrylamide-maleic acid hydrogel (AAm/MA) prepared by γ-radiation . Swelling tests of AAm/MA hydrogel were made in buffer solution and amino acid solutions at various pH at 37°C. The pHs values were resulted from the ionization of α - carboxyl groups (pK_1), α - amino groups (pK_2) and, isoelectric points (pI) of amino acids. The swelling of AAm/MA hydrogel increased when pH values of solutions were increased. The value of equilibrium swelling of AAm/MA hydrogel was 1035% at pH 10 buffer, while it was 880% at pH 2 buffer. The values of equilibrium swelling of AAm/MA hydrogel in phenylalanine, tryptophan and histidine solutions varied among 1130-1245% at pH 10, while they were among 790-975% at pH 2. The rate constant of swelling, diffusional exponent, network parameter and, diffusion and intrinsic diffusion coefficient were calculated by swelling kinetics. Diffusion of the penetrants into the hydrogel was found to be *non-Fickian* character. The diffusion coefficients of the hydrogel varied between 3.33×10^{-6} - 7.71×10^{-6} $cm^2 s^{-1}$, while the intrinsic diffusion coefficients varied between 4.03×10^{-6} - 8.48×10^{-6} $cm^2 s^{-1}$.

Okay et al., [28] prepared a series of hydrogels from acrylamide and 2-acrylamido-2-methylpropanesulfonic acid (AMPS) monomers with 0-80 mol% AMPS and using *N,N'*-methylenebisacrylamide as the crosslinker. The swelling capacities of hydrogels were measured in water and in aqueous NaCl solutions. The volume swelling ratio q_v of hydrogels in water increased sharply when the mole fraction f_c of AMPS increased from 0 to 0.06. At higher values of f_c from 0.06 up to 0.18, no change in the swelling capacities of hydrogels was observed; in this range of f_c, q_v became nearly constant at 750. However, as f_c further increased, q_v started to increase again monotonically over the entire range of f_c. At a fixed value of f_c, the swelling ratio of hydrogels decreased with increasing salt concentration in the external solution. The results of the swelling measurements in aqueous salt solutions were compared with the predictions of the Flory-Rehner theory of swelling equilibrium. It was shown that the theory correctly predicted the swelling behavior of hydrogels up to 80 mol % charge densities. However, the method of estimation of the network parameters was found to be unimportant in the prediction of the experimental swelling data. The network parameters used in the simulation only correct the deficiency of the swelling theory.

Guven and Sen [29] predicted the swelling behaviour of hydrogels containing diprotic acid moieties, sensitive to pH and ionic strength changes of the swelling medium. The equations derived for the prediction of the theoretical swelling curves were based on the phantom network theory of Erman *et al.* and the approaches of Peppas *et al.* For all predictions, a number of polymer-based parameters, solution property parameters and polymer-solvent combination type parameters were evaluated for typical dicarboxylated copolymers. The advantages of the derived equations for the determinations of average molecular weight between the cross-links and also a polymer-solvent interaction parameter had been exemplified.

Sen et al., [30] prepared hydrogels with varying crosslink densities and ionic moieties from the ternary systems N-vinyl 2-pyrrolidone/itaconic acid/water by irradiation with γ rays at ambient temperature. The influence of external stimuli such as pH, temperature and ionic strength of the swelling media and the type of buffer on the equilibrium swelling properties were investigated. Hydrogels showed typical pH and temperature responses, such as high-pH and low-temperature swelling and low-pH and high-temperature deswelling. A change in the ionic strength of the swelling solution from 0.01 to 0.20 caused a decrease in the equilibrium degree of swelling of hydrogels. Oscillatory swelling behaviour was also observed and investigated in response to changes in the pH of the solution.

Sen et al., [31] investigated the average molecular weight between cross-links (M_c) of itaconic acid-containing poly(vinyl pyrrolidone) and maleic acid containing poly(acrylamide) hydrogels sensitive to pH changes of the swelling medium. Polyelectrolyte hydrogels with varying compositions were prepared in the form of rods from ternary mixtures of *N*-vinyl 2-pyrrolidone/itaconic acid/water and acrylamide/maleic acid/water. Gelation was achieved by irradiating the system with γ rays at ambient temperature. The equation modified by the authors recently for the determination of M_c was observed to describe very well the swelling behaviour of charged polymeric networks. In addition to the evaluation of M_c from swelling data, the same equation also provided the simultaneous measurement of polymer-solvent interaction parameter of the systems investigated.

Tumturk et al., [32] prepared poly(acrylamide/maleic acid) [P(AAm/MA)] hydrogels by irradiating the ternary mixtures of AAm/MA and water by γ rays at ambient temperature. The influence of the MA on the adsorption capacity of hydrogels were found to increase from 0.40 to 0.71 mg α-amylase/g dry gel with increasing amount of MA in the gel system. Maximum enzyme activities were observed at lower pH values and higher temperatures for adsorbed enzyme compared with free enzyme. Kinetic parameters were calculated as 2.51 g dm^{-3} for K_m and 1.67 x 10^{-3} g dm^{-3} min^{-1} for V_{max} of the free enzyme, in the range of 12.3-12.9 g dm^{-3} for K_m and 1.63 x 10^{-3} - 1.96 x 10^{-3} g dm^{-3} min^{-1} for V_{max} depending on the amount of MA in the hydrogel. While the enzymatic activity of free enzyme was completely lost after 20 days, the adsorbed enzyme retained 47-59% of its original activity after 20 days, depending on the amount of MA in the hydrogels.

Kiatkamjornwong et al., [33] studied graft copolymerizations of acrylamide and/or acrylic acid onto cassava starch by a simultaneous irradiation technique using gamma-rays as the initiator with regards to various parameters of importance: the monomer-to-cassava starch ratio, total dose (kGy), dose rate (kGy h^{-1}), acrylamide-to-acrylic acid ratio, and the addition of nitric acid and maleic acid as the additives. Grafting parameters were determined in relation to the water absorption of the saponified graft copolymer. The water absorption of the saponified graft copolymer in salt and buffer solutions of different ionic strengths was also measured, from which the superabsorbent properties were found to be pH sensitive. The starch graft copolymers of acrylamide and acrylic acid gave higher water absorption than the starch graft copolymers of either acrylamide or acrylic acid alone. The porosity of the saponified starch graft copolymers prepared by the acrylamide/acrylic acid ratios of 70:30 and 50:50 was much higher than the porosity of copolymers in terms of fine networks. Ionic strength and multi-oxidation states of the saline and buffer solutions markedly decreased the water absorption of the saponified cassava starch grafted superabsorbent polymers.

CHAPTER 3

EXPERIMENTAL

3.1 Materials

3.1.1 Chemicals

Cassava starch was obtained, in one lot, from Thai Wah Co., Ltd. It was produced from tapioca cultivated in summer. It contained 13.5% moisture, 0.20% ash, pH value 4.0-7.0 and viscosity of 550 B.U. min.

Acrylamide, AM, and acrylic acid, AA were provided by Siam Resin & Chemical Co., Ltd. They were use as received.

Methanol, commercial grade from BDH, Poole England, was purified by fractional distillation at atmospheric pressure.

Acetone, commercial grade from Merck, Darmstadt Germany, was purified by fractional distillation at atmospheric pressure.

Other chemicals, as shown in Table 3.1, which were of analytical grade, were used without further purification.

3.1.2 Equipment and Glassware

Water bath circulator, hot plate and magnetic stirrer, mechanical stirrer, heating mantle, reactor, 3-necked round bottom flask, flat bottom flask, condenser, centrifuge bottle, desiccator, grinder, beaker, funnel, erlenmeyer flask, analytical balance, oven and general laboratory glassware and equipment.

Table 3.1 Chemicals

Chemicals	Source
Hydrochloric acid (HCl)	Merck (Darmstadt Germany)
Maleic acid, MA, ($C_4H_4O_4$)	Merck (Darmstadt Germany)
Potassium hydroxide (KOH)	J.T.Baker (Phillipsburg USA)
Sodium chloride ($NaCl$)	Merck (Darmstadt Germany)
Magnesium Chloride ($MgCl_2.6H_2O$)	Merck (Darmstadt Germany)
Calcium Chloride ($CaCl_2.2H_2O$)	Carlo Erba (Milan Italy)
Boric acid (H_3BO_3)	BDH (Poole England)
Citric acid ($H_3C_6H_5O_7.H_2O$)	Carlo Erba (Milan Italy)
Tri-sodium phosphate ($Na_3PO_4.12H_2O$)	Merck (Darmstadt Germany)

3.1.3 Apparatus

Cobalt 60 Source, Gamma beam 650 of 42,750 Curies from Nordian International Inc., Toronto Canada

Fourier Transform Infrared Spectroscopy, Nicolet Impact 410, U.S.A.

Elemental Analyzer, Perkin Elmer PE 2400 series II, Norwalk Connecticut U.S.A.

Scanning Electron Microscope, JEOL, JSM-T220 A, Tokyo Japan

3.2 Procedure

3.2.1 Gelatinization of Cassava Starch

Into a 500 cm^3 reactor, 10 g of cassava starch was mixed with 200 cm^3 of distilled water. The system was stirred at 400 rpm and heated at around 85 ± 3 °C at the same time for one hour to form a paste-like slurry.

Part I: Effect of Diprotic Acids on Grafting Efficiency and Water Absorption of Cassava Starch-Polyacrylamide via γ-Irradiation.

3.2.2 Graft Copolymerization of Acrylamide and Maleic Acid onto Cassava Starch by Simultaneous Irradiation

The gelatinized starch was then cooled at room temperature. Twenty grams of acrylamide and 2% maleic acid (by weight of the monomer) were added into the gelatinized starch. The mixture was stirred at 400 rpm at room temperature for 30 minutes. The gelatinized starch-AM/MA mixture was removed into the 250-cm^3 aluminium tube covered the inner wall with aluminium foil, and purged with nitrogen gas for 20 minutes. It was closed tightly with foil and paraffin film, and then irradiated under gamma rays. The reaction product was precipitated with methanol and dried in a vacuum oven at 65°C for 24 hours.

Several important parameters involved gamma-irradiation of cassava starch mixed with AM and MA were studied so as to produce a cassava starch graft copolymer with the highest water absorption capacity. The parameters of which were the following.

3.2.2.1 Effect of Total Dose (kGy) and Dose Rate (kGy h^{-1}) on Graft copolymerization

The mixture was irradiated under gamma rays at various total doses and dose rate as shown in Table 3.2.

Table 3.2 Various Numbers of Total Dose (kGy) and Dose Rate (kGy h^{-1}) for Graft Copolymerization of Acrylamide and Maleic Acid onto Cassava Starch

Dose Rate (kGy h^{-1})	**Total Dose (kGy)**
1.71	0.5
	1.0
	2.0
	4.0
	6.0
	8.0
	10.0
	12.0
4.34	0.5
	1.0
	2.0
	4.0
	6.0
	8.0
	10.0
	12.0

Table 3.2 Various Numbers of Total Dose (kGy) and Dose Rate (kGy h^{-1}) for Graft Copolymerization of Acrylamide and Maleic Acid onto Cassava Starch (continued)

Dose Rate (kGy h^{-1})	**Total Dose (kGy)**
11.0	0.5
	1.0
	2.0
	4.0
	6.0
	8.0
	10.0
	12.0

Thereafter, the effects of total dose (kGy) and dose rate (kGy h^{-1}) on grafting characteristics and water absorption were carried out.

3.2.2.2 Effect of Monomer-to-Starch Ratio on Graft Copolymerization

Various amounts of acrylamide as 10, 15, 20, 25 and 30 g (at each monomer-to-starch ratio 1:1, 1.5:1, 2:1, 2.5:1 and 3:1, respectively) and 2% maleic acid (by weight of the monomer) were added to each of the gelatinized starches. The reaction mixture was irradiated at the optimum total dose (kGy) and dose rate (kGy h^{-1}), which was derived from Section 3.2.2.1. The effect of monomer-to-starch ratio on grafting characteristics and water absorption were determined.

3.2.2.3 Effect of Maleic Acid on Graft Copolymerization

The amounts of maleic acid to be mentioned were added in each batch of gelatinized starch-monomer mixture with the optimum monomer-to-starch ratio (Section 3.2.2.2): 0, 1, 2, 3, 4, 8 and 12% maleic acid (by weight of the monomer). Each batch of reaction mixture was irradiated at optimum total dose (kGy) and dose rate (kGy h^{-1}), which was derived from Section 3.2.2.1 . The effect of the acids on grafting characteristics and water absorption was then evaluated.

3.2.3 Removal of Homopolymer and Free Copolymer.

The dried product (about 10 g) derived from the above sections that was ground previously into a powder form was stirred in 1,500 cm^3 distilled water at room temperature for 24 hours. The mixture was centrifuged to separate the graft copolymer which was washed with distilled water and centrifuged to allow another separation of grafted copolymer. Then it was precipitated with methanol, dried in the vacuum oven at 65°C for 24 hours and weighed to determine the amount of the homopolymer and free copolymer.

3.2.4 Saponification of the Graft Copolymer

Into a 500-cm^3 reactor, 5 g of graft copolymer was mixed with 125 cm^3 of 5% potassium hydroxide solution. The mixture was stirred with a mechanical stirrer at 400 rpm and the reaction was carried out at room temperature for 90 minutes. The reaction product was washed until pH 7 was reached and precipitated with methanol. It was dried at 65°C in a vacuum oven for 24 hours. The dried product was ground into a powder form.

3.2.4.1 Determination of Optimum Time and Temperature for saponification of Acrylamide and Maleic Acid Moieties.

To achieve the optimum time and temperature for saponification which could give the product with the highest water absorption value, the starch-*g*-polyacrylamide/maleic acid (2% w w^{-1}) sample prepared by a dose rate of 1.71 kGy h^{-1} to the total dose of 6.0 kGy was saponified with 5% potassium hydroxide solution for various periods of time and temperatures as follows.

1) A series of reaction time of 30, 60 and 90 minutes was used for the saponification.

2) A series of temperature of room temperature, 50 and 75°C was used for the saponification.

Saponified starch-*g*-polyacrylamide/maleic acid samples were subjected to determination of the amount of nitrogen by elemental analysis. They were characterized by pyrolysis in high purity oxygen (a static-state oxidation), separated by the frontal analysis in a gas chromatography and quantitatively detected by a thermal conductivity detector (CHNS/O analyzer, Perkin Elmer PE 2400 Series II). The optimum saponification time and temperature found was then used for further saponification of the other products.

3.2.5 Characterization of Copolymer

3.2.5.1 Existence of Functionalities by IR Spectroscopy

The infrared spectra of cassava starch, graft copolymer, and saponified graft copolymer were measured by IR spectroscopy on an FT-IR spectrophotometer using a KBr pellet.

3.2.5.2 Determination of percentage conversion

The experimental procedures described in the above section were carried out. The weight of the graft copolymer along with homopolymer was regarded as the total amount of polymer obtained from the weight of monomer charged. Percentage conversion was subsequently calculated.

3.2.5.3 Determination of percentage Gel Content

One gram of the dried products derived from Section 3.2.2 were extracted by water in a Soxhlet extractor for 24 hours. Then the gels were precipitated with methanol, dried to a constant weight in the vacuum oven at 65^{o}C for 24 hours and weighed to determine the amount of the gel content

3.2.5.4 Determination of Percentage Homopolymer and Free Copolymer

The weights obtained from Section 3.2.3 were the amount of free polyacrylamide and copolymer produced as by-products, which were then calculated.

3.2.5.5 Determination of Percentage Add-on

In a 500-cm^3 flat bottom flask equipped with a condenser, 1.0 g of the graft copolymer was stirred in 250 cm^3 of 1.5 *M* HCl and the mixture was refluxed for 2 hours. The polymer was filtered and it was then washed with methanol until pH 7 of the washed solution was reached and then the polymer was dried.

To observe the completion of reaction, the residue starch (substrate) after acid hydrolysis was checked with iodine solution.

The weight percentages of polyacrylamide in the graft copolymer or the so called "percentage add-on" were computed from the weight difference between the graft copolymer and soluble starch, which was removed by the acid hydrolysis.

3.2.5.6 Determination of Percentage Grafting Efficiency

The experimental procedures of Sections 3.2.1-3.2.3 and 3.2.5.5 were carried out with the grafted product. The percentage of total synthetic polymer formed that had been grafted to starch or the 50 called "percentage grafting efficiency" was computed.

3.2.5.7 Determination of surface Morphology of the Copolymers

The surface morphology of the copolymers was investigated using a scanning electron microscope (SEM), model JSM-T 220 A JEOL without cross-section. The thickness of gold coated on the copolymer was 25 nm and SEM was operated with a 15 or 20 kV accelerating voltage.

3.2.6 Water Absorption/Retention Capacities of the Copolymer

3.2.6.1 In Distilled Water

One hundred and fifty gram of distilled water was added to 0.05 g of dried and saponified graft copolymer in a 250-cm^3 glass beaker and allowed to stand for 30 minutes for swelling. The fully swollen polymer was filtered through a 100-mesh aluminium screen for 3 hours and the drained water was weighted. The amount of water retained by the saponified graft copolymer was calculated as in gram per gram of the dry modified starch.

3.2.6.2 In Sodium Chloride, Magnesium Chloride, and Calcium Chloride Solutions

The same experimental procedure as described in Section 3.2.6.1 was carried out, except that a series of sodium chloride, magnesium chloride, and calcium chloride solutions of 0.9% w v^{-1} was used instead of distilled water.

3.2.6.3 In Buffer Solutions

The same experimental procedure as described in Section 3.2.6.1 was carried out, except that a series of buffer solutions ranging from pH 3 to 11 was used instead of distilled water. The buffer solutions of pH 3 to 11 were prepared from mixing of 0.20 *M* boric acid, 0.05 *M* citric acid, and 0.10 *M* tri-sodium phosphate [34].

3.2.6.4 Effect of Particle Size on Water Absorption

The same experimental procedure as described in Section 3.2.6.1 was carried out, except that a series of dried and saponified graft copolymer of particle sizes ranging from 30 to 100 mesh was used for determining the water absorption.

3.2.7 Water Absorption Under Load of The Copolymer (AUL)

The test apparatus consists of a plastic cylinder, 2.6 cm inside diameter, with 100-mesh wire cloth fastened across the bottom of the cylinder. A piece of filter paper is placed on a wire net to ensure good contact of the liquid with the polymer.

A sample of saponified graft copolymer is screened to the desired particle size, typically 30-50 mesh. A 0.1 gram sample of saponified graft copolymer is loaded into the plastic cell so that it is uniformly distributed over the screen. At the atmosphere the pressure is 101.32 kPa, different addition weights (typically 54, 108, 162, 216 and 270 g for 1, 2, 3, 4 and 5 kPa loads, respectively) are placed on top of the sample. The level of the liquid to be absorbed is adjusted to the height of the wire cloth and the water is sucked into the polymer layer. The amount (in grams) of fluid picked up after 60 minutes, divided by the weight of the sample is the AUL value in grams of fluid picked up per gram of sample (g g^{-1}) [35].

Part II: Effect of Acid Additives on Grafting Efficiency and Water Absorption of Cassava Starch-Polyacrylamide/acrylic acid via γ-Irradiation.

3.2.8 Graft Copolymerization of Acrylamide and Acrylic Acid onto Cassava Starch by Simultaneous Irradiation.

Twenty grams of monomer mixture (10 g of AM and 10 g of AA) were added into the gelatinized starch. The mixture was stirred at 400 rpm at room temperature for 30 minutes. The gelatinized starch-AM/AA mixture was removed into the 250-cm^3 aluminium tube covered the inner wall with aluminium foil, and purged with nitrogen gas for 20 minutes. It was closed tightly with foil and paraffin film, and then irradiated under gamma rays at a dose rate 1.71 kGy h^{-1} and a total dose 6.0 kGy [33]. The reaction product was precipitated with acetone and dried in a vacuum oven at 56°C for 24 hours.

In the case of graft copolymerization of acrylamide or acrylic acid onto cassava starch, twenty grams of acrylamide or acrylic acid was used instead of the monomer mixture.

3.2.8.1 Effect of Acid Additives on Graft Copolymerization.

The amounts of acids to be mentioned were added in each batch of gelatinized starch-monomer mixture: 10 cm^3 of 0.001, 0.01 and 0.1 *M* H_2SO_4, 0.01 *M* HNO_3 and 1, 2 and 3% maleic acid. Each batch of reaction mixture was irradiated at the dose rate 1.71 kGy h^{-1} and the dose rate 6.0 kGy. The effect of the additives on grafting characteristics and water absorption was then evaluated.

3.2.9 Removal of Homopolymer and Free Copolymer.

In the case of starch-*g*-polyacrylamide and starch-*g*-poly(acrylamide-*co*-acrylic acid), the same experimental procedure as described in Section 3.2.3 was carried out, except that it was precipitated with acetone, dried in the vacuum oven at 56°C for 24 hours and it was weighed later to determine the amount of the homopolymer and free copolymer.

In the case of starch-*g*-poly(acrylic acid), the dried product (about 9 g) derived from the above sections, ground previously into a powder form, was extracted in 1,000-cm^3 methanol by a Soxhlet extractor at 65°C for 24 hours. The extracted product was dried in a vacuum oven at 65°C for 24 hours and weighed to determine the amount of the homopolymer.

3.2.10 Saponification of the Graft Copolymer.

The graft copolymer (5 g) was mixed with 125 cm^3 of 5% potassium hydroxide solution. The mixture was stirred with a mechanical stirrer at 400 rpm and the reaction was carried out at room temperature for 30 minutes [33]. The reaction product was washed until pH 7 was reached and precipitated with methanol. Then it was dried at 65°C in a vacuum oven for 24 hours and ground into a powder form.

3.2.11 Characterization of Copolymer.

3.2.11.1 Existence of Functionalities by IR Spectroscopy.

The same experimental procedure as described in Section 3.2.5.1 was carried out.

3.2.11.2 Determination of Percentage Conversion.

The same experimental procedure as described in Section 3.2.5.2 was carried out.

3.2.11.3 Determination of Percentage Homopolymer.

The weights obtained from Section 3.2.9 were the amount of free polyacrylamide, poly(acrylic acid) and poly(acrylamide-*co*-acrylic acid) produced as by product, which were then calculated.

3.2.11.4 Determination of Percentage Add-on.

In the case of starch-*g*-polyacrylamide and starch-*g*-poly(acrylamide-*co*-acrylic acid), the same experimental procedure as described in Section 3.2.5.5 was carried out.

In the case of starch-*g*-poly(acrylic acid), determination of percentage add-on was based on Dennenberg and Abbott's method [36]. The graft copolymer (1.0 g) was added to 100-cm^3 glacial acetic acid that was then heated to 90-100 ^oC. The mixture was stirred for 1 hour to swell the grafted side chains. Perchloric acid (65%) of 2 cm^3 was added dropwise, and the reaction was completed within 1-2 minutes. The reaction was cooled to room temperature and centrifuged to separate the poly(acrylic acid) side chain. The polymer was washed with acetone until pH 7 of the washed solution was reached and then it was dried.

3.2.11.5 Determination of Percentage Grafting Efficiency.

The experimental procedure of Sections 3.2.8, 3.2.9 and 3.2.11.4 was carried out with the grafted product. The percentage grafting efficiency was computed.

3.2.11.6 Determination of Surface Morphology of the Copolymers.

The same experimental procedures as described in Section 3.2.5.7 were carried out.

3.2.11.7 Determination of Water Absorption Capacities in Distilled Water

The same experimental procedures as described in Section 3.2.6.1 were carried out.

CHAPTER 4

RESULTS AND DISCUSSION

Part I: Effect of Diprotic Acids on Grafting Efficiency and Water Absorption of Cassava Starch-Polyacrylamide via γ-Irradiation.

4.1 Characterization the Functional Groups of the Copolymer by FTIR.

FT-IR technique was used to follow up changes in graft copolymerization. The FT-IR spectra of cassava starch, and the graft copolymer before extraction, after extraction, and after saponification are given in Tables 4.1-4.2 and Figures 4.1-4.7 .

The infrared absorption of cassava starch in Figure 4.1 gives the broad peak of O – H stretching at 3,397 cm^{-1}, the weak peak of C – H stretching at 2,929 cm^{-1}, the weak peak of C – H bending at 1,455 cm^{-1}, the weak peak of O – H bending at 1,366 and 1,421 cm^{-1}, and the strong peak of C – O stretching at 1,017 cm^{-1}.

The IR spectra of polyacrylamide grafted onto the starch backbone (starch-*g*-polyacrylamide) before and after extraction are shown in Figures 4.2-4.4. All the characteristic absorption peaks of cassava starch still exist. Additional broad peak at 3,192 cm^{-1}, sharp peak at 1,664 cm^{-1}, weak peak at 1,611 cm^{-1} and weak peak at 1,325 and 1,354 cm^{-1} indicate the N – H stretching, C = O stretching of carboxamide, N – H bending and C – N stretching, respectively which are the characteristics of the -$CONH_2$ group containing in the acrylamide. When the starch-*g*-polyacrylamide was saponified for 90 minutes, the additional weak peak at 1,558

cm^{-1} indicates the C = O stretching, which is the characteristic of the carboxylate group.

For the IR spectra of starch-*g*-poly(acrylamide-*co*-maleic acid) in both before and after extraction (Figures 4.5-4.6) give all the absorption peaks of cassava starch and acrylamide. The additional weak peak at 2,786 cm^{-1}, strong peak at 1,664 cm^{-1}, weak peak at 1,206 cm^{-1} and weak peak at 937 cm^{-1} are for the O – H stretching, C = O stretching, C – O stretching and O – H bending of -COOH group containing in maleic acid, respectively. When starch-*g*-poly(acrylamide-*co*-maleic acid) was saponified, the stronger peak at 1,383 cm^{-1} of C = O stretching of the carboxylate ion indicates that acrylamide and maleic acid moieties have been converted to acrylate group (Figure 4.7)

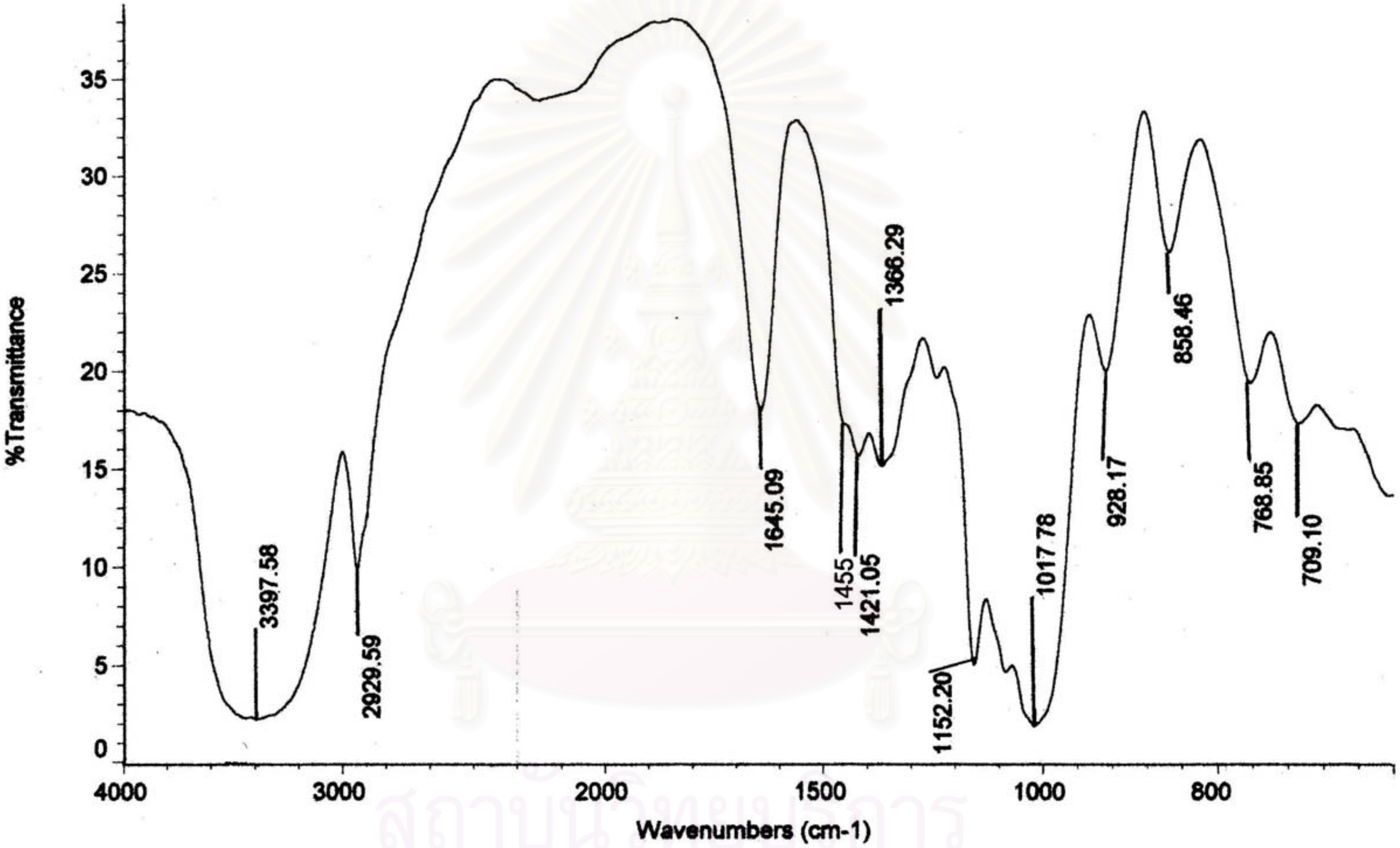

Figure 4.1 Infrared spectrum of cassava starch.

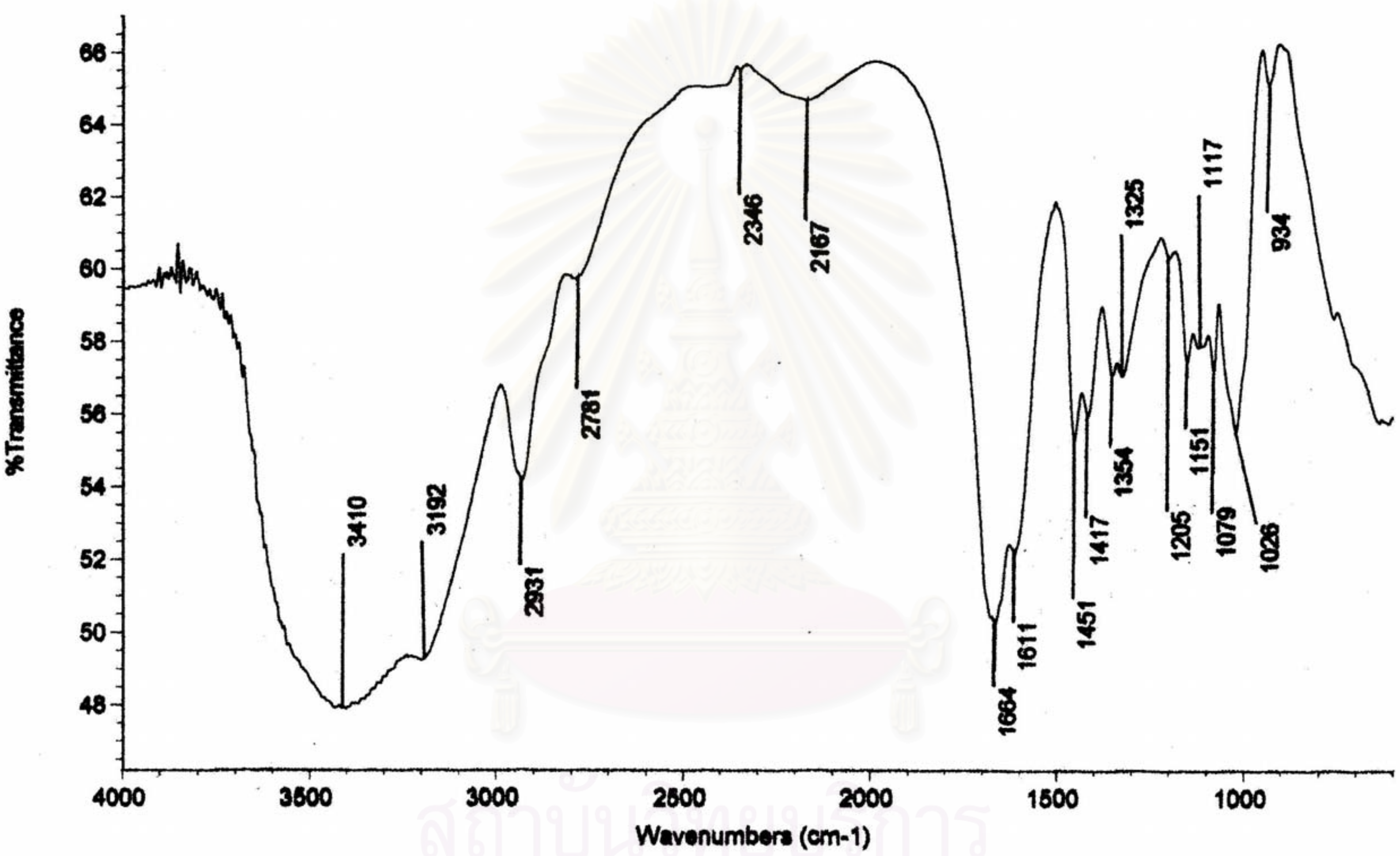

Figure 4.2 Infrared spectrum of the starch-g-polyacrylamide before extraction.

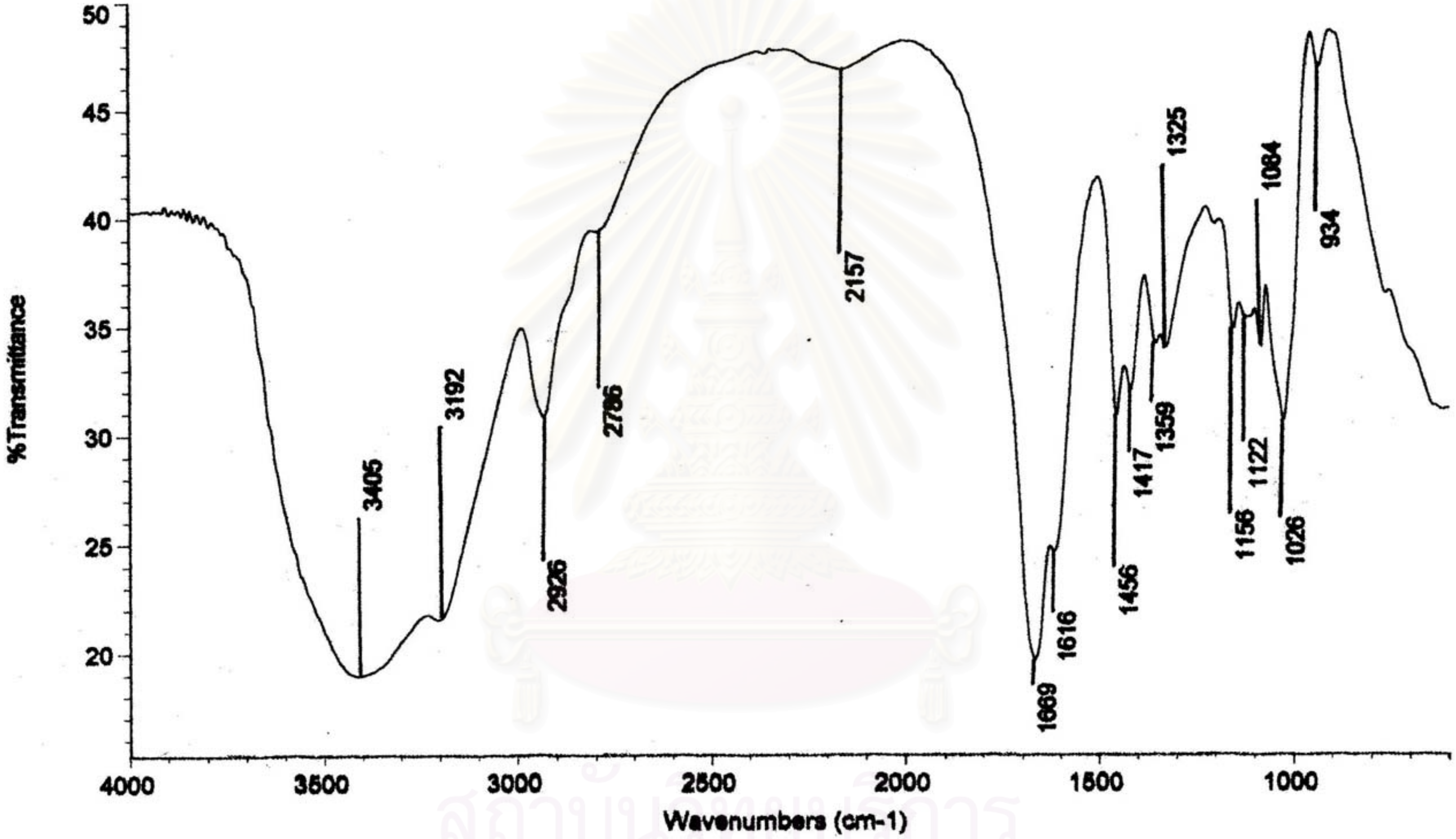

Figure 4.3 Infrared spectrum of the starch-g-polyacrylamide after extraction.

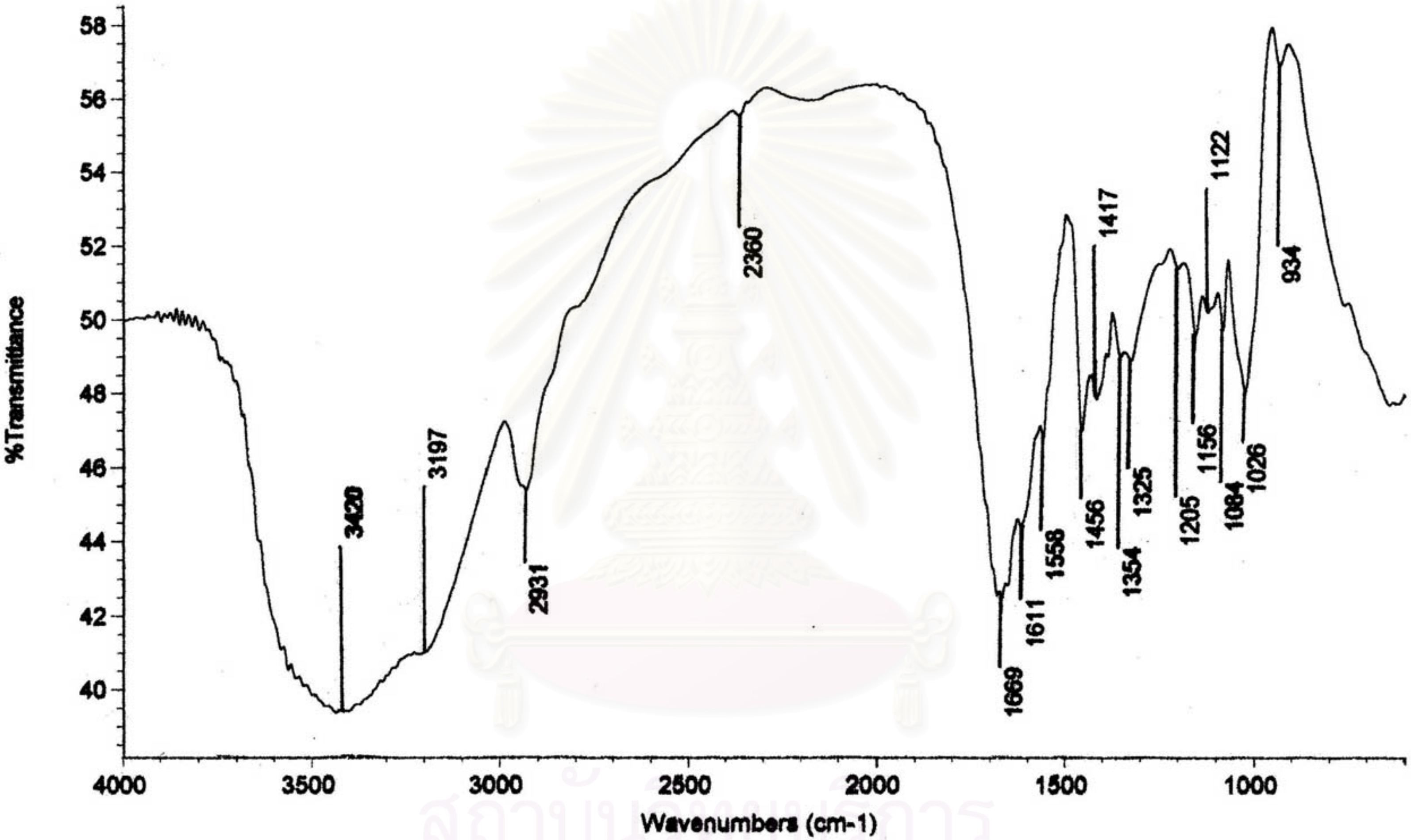

Figure 4.4 Infrared spectrum of the starch-g-polyacrylamide after saponification.

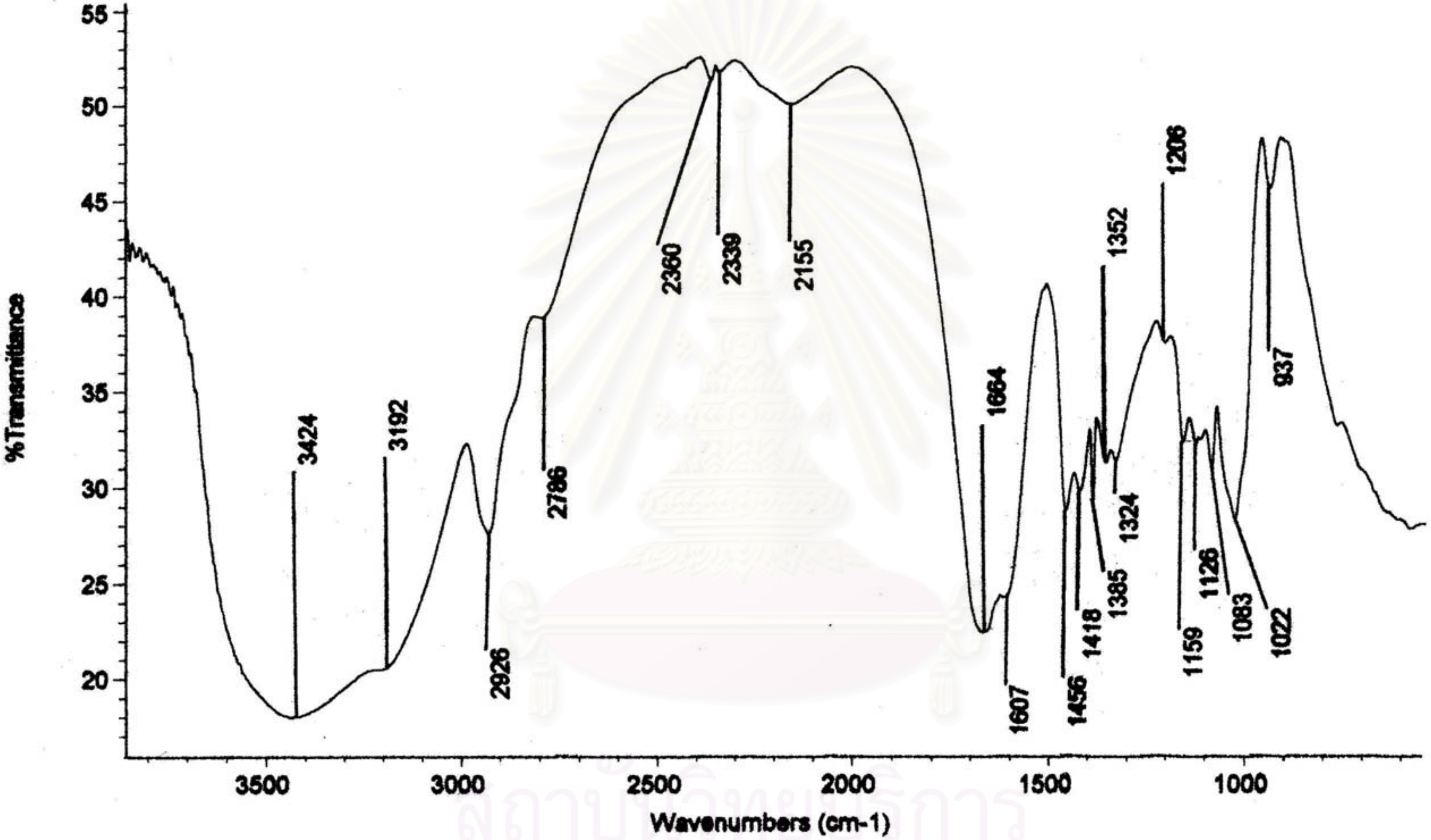

Figure 4.5 Infrared spectrum of the starch-g-poly(acrylamide-co- maleic acid) before extraction.

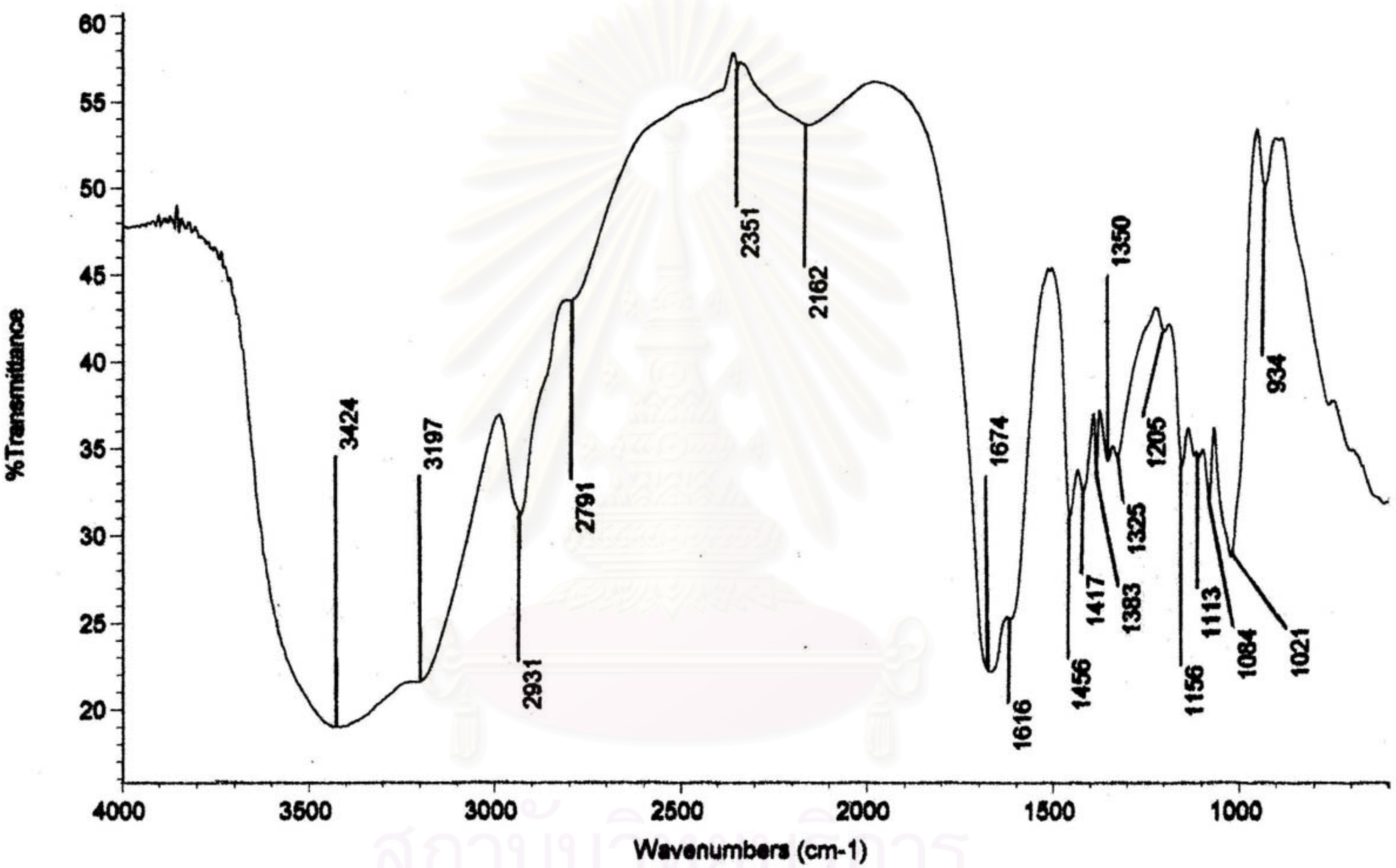

Figure 4.6 Infrared spectrum of the starch-g-poly(acrylamide-co-maleic acid) after extraction.

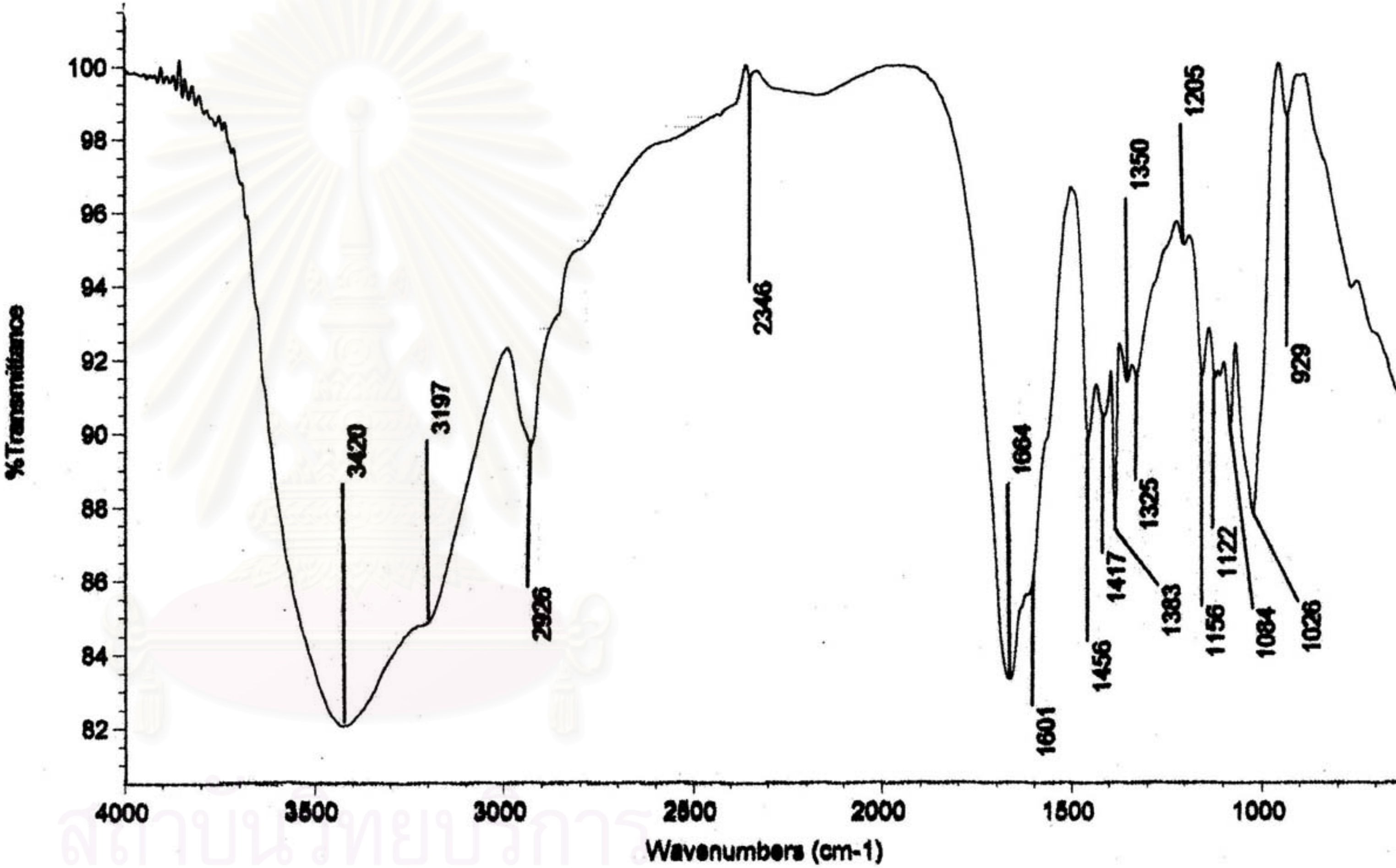

Figure 4.7 Infrared spectrum of the starch-g-poly(acrylamide-co-maleic acid) after saponification.

Table 4.1 The Infrared Absorption of Functional Groups in Cassava Starch and Starch-*g*- polyacrylamide Before Extraction, After Extraction, and After Saponification.

Starch		Starch-*g*-polyacrylamide before extraction		Starch-*g*-polyacrylamide after extraction		Starch-*g*-polyacrylamide after saponification	
wave number (cm^{-1})	assignment	wave number (cm^{-1})	assignment	wave number (cm^{-1})	assignment	wave number (cm^{-1})	assignment
3,397	O – H stretching	3,410	O – H stretching	3,405	O – H stretching	3,420	O – H stretching
2,929	C – H stretching of CH$_2$	2,931	C – H stretching of CH$_2$	2,926	C – H stretching of CH$_2$	2,931	C – H stretching of CH$_2$
1,455	C – H bending of CH$_2$	1,451	C – H bending of CH$_2$	1,456	C – H bending of CH$_2$	1,456	C – H bending of CH$_2$
1,366 and 1,421	O – H bending	1,417	O – H bending	1,417	O – H bending	1,417	O – H bending
1,017	C – O stretching	1,026	C – O stretching	1,026	C – O stretching	1,026	C – O stretching
		3,192	N – H stretching	3,192	N – H stretching	3,197	N – H stretching
		1,664	C = O stretching of carboxamide	1,669	C = O stretching of carboxamide	1,669	C = O stretching of carboxamide
		1,611	N – H bending	1,616	N – H bending	1,611	N – H bending
		1,325 and 1,354	C – N stretching	1,325 and 1,359	C – N stretching	1,325 and 1,354	C – N stretching
						1,558	C = O stretching of carboxylate

Table 4.2 The Infrared Absorption of Functional Groups in Cassava Starch and Starch-*g*-poly(acrylamide-*co*-maleic acid) Before Extraction, After Extraction, and After Saponification.

Starch		**Starch-*g*-poly(acrylamide-*co*-maleic acid) before extraction**		**Starch-*g*-poly(acrylamide-*co*-maleic acid) after extraction**		**Starch-*g*-poly(acrylamide-*co*-maleic acid) after saponification**	
wave number (cm^{-1})	assignment	wave number (cm^{-1})	assignment	wave number (cm^{-1})	assignment	wave number (cm^{-1})	assignment
3,397	O – H stretching	3,424	O – H stretching	3,424	O – H stretching	3,420	O – H stretching
2,929	C – H stretching of CH_2	2,926	C – H stretching of CH_2	2,931	C – H stretching of CH_2	2,926	C – H stretching of CH_2
1,455	C – H bending of CH_2	1,456	C – H bending of CH_2	1,456	C – H bending of CH_2	1,456	C – H bending of CH_2
1,366 and 1,421	O – H bending	1,418	O – H bending	1,417	O – H bending	1,417	O – H bending
1,017	C – O stretching	1,022	C – O stretching	1,021	C – O stretching	1,026	C – O stretching
		3,192	N – H stretching	3,197	N – H stretching	3,197	N – H stretching
		1,664	C = O stretching of carboxamide	1,674	C = O stretching of carboxamide	1,664	C = O stretching of carboxamide
		1,607	N – H bending	1,616	N – H bending	1,601	N – H bending
		1,324 and 1,352	C – N stretching	1,325 and 1,350	C – N stretching	1,325 and 1,350	C – N stretching

Table 4.2 The Infrared Absorption of Functional Groups in Cassava Starch and Starch-*g*-poly(acrylamide-*co*-maleic acid) Before Extraction, After Extraction, and After Saponification(continued).

Starch		**Starch-*g*-poly(acrylamide-*co*-maleic acid) before extraction**		**Starch-*g*-poly(acrylamide-*co*-maleic acid) after extraction**		**Starch-*g*-poly(acrylamide-*co*-maleic acid) after saponification**	
wave number (cm^{-1})	assignment	wave number (cm^{-1})	assignment	wave number (cm^{-1})	assignment	wave number (cm^{-1})	assignment
		2,,786	O – H stretching of carboxylic acid	2,791	O – H stretching of carboxylic acid	2,791	O – H stretching of carboxylic acid
		1664	C = O stretching of carboxylic acid	1,674	C = O stretching of carboxylic acid	1,664	C = O stretching of carboxylic acid
		1,206 and 1,385	C – O stretching of carboxylic acid	1,205 and 1,383	C – O stretching of carboxylic acid	1,205 and 1,383	C – O stretching of carboxylic acid
		937	O – H bending of carboxylic acid	934	O – H bending of carboxylic acid	929	O – H bending of carboxylic acid
						stronger 1,383	C = O stretching of carboxylate

4.2 Effect of Saponification Time and Temperature on Acrylamide and Maleic Acid Moiety.

The degree of saponification depends on reaction time, temperature, and concentration of alkaline solution [37]. The degree of saponification of starch-g-poly(acrylamide-co-maleic acid) prepared at the dose rate 1.71 kGy h^{-1} and the total dose 6.0 kGy with 5% potassium hydroxide solution for various periods of time and temperature is presented in terms of the nitrogen content and water absorption capacity as shown in Table 4.3

Table 4.3 Effect of Reaction Time and Temperature on Degree of Saponification and Water Absorption.

Period of time and temperature for saponification	Composition of the elements (%)			WA ($g\ g^{-1}$)
	C	H	N	
Unsaponified sample	43.956	5.178	11.922	81 ± 6
Room temperature, 30 min.	42.855	6.526	10.780	592 ± 30
Room temperature, 60 min.	41.420	6.055	9.629	1,057 ± 21
Room temperature, 90 min.	41.194	6.405	9.251	1,216 ± 14
50°C , 30 min.	37.206	5.691	6.153	934 ± 54
50°C , 60 min.	37.902	5.692	5.935	946 ± 12
50°C , 90 min.	38.003	5.391	5.899	972 ± 28
75°C , 30 min.	36.434	5.620	4.905	960 ± 10
75°C , 60 min.	36.664	5.607	4.723	1,296 ± 41
75°C , 90 min.	36.879	5.519	4.579	1,159 ± 19

4.2.1 Relationship between Time and Degree of Saponification.

Table 4.3 shows a continuous increase in the degree of saponification as the saponification time increases. The longer the saponification time, the more the amide groups on the poly(acrylamide-*co*-maleic acid) chains change to the carboxylate groups through the following chemical reaction (eq. 4.1)

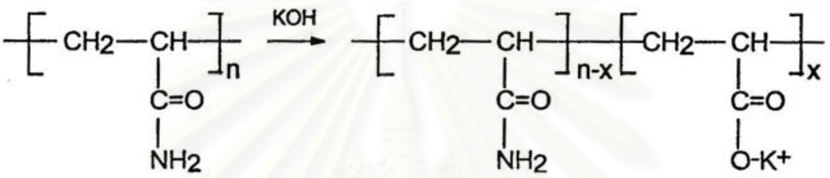

$$\left[CH_2-\underset{\underset{NH_2}{|}}{\underset{C=O}{\underset{|}{CH}}}\right]_n \xrightarrow{KOH} \left[CH_2-\underset{\underset{NH_2}{|}}{\underset{C=O}{\underset{|}{CH}}}\right]_{n-x}\left[CH_2-\underset{\underset{O^-K^+}{|}}{\underset{C=O}{\underset{|}{CH}}}\right]_x \qquad (4.1)$$

4.2.2 Relationship between Temperature and Degree of Saponification.

The experimental data for the effect of temperature on the degree of saponification of poly(acrylamide-*co*-maleic acid) are also given in Table 4.3. Poly(acrylamide-*co*-maleic acid) undergoes an extensive saponification at higher temperature.

4.2.3 Relationship between Degree of Saponification and Water Absorption.

From Table 4.3, the water absorption increases with increasing of the degree of saponification up to at which the nitrogen content is 9.25% at the reaction time of 90 minutes at room temperature. Thereafter, water absorption was not increased until the percentage nitrogen content was 4.7%. At this condition of saponification, water absorption is as high as 1296 $\pm$ 41 g g^{-1} of its dried weight at the reaction time of 60 minutes at 75°C.

To save the energy, ninety minutes at room temperature saponification is an optimum condition to convert acrylamide and maleic acid moieties to acrylate salt, which give the highest water absorption.

At low degrees of saponification, the number of carboxyl groups is very low and randomly distributed: any hydrogen bonds formed will be unable to sustain a stable intramolecular complex. At a higher degree of saponification, an increase in the number of acid groups on the acrylamide chain will enhance intramolecular bonding between the amide and acid groups of the same molecule. The decrease of water absorption can be attributed to the decreased mobility of the saponified poly(acrylamide-*co*-maleic acid) chains due to such intramolecular hydrogen bonding [38].

4.3 Graft Copolymerization of Acrylamide and Maleic Acid onto Cassava Starch by Simultaneous Irradiation.

4.3.1 Effect of Total Dose and Dose Rate on Graft Copolymerization.

The effects of total dose and dose rate on the grafting of AM and MA onto cassava starch are presented in terms of the conversion of monomer, gel content, homopolymer and free copolymer formed, grafting efficiency, percentage add-on, and water absorption as shown in Table 4.4

Table 4.4 Effect of Total Dose and Dose Rate on the Graft Copolymerization of Acrylamide and Maleic Acid onto Cassava Starch

DR (kGy h^{-1})	TD (kGy)	Conv (%)	Gel (%)	Homo (%)	Add-on (%)	GE (%)	WA (g g^{-1})
1.71	0.5	80.8	55.7	77.7	40.9	10.5	808±7
	1.0	90.8	65.8	66.7	49.9	19.9	866±11
	2.0	96.6	69.3	48.4	54.6	36.8	1877±16
	4.0	97.7	77.3	30.8	60.5	57.6	2026±18
	6.0	98.7	78.9	22.9	60.8	67.2	1216±14
	8.0	99.9	81.2	17.8	61.9	74.1	645±5
	10.0	98.4	82.3	16.0	63.2	76.8	661±18
	12.0	98.5	87.1	14.9	67.9	79.5	620±37
4.34	0.5	68.4	28.7	82.1	26.6	5.4	718±13
	1.0	86.5	42.2	79.4	31.6	7.6	748±6
	2.0	89.8	52.8	70.8	36.6	13.0	1059±9
	4.0	93.0	67.6	45.2	51.3	38.3	1229±9
	6.0	94.4	68.0	29.7	58.0	57.9	1357±7
	8.0	96.1	75.7	24.7	59.7	64.6	1123±10
	10.0	96.5	76.6	21.4	62.2	69.6	941±17
	12.0	97.4	81.5	18.7	59.1	72.0	857±7

DR = Dose Rate; TD = Total Dose; Conv = Conversion; Gel = Gel Content; Homo = Homopolymer; GE = Grafting Efficiency; WA = Water Absorption; AM-to-Starch ratio = 2 : 1; MA = 2% w w^{-1} of the acrylamide monomer

Table 4.4 Effect of Total Dose and Dose Rate on the Graft Copolymerization of Acrylamide and Maleic Acid onto Cassava Starch (continued)

DR (kGy h^{-1})	TD (kGy)	Conv (%)	Gel (%)	Homo (%)	Add-on (%)	GE (%)	WA (g g^{-1})
11.0	0.5	56.3	27.8	88.5	26.7	3.4	608±7
	1.0	75.6	32.9	83.8	30.1	5.5	667±5
	2.0	84.2	45.3	79.0	34.1	8.4	1071±47
	4.0	91.9	45.8	73.9	38.8	12.0	1249±39
	6.0	94.6	47.8	57.6	45.6	25.1	1540±22
	8.0	95.8	59.3	47.3	51.5	36.4	1887±9
	10.0	96.6	62.3	43.1	54.3	41.8	1700±17
	12.0	97.5	64.9	36.4	58.0	50.3	1690±24

DR = Dose Rate; TD = Total Dose; Conv = Conversion; Gel = Gel Content; Homo = Homopolymer; GE = Grafting Efficiency; WA = Water Absorption; AM-to-Starch ratio = 2 : 1; MA = 2% w w^{-1} of the acrylamide monomer

4.3.1.1 Relationship between Total Dose, Dose Rate and Percentage Conversion.

Table 4.4 and Figure 4.8 illustrate the conversion of monomer as a function of total dose and dose rate of graft copolymerization of AM and MA onto starch. We found that graft copolymerization of AM and MA onto starch at the dose rate of 1.71 kGy h^{-1}, the conversion of monomer increases with increasing the amounts of total irradiation dose up to 8 kGy. Higher than 8 kGy, the conversion of the monomer decreases. However, in the case of graft copolymerization of AM and MA onto starch at the dose rate of 4.34 and 11.0 kGy h^{-1}, the percentage conversion increases with increasing in the total dose. An increase in the total dose enhances the formation of radicals in the reaction mixture: monomer, starch, and water. All molecules are activated to induce a higher conversion for both homopolymer formation and the grafting reaction. However when the amounts of total dose are higher than 8 kGy at the dose rate of 1.71 kGy h^{-1}, the percentage conversion decreases which may be the chain scission effect of the polymer at a longer reaction time.

Increasing the dose rate reduces the percentage conversion especially at low total dose. Increasing the dose rate is to increase the radical density. At the high radical density, radical recombination can probably occur. This deteriorates the conversion of monomer. In addition, the effect of high dose rate enhances the degradation of the starch backbones [17].

4.3.1.2 Relationship between Total Dose, Dose Rate and Percentage Gel Content.

Table 4.4 and Figure 4.9 show the effect of total dose and dose rate on percentage gel content. The amount of gel content is related to the crosslink density. Crosslinking of graft copolymer is formed rapidly during the initial period of irradiation and gel content increases with total dose. At the higher total dose, more radicals are generated to produce homopolymer and copolymer. Acrylamide polymers are crosslinked under irradiation. When the rupture of hydrogen or substituent occurs in the chain by the action of radiation, the resultant polymer radicals may react with polymer radicals at adjacent sites on neighboring chain and thus the crosslink of two polymer chains is formed [39].

Increasing the dose rate reduces the percentage gel content. Crosslinking occurs at the lower dose rate of gamma radiation and molecular chain scission at higher dose rate especially in polysaccharides, resulting in a decrease of the crosslinking extent.

4.3.1.3 Relationship between Total Dose, Dose Rate and Percentage Homopolymer.

The correlation between total dose, dose rate, and percentage homopolymer of graft copolymerization of AM and MA onto starch is shown in Table 4.4 and Figure 4.10. It appears that increasing total dose reduces the content of homopolymer, at all dose rates studied, because high total dose can induce ample active sites on the starch backbone for the monomer to be grafted on.

At a fixed total dose, the percentage homopolymer increases when increasing the dose rate because the generation of free radicals is enormously increased accordingly. Recombination of primary radicals into any inert species in the bulk medium are very significant. As a theoretical consequence, at a higher dose rate, there are a great deal of free radicals generated, yet there are only a few free radicals available to start the graft copolymerization. Most radicals undergo recombination or initiate homopolymerization [40]. The lower dose rates which produce a smaller amount of homopolymer may probably suggest a diffusion control mechanism of homopolymer formation as that only a few radicals produced can encounter each other to form a homopolymer.

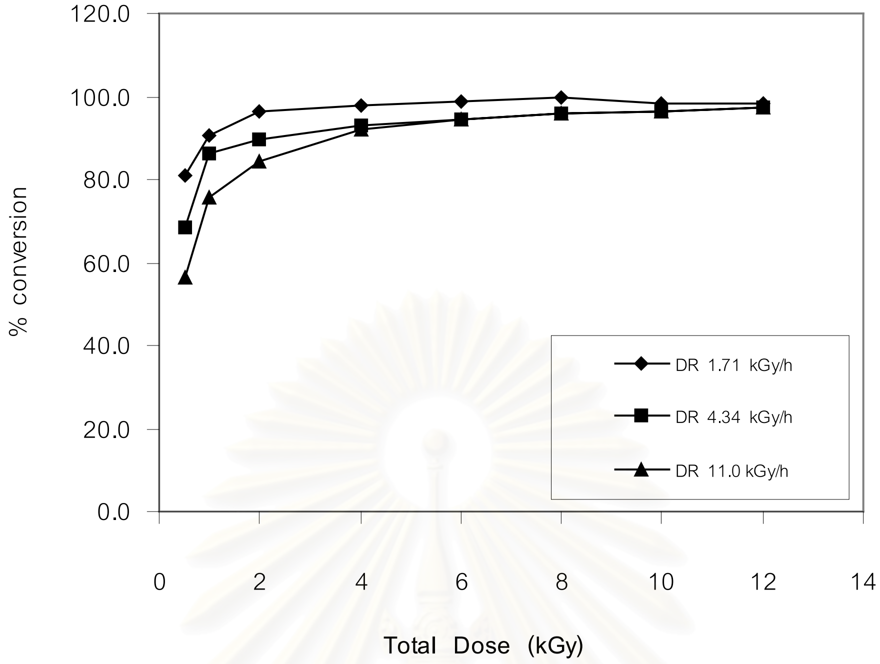

Figure 4.8 Effect of total dose and dose rate on the percentage conversion of graft copolymerization of AM/MA onto starch

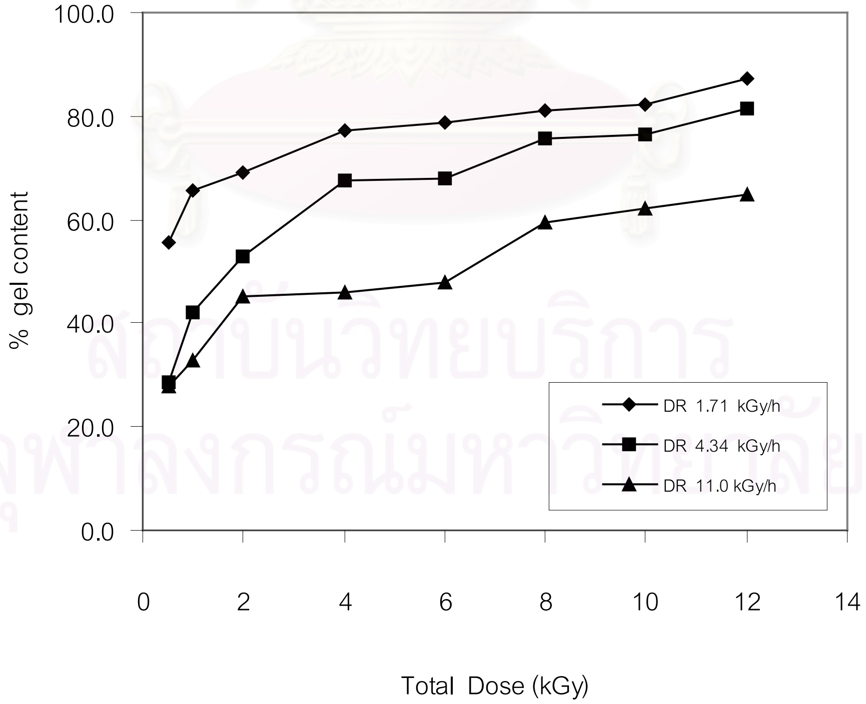

Figure 4.9 Effect of total dose and dose rate on the percentage gel content of graft copolymerization of AM/MA onto starch

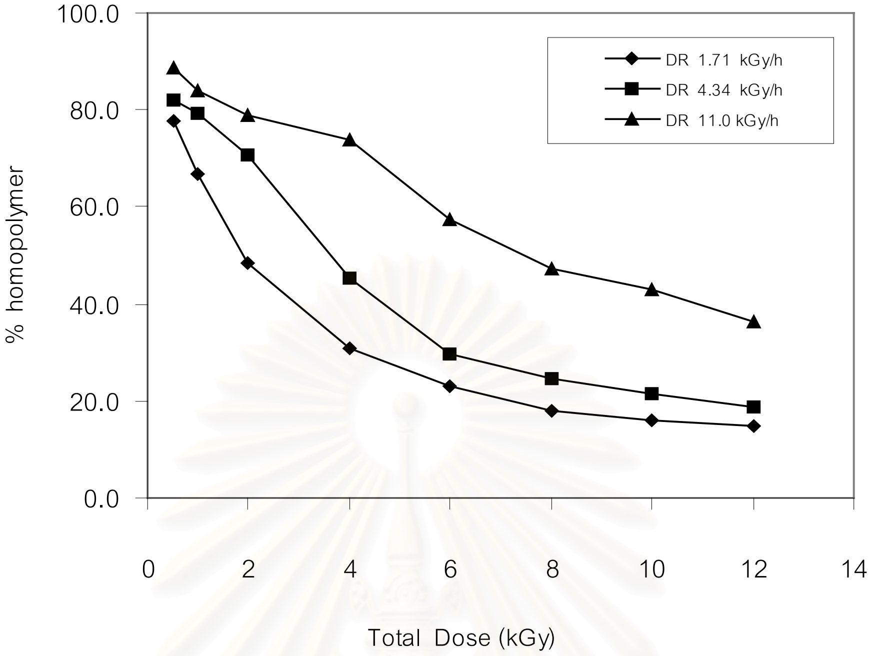

Figure 4.10 Effect of total dose and dose rate on the percentage homopolymer of graft copolymerization of AM/MA onto starch

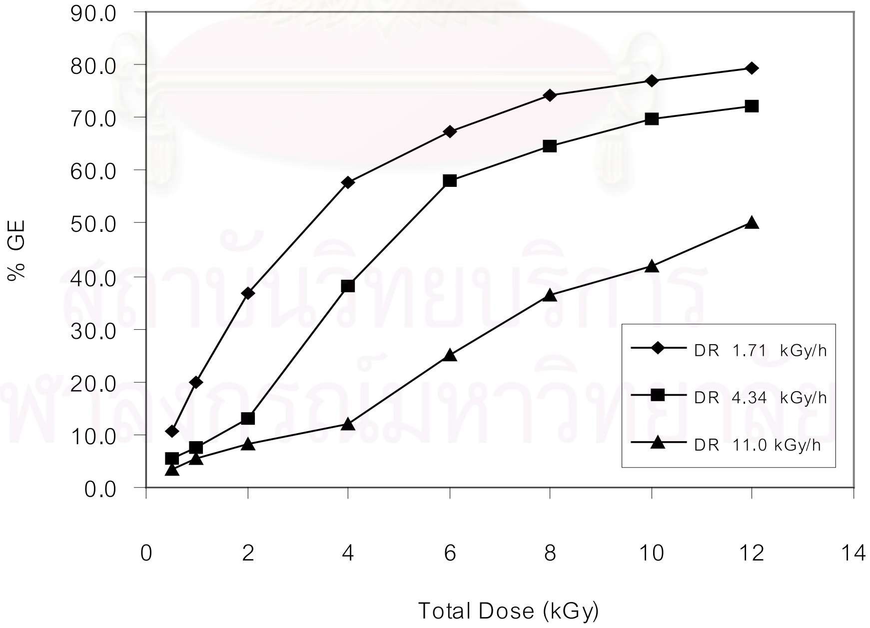

Figure 4.11 Effect of total dose and dose rate on the percentage grafting efficiency of graft copolymerization of AM/MA onto starch

4.3.1.4 Relationship between Total Dose, Dose Rate, and Grafting Efficiency.

The experimental data of the effect of the total dose and dose rate on grafting efficiency of graft copolymerization of AM and MA onto starch are given in Table 4.4 and Figure 4.11. Grafting Efficiency increases with increasing total dose. At higher total dose, there are many active sites on the starch backbone and many monomers can diffuse to graft on the starch backbone.

At a fixed total dose studied, the lower dose rate produces a higher grafting efficiency. It suggests that the monomer molecules and/or radicals are available at all active grafting sites on the starch backbones. The grafting reaction takes place in the accessible regions of the starch and grafting efficiency is therefore enhanced. The grafting efficiency decreases when increasing the dose rate because too high the radicals tend to terminate the active radicals before they can lead to the adequate grafting.

4.3.1.5 Relationship between Total Dose, Dose Rate and Percentage Add-on.

Table 4.4 and Figure 4.12 show the effect of total dose and dose rate on percentage add-on of the graft copolymerization of AM and MA onto starch. The experimental data show a continuous increase in percentage add-on. At a higher irradiation dose, higher radicals generated produced many growing chains to be grafted on a plenty of active sites on the starch backbone. When the total dose higher than 10 kGy at the dose rate of 4.34 kGy h^{-1}, the percentage add-on decreases. It then suggests that the decreasing percentage add-on could be due to the formation of small fragments of $OH^{\bullet}$ and e_{aq}^{-} to form the homopolymer at the expense of grafting reaction.

A declining trend of percentage add-on is found when increasing the dose rates. The small quantity of free radicals produced from a low dose rate is more effective towards a grafting reaction than a homopolymer formation. There are a small number of free radical populations in the aqueous phase to collide among themselves which would, otherwise, result in a greater amount of homopolymer formation. The free radicals are consequently allowed to diffuse to the starch backbones to be grafted on [41].

4.3.1.6 Relationship between Total Dose, Dose Rate and Water Absorption.

Water Absorption in distilled water by the saponified starch-*g*-poly (acrylamide-*co*-maleic acid) is shown in Table 4.4 and Figure 4.13. The total dose and dose rate of gamma rays influence the grafting parameters very significantly. The swelling of these polymers depends on the precise structure of the polymer network and primarily on the cross-link density. High water absorption is affected positively by percentage add-on, grafting efficiency and conversion. Homopolymer formation has a strong negative effect on water absorption. At the total dose of 4 kGy and dose rate of 1.71 kGy h^{-1}, the highest water absorption of saponified product is obtained.

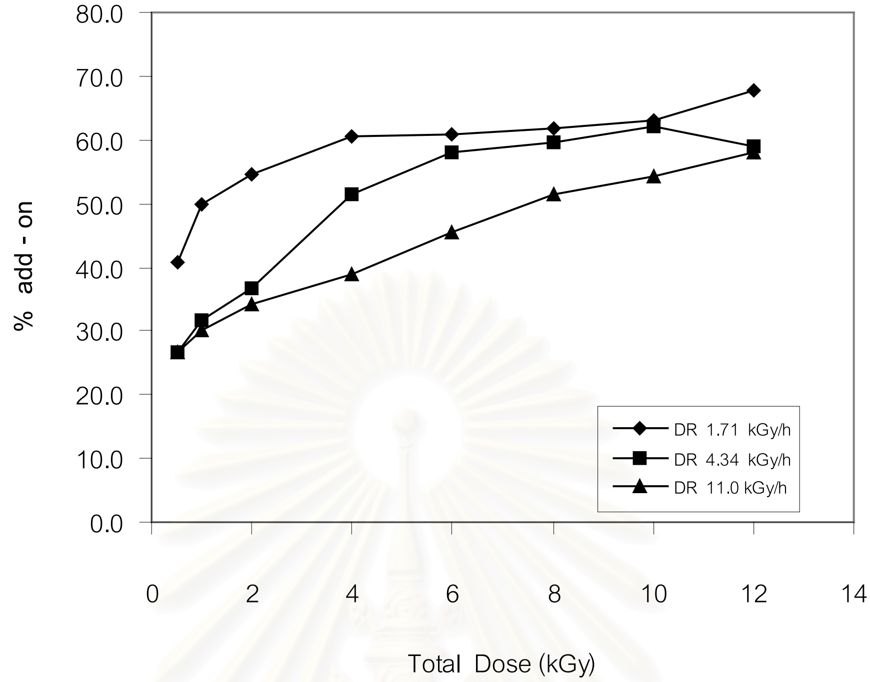

Figure 4.12 Effect of total dose and dose rate on the percentage add-on of graft copolymerization of AM/MA onto starch

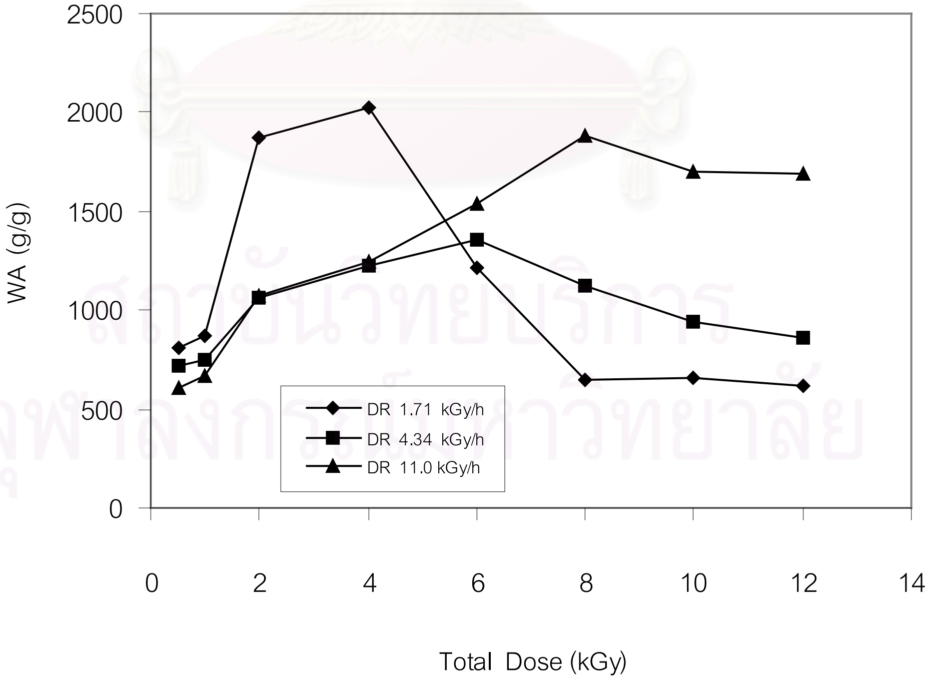

Figure 4.13 Effect of total dose and dose rate on water absorption of graft copolymerization of AM/MA onto starch

4.3.2 Effect of Monomer-to-Starch Ratio on Graft Copolymerization.

The effect of monomer-to-starch ratio on the grafting of AM and MA onto cassava starch is presented in terms of the conversion of monomer, gel content, homopolymer and free copolymer formed, grafting efficiency, percentage add-on, and water absorption as shown in Table 4.5.

Table 4.5 Effect of Monomer-to-Starch Ratio on the Graft Copolymerization of Acrylamide and Maleic Acid onto Cassava Starch

AM:St ratio	**Conv (%)**	**Gel (%)**	**Homo (%)**	**Add-on (%)**	**GE (%)**	**WA ($g\ g^{-1}$)**
1 : 1	80.4	51.0	38.0	32.2	34.5	682±12
1.5 : 1	86.1	57.4	31.3	48.3	51.5	1582±30
2 : 1	97.7	69.3	30.8	60.5	57.6	2026±18
2.5 : 1	96.6	72.5	24.5	63.2	66.1	2256±25
3 : 1	97.9	74.3	22.4	69.6	70.7	2037±21

AM:St = Acrylamide-to-Starch Ratio; Conv = Conversion; Gel = Gel Content; Homo = Homopolymer; GE = Grafting Efficiency; WA = Water Absorption; MA = 2% w w^{-1} of monomer with a dose rate of 1.71 kGy h^{-1}, and a total dose of 4.0 kGy

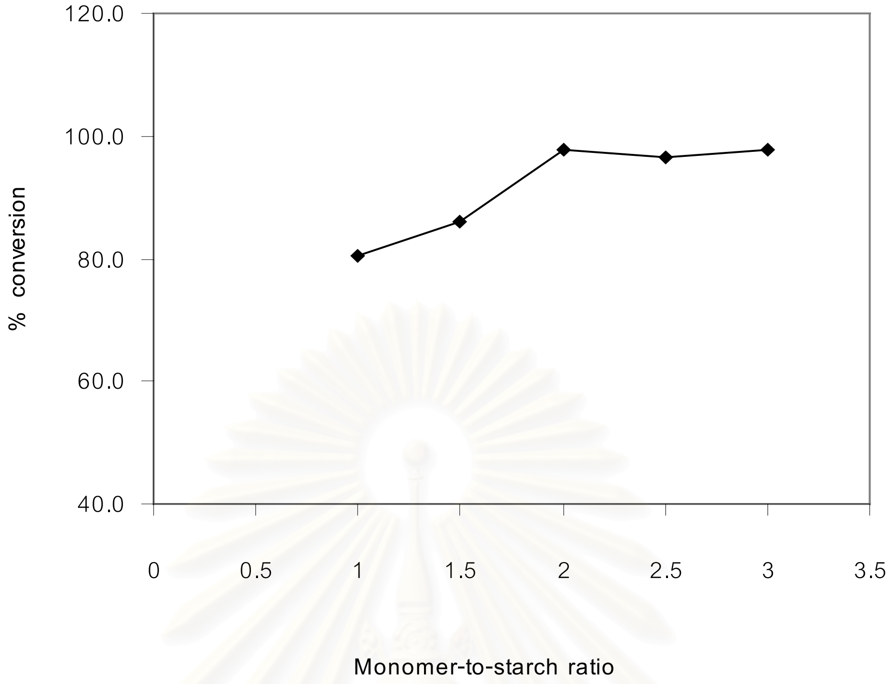

Figure 4.14 Effect of monomer-to-starch ratio on the percentage conversion of graft copolymerization of AM/MA onto starch

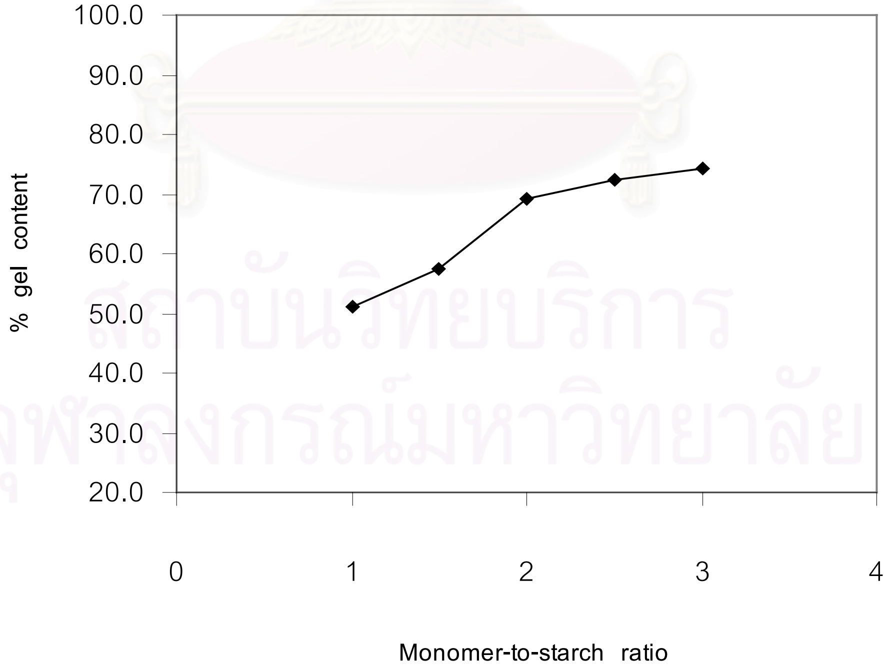

Figure 4.15 Effect of monomer-to-starch ratio on the percentage gel content of graft copolymerization of AM/MA onto starch

4.3.2.1 Relationship between Monomer-to-Starch Ratio and Percentage Conversion.

Table 4.5 and Figure 4.14 show the correlation between the monomer-to-starch ratio and the conversion of monomer. As the quantity of AM monomer increases from 1:1 to 2:1, percentage conversion also increases proportionally to the quantity of the monomer. The percentage conversion does not change as the quantity of the AM increases from 2:1 to 3:1. This is the upper limit of monomer quantity given that can eventually affect polymerizations.

During the irradiation, a temperature rise is detected. The increase in temperature may lead to a broader distribution of primary species and thereby an increase in G_R values of $H^\bullet$, $OH^\bullet$ or e_{aq}^- and a decrease in G_M values of molecular hydrogen, H_2, or H_2O_2 [37]. This result in a higher yield of polymer when higher quantity AM monomer is irradiated.

4.3.2.2 Relationship between Monomer-to-Starch Ratio and Percentage Gel Content.

Table 4.5 and Figure 4.15 shows that the percentage gel content increases with increasing monomer-to-starch ratio. At the higher quantity of AM, the number of reactive sites for a crosslink formation is greater, thus giving a higher amount of gel fraction. This due to the occurrence of imidization that usually takes place in the polymerization of acrylamide in concentrated solution and at high temperature or very long reaction times. Imidization is accelerated by strong acids [42]. The imidization of the amide pendants in the copolymer is shown in Equation 4.2.

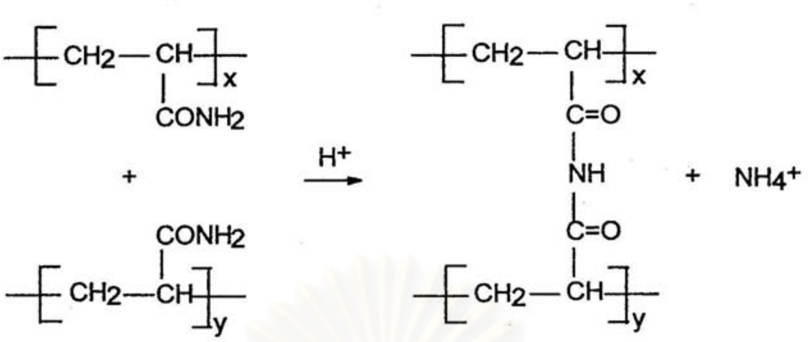

(4.2)

In addition, the chain transfer to polymer increases with monomer concentration, especially at high extent of conversion, and this results in increasing amounts of branching and self-crosslinking reactions.

4.3.2.3 Relationship between Monomer-to-Starch Ratio and Percentage Homopolymer.

The correlation between the monomer-to-starch ratio and percentage homopolymer of graft copolymerization of AM and MA onto starch is shown in Table 4.5 and Figure 4.16. It appears that the percentage of homopolymer formed decreases with increasing monomer-to-starch ratio. At the lower monomer mixture concentration, a small number of monomers can diffuse to graft on the starch backbone. Most of the monomers are used for homopolymer formation through collision due to the viscous grafting substrate. At a high monomer-to-starch ratio, the percentage homopolymer may not be correctly determined simply by extraction because cross-linked or interentangled high molecular weight homopolymers remained in the starch. It is anticipated that a semi-interpenetrating polymer network could be formed, either chemically or physically with cassava starch, at the higher ratios of monomer to starch. Homopolymers of PAM along with ungrafted, free copolymer of AM/MA could be formed [33].

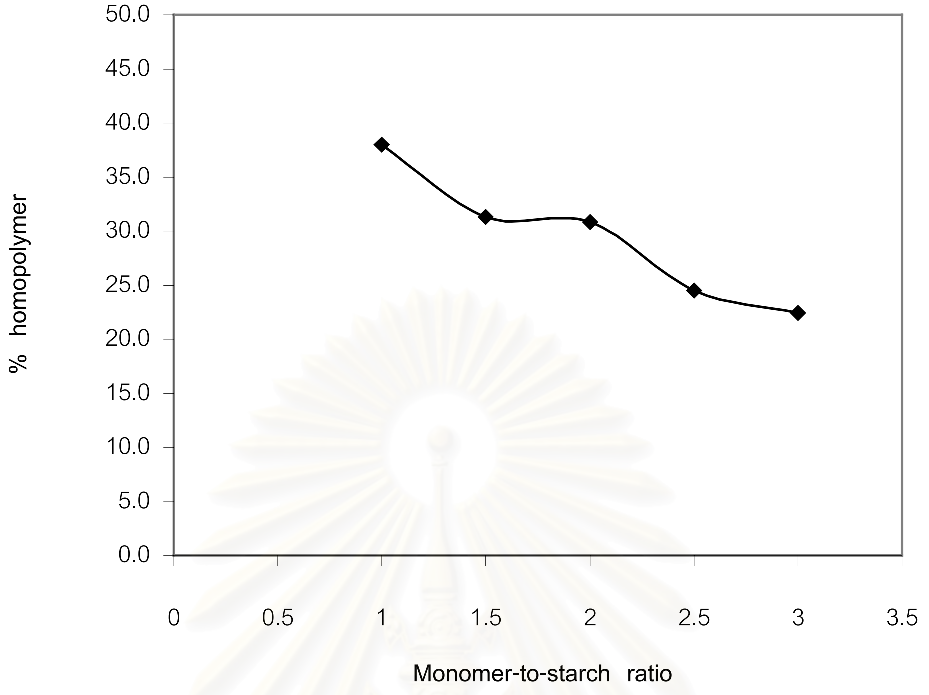

Figure 4.16 Effect of monomer-to-starch ratio on the percentage homopolymer of graft copolymerization of AM/MA onto starch

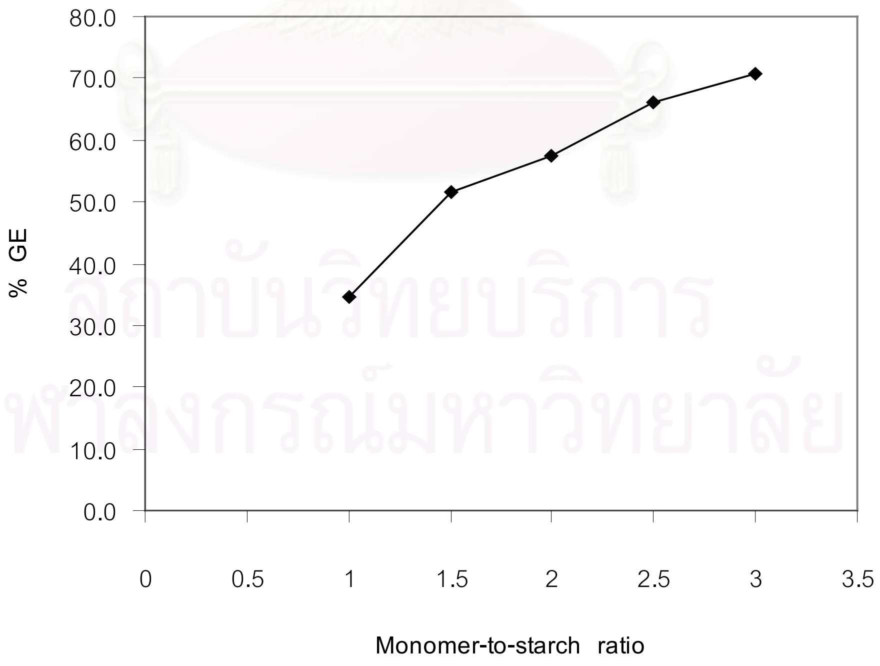

Figure 4.17 Effect of monomer-to-starch ratio on the percentage grafting efficiency of graft copolymerization of AM/MA onto starch

4.3.2.4 Relationship between Monomer-to-Starch Ratio, Grafting Efficiency and Percentage Add-on.

The effect of the monomer-to-starch ratio on grafting efficiency and percentage add-on is given in Table 4.5 and Figures 4.17-4.18. The result shows that grafting efficiency and percentage add-on increase with increasing monomer-to-starch ratio. This result indicates that a higher AM concentration can enhance grafting yield due to that more monomers can react at grafting sites in the starch trunk polymer.

4.3.2.5 Relationship between Monomer-to-Starch Ratio and Water Absorption.

The effect of monomer-to-starch ratio on the water absorption of saponified starch-*g*-poly(acrylamide-*co*-maleic acid) in distilled water is shown in Table 4.5 and Figure 4.19. The experimental data shows that the highest water absorption occurred at the quantity of monomer-to-starch ratio of 2.5:1.

The absorbency of crosslinked polymer can be explained in terms of swelling. Swelling is a diffusion phenomenon driven by the affinity of the molecules of the contracting fluid. The swelling equilibria of ionized hydrogels are determined by a balance of three primary forces, as follows :

1. The free energy of mixing of the network chains with solvent,
2. The net osmotic pressure within the network resulting from the mobile counterions surrounding the fixed charged groups (ion osmotic pressure), and
3. The elastic retractile response of the network (network swelling pressure).

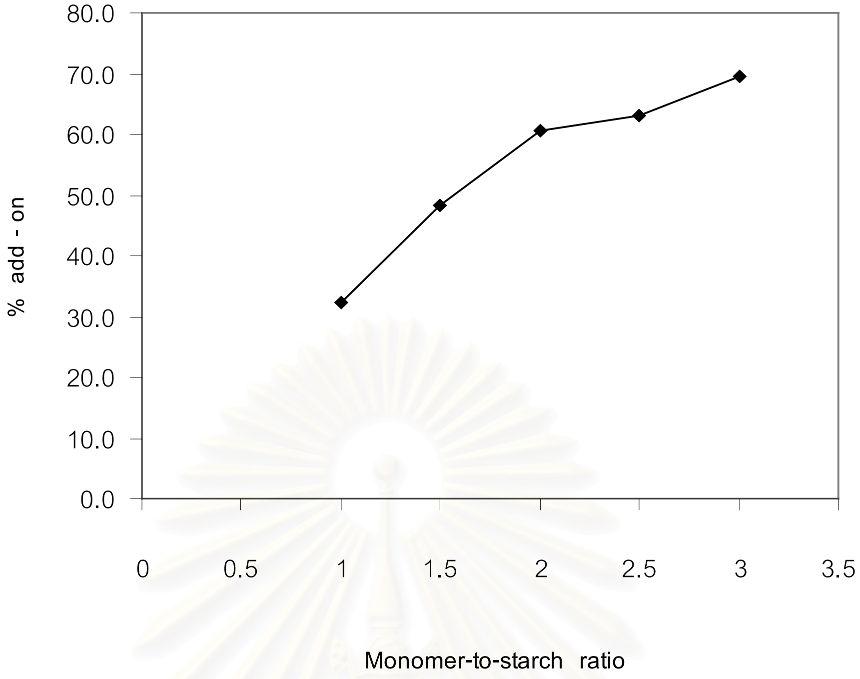

Figure 4.18 Effect of monomer-to-starch ratio on the percentage add-on of graft copolymerization of AM/MA onto starch

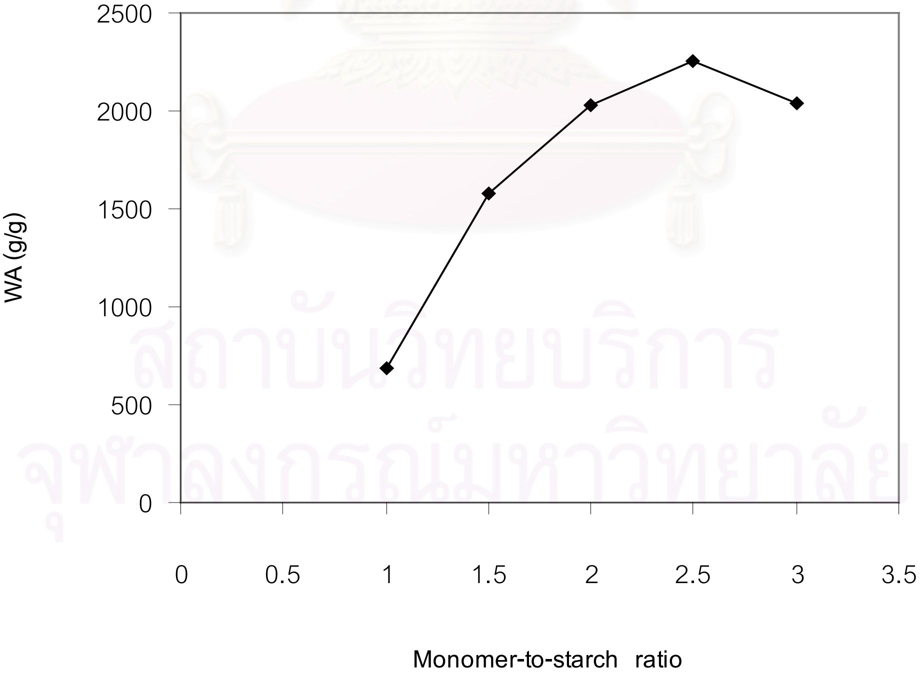

Figure 4.19 Effect of monomer-to-starch ratio on water absorption of graft copolymerization of AM/MA onto starch

Forces (1) and (2) favor hydrogel swelling, while force (3) opposes it. The saponified starch-*g*-poly(acrylamide-*co*-maleic acid) is swollen in water on account of the hydrophilic pendants (amide and carboxylate groups) in its structure. The graft copolymerization with the higher grafting efficiency gives the graft copolymer containing the higher concentration of mobile K^+ ions, resulting from the saponification step. Thus the swelling increases due to the increase of the different osmotic pressure between inside and outside of the gel. However, monomer-to-starch ratio higher than 2.5:1, the water absorption decreases. This may be due to the higher crosslink density at higher monomer concentration. For a given polymer-solvent system the equilibrium swelling is inversely related with the crosslink density [43]. The polymer chains are restricted in swelling by elastic retraction forces of the network. The more the chains separate from each other, the more stiffness the originally coiled polymer chains become.

4.3.3 Effect of Maleic Acid Content on Graft Copolymerization.

The effect of maleic acid content on starch-*g*-poly(acrylamide-*co*-maleic acid) prepared at the dose rate of 1.91 kGy h^{-1}, to the total dose of 4.0 kGy, the acrylamide-to-starch ratio of 2.5:1 and saponified at room temperature for 90 minutes with 5% KOH solution is presented in terms of the amount of carbon and hydrogen as shown in Table 4.6.

Table 4.6 Compositions of Elemental Analysis.

Maleic Acid Content (% $w\,w^{-1}$ of monomer)	Composition of the elements (%)		
	Carbon	**Hydrogen**	**Nitrogen**
Non MA	44.463	6.595	11.044
MA 1%	44.097	6.569	10.785
MA 2%	44.045	6.595	10.419
MA 3%	43.995	6.366	10.137
MA 4%	43.797	6.177	9.646
MA 8%	43.831	6.178	9.338
MA 12%	43.813	6.430	8.993

When the maleic acid content increases, the percentage carbon slightly decreases, while the percentage hydrogen does not change significantly and the percentage nitrogen decreases. Because the higher percentage homopolymer of polyacrylamide and ungrafted, free copolymer of low molecular weight poly(acrylamide-*co*-maleic acid) are removed from the grafted copolymer of starch/AM

Table 4.7 shows the effect of maleic acid content on the grafting of AM and MA onto cassava starch in the terms of the conversion of monomer, homopolymer and free copolymer formed, grafting efficiency, percentage add-on and water absorption, respectively.

Table 4.7 Effect of Maleic Acid Content on the Graft Copolymerization of Acrylamide and Maleic Acid on to Cassava Starch

MA content (%)	**Conv (%)**	**Gel (%)**	**Homo (%)**	**Add-on (%)**	**GE (%)**	**WA ($g\ g^{-1}$)**
0%	95.7	84.2	13.4	67.0	81.2	1679±16
1%	96.6	79.9	20.6	65.9	71.7	1637±15
2%	96.6	72.5	24.5	63.2	66.1	2256±25
3%	95.4	71.8	29.1	62.7	60.5	2166±6
4%	95.1	71.4	32.5	61.4	56.0	2020±12
8%	96.4	69.5	39.4	59.1	47.6	1972±10
12%	98.4	62.4	45.6	56.5	40.2	1718±9

MA content = Maleic Acid Content; Conv = Conversion; Gel = Gel Content; Homo = Homopolymer; GE = Grafting Efficiency; WA = Water Absorption; Acrylamide-to-starch ratio = 2.5:1 with a dose rate of 1.71 kGy h^{-1}, and a total dose of 4.0 kGy

4.3.3.1 Relationship between Maleic Acid Content and Percentage Conversion.

The correlation between percentage conversion of the monomer and the amount of maleic acid is shown in Table 4.7 and Figure 4.20. The increasing amount of maleic acid does not increase the conversion of the reaction significantly and it nearly approached 100%. Thus it indicates that a nearly complete conversion is obtained using this radiation dose and acrylamide-to-starch ratio. The ionizing radiation can initiate a certain number of free radicals. It can be also seen in Table 4.6 that the amount of carbon does not increase when increasing the maleic acid content.

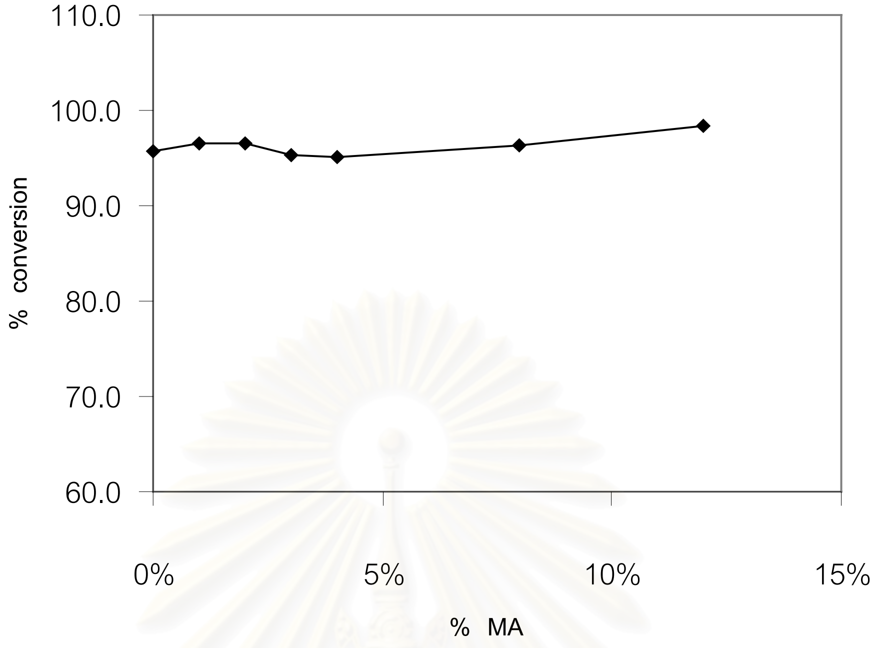

Figure 4.20 Effect of maleic acid content on the percentage conversion of graft copolymerization of AM/MA onto starch

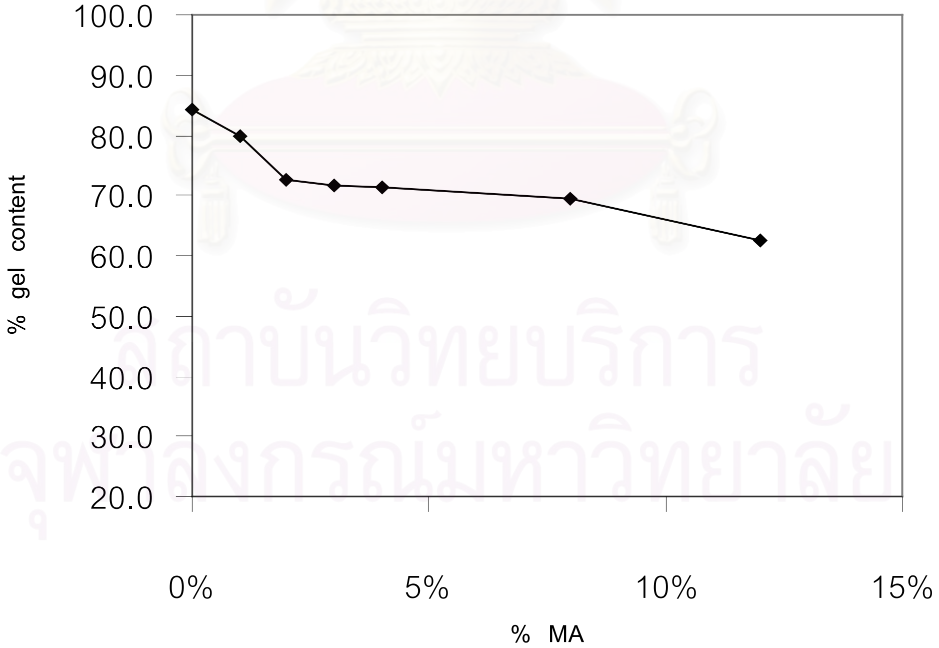

Figure 4.21 Effect of maleic acid content on the percentage gel content of graft copolymerization of AM/MA onto starch

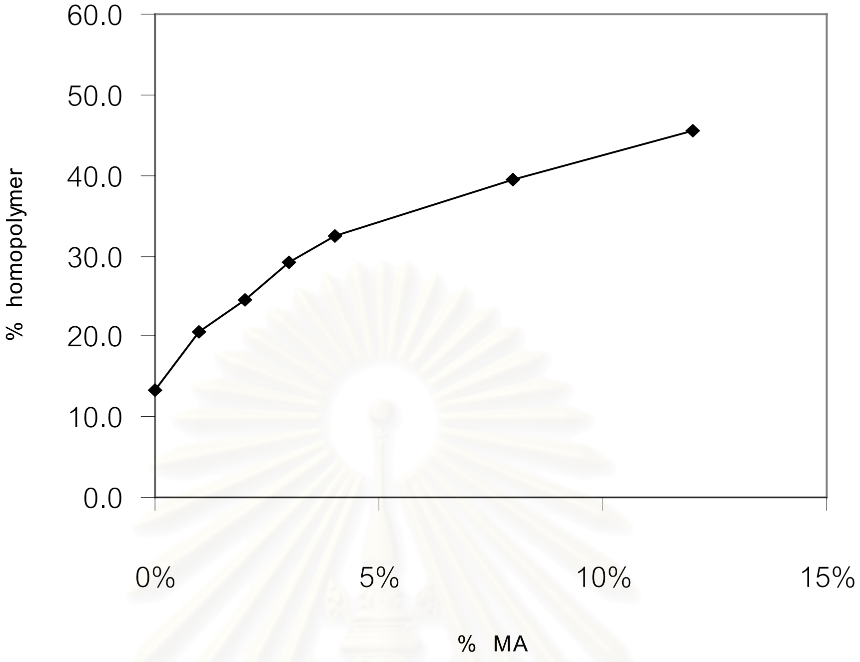

Figure 4.22 Effect of maleic acid content on the percentage homopolymer of graft copolymerization of AM/MA onto starch

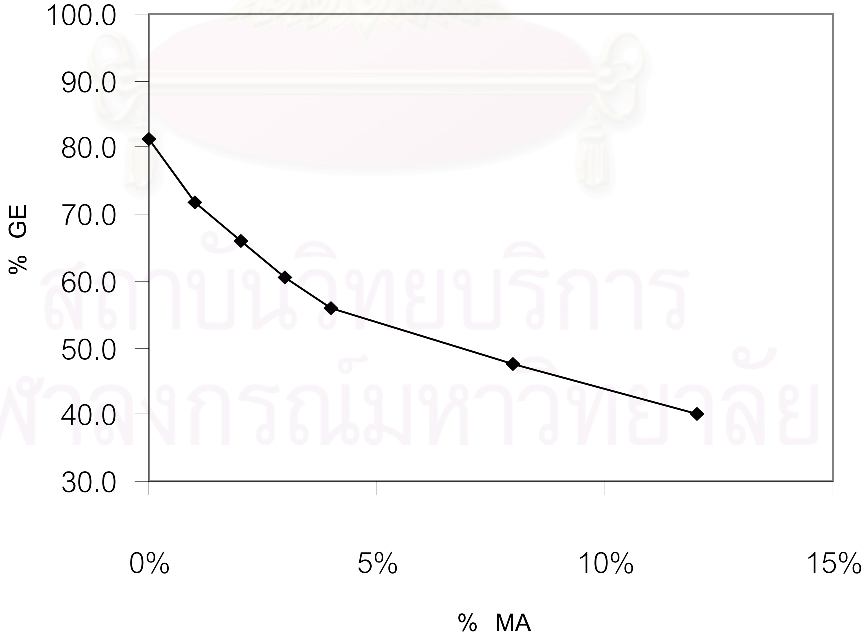

Figure 4.23 Effect of maleic acid content on the percentage grafting efficiency of graft copolymerization of AM/MA onto starch

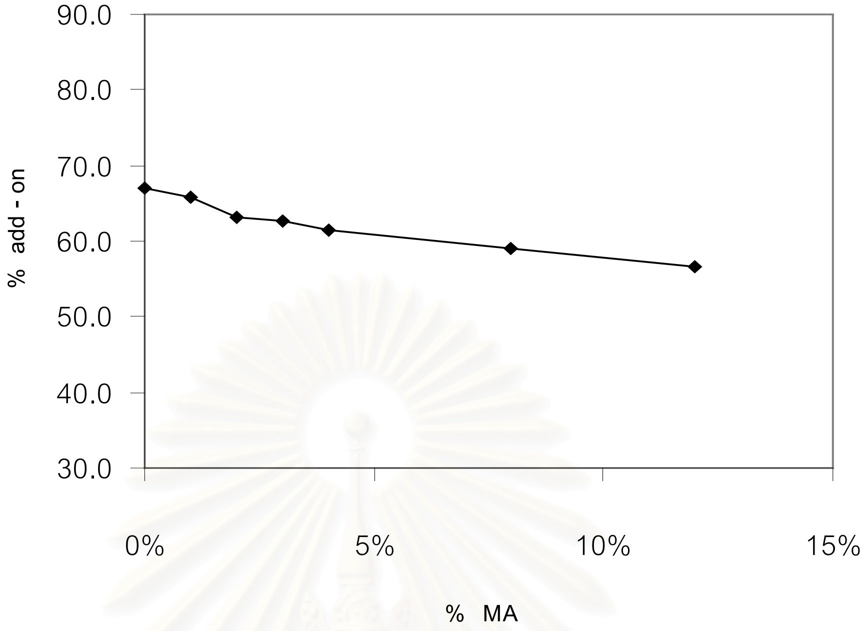

Figure 4.24 Effect of maleic acid content on the percentage add-on of graft copolymerization of AM/MA onto starch

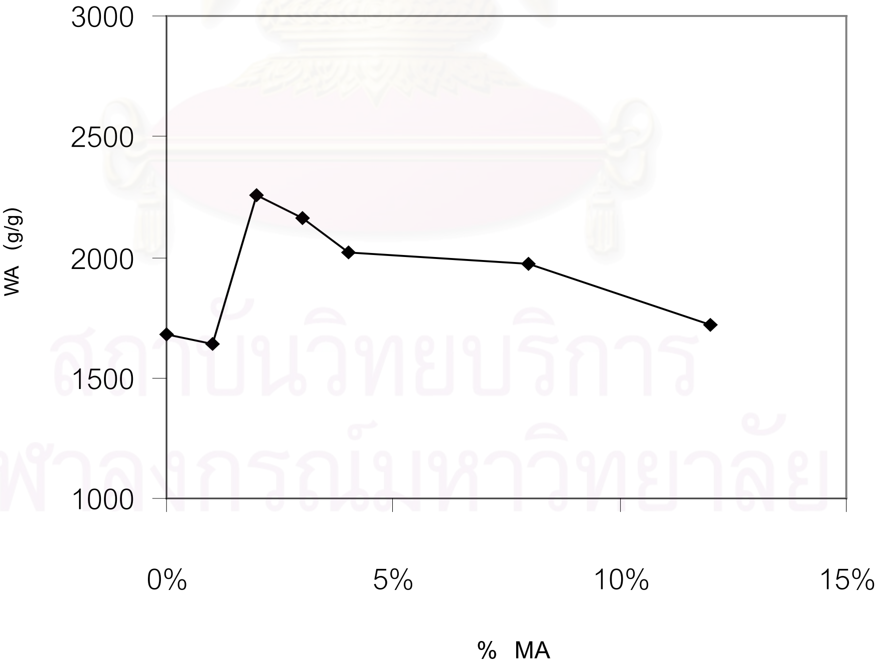

Figure 4.25 Effect of maleic acid content on water absorption of graft copolymerization of AM/MA onto starch

4.3.3.2 Relationship between Maleic Acid Content and Percentage Gel Content.

The Experimental data of the effect of maleic acid content on percentage gel content are given in Table 4.7 and Figure 4.21. Percentage gel content decreases with increasing maleic acid content. This result indicates that maleic acid does not act as a crosslinking agent and both monomer preferred to copolymerize as an ungrafted, free copolymer rather than grafted copolymer onto the starch backbone.

As shown in Table 4.6, the amount of carbon and hydrogen slightly decrease when maleic acid content increases.

4.3.3.3 Relationship between Maleic Acid Content, Percentage Homopolymer, Grafting Efficiency and Percentage Add-on.

Table 4.7 and Figures 4.22-4.24 show the effect of maleic acid content on percentage homopolymer and free copolymer, grafting efficiency and percentage add-on of graft copolymerization of AM and MA onto cassava starch. The experimental data show that increasing maleic acid content increases the homopolymer and free-copolymer formed.

For the radical copolymerization of AM (M_1) – MA (M_2) with $r_1 = 2.2$ and $r_2 = 0$ [44]. In this case, the acrylamide monomer is more reactive than the maleic acid toward the propagation species. Consequently, the copolymer will contain a greater proportion of acrylamide monomers in the random sequence of monomer units and the greater reactivity of the AM results in its being incorporated preferentially into the first – formed copolymer. In addition, determination of monomer reactivity ratios r_1 and r_2, maleic acids cannot polymerize to obtain homopolymer. Thus the increasing homopolymer may be from the formation of polyacrylamide or the random reactions of AM and

MA radicals with the monomers lead to the formation of ungrafted, free copolymer of AM and MA as shown in the IR spectrum for homopolymer or mixed with starch-*g*-poly(acrylamide-*co*-maleic acid) (Figure 4.26). All characteristic absorption peaks of acrylamide and maleic acid are observed. The broad peak of O – H stretching at 3,395 cm^{-1}, the weak peak of C – H stretching at 2,931 cm^{-1}, the weak peak of C – H bending at 1,456 cm^{-1}, the weak peak of O – H bending at 1,383 and 1,422 cm^{-1}, and the strong peak of C – O stretching at 1,026 cm^{-1} are the characteristics of cassava. The broad peak at 3,192 cm^{-1}, sharp peak at 1,669 cm^{-1}, weak peak at 1,616 cm^{-1} and weak peak at 1,330 and 1,354 cm^{-1} indicate the N – H stretching, C = O stretching of carboxamide, N – H bending and C – N stretching, respectively which are the characteristics of the -CONH$_2$ group containing in the acrylamide. The additional weak peak at 2,931 cm^{-1}, strong peak at 1,669 cm^{-1}, weak peak at 1,205 cm^{-1} and weak peak at 934 cm^{-1} are for the O – H stretching, C = O stretching, C – O stretching and O – H bending of -COOH group containing in maleic acid, respectively. The percentage grafting efficiency and percentage add-on decrease due to an increase of these ungrafted material.

4.3.3.4 Relationship between Maleic Acid Content and Water Absorption.

To raise the water retention capacity of the starch-*g*- polyacrylamide, a dienoic organic acid containing hydrophilic groups such as maleic acid monomer is used to prepare graft copolymer. It is known that many studies have been published on the polyelectrolyte behavior of alternating copolymers of maleic acid in aqueous solutions. In aqueous solutions, several characteristic properties have been observed: conformational transition, two-step dissociation process of dicarboxylate groups, binding of counterions, etc. These properties of maleic acid copolymers are attributed to two factors: (a) hydrophobic interaction

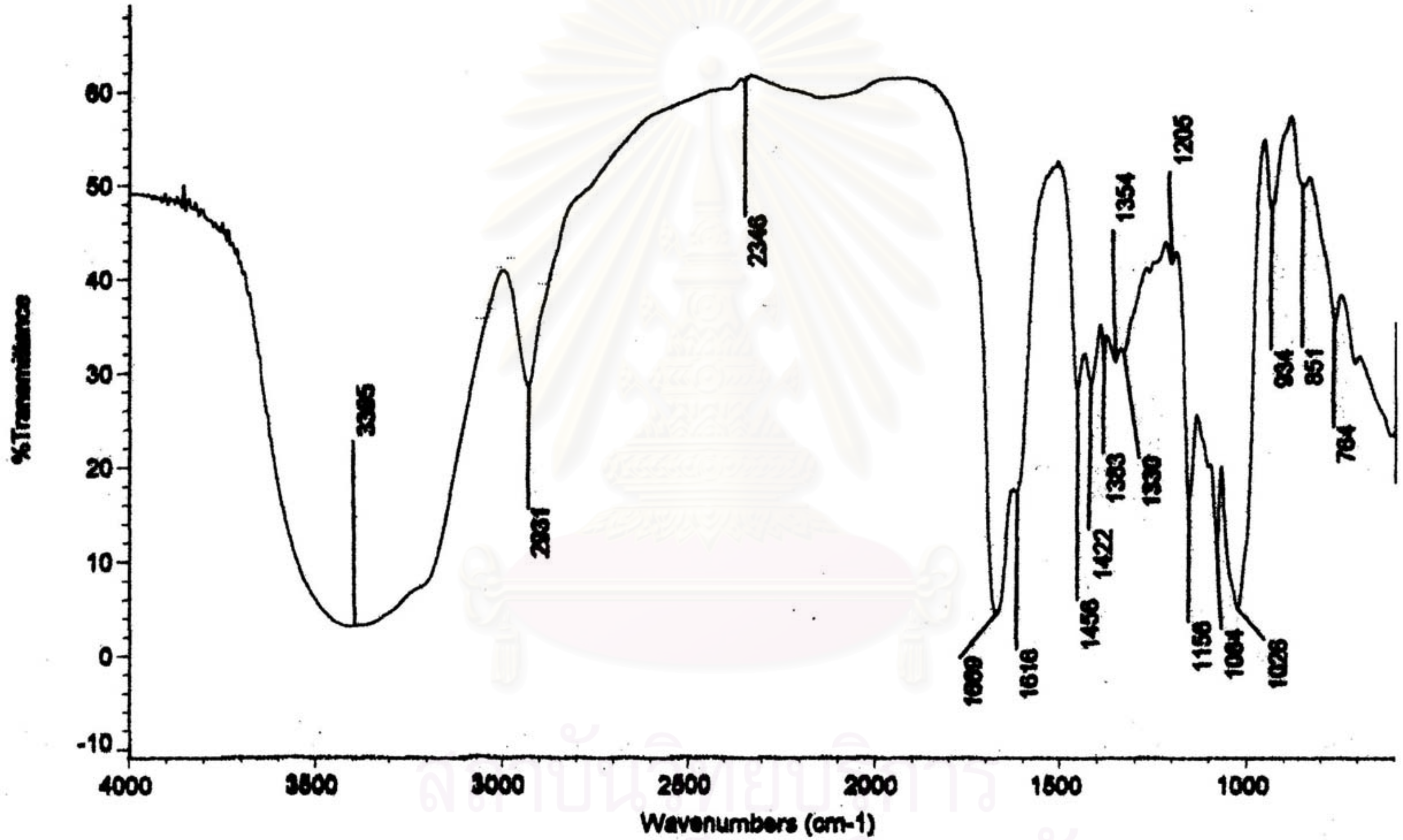

Figure 4.26 Infrared spectrum of homopoloymer and free copolymer of starch-g-poly(acrylamide-co-maleic acid)

of non polar side chains, and (b) short-range electrostatic interaction of a pair of adjacent nearest neighbor corboxylate groups. [21, 45]

The relationship between maleic acid content and water absorption is shown in Table 4.7 and Figure 4.25. It shows that the highest water absorption occurs at the quantity of maleic acid about 2% $w\,w^{-1}$ of acrylamide. At lower maleic acid content, the water absorption increases with increasing of maleic acid content. These may be due to copolymerization reactions via charge transfer (CT) complexes of monofunctional acceptors and donors (DA). In a detailed series of papers the background theory of the role of CT complexes in photopolymerization has been discussed, in particular their participation in UV curing systems under photoinitator free conditions has been explained. (Jonsson et. al. [46]; Hall et. al. [47]; Garnett et. al. [48]). Briefly, DA complexes involving donor and acceptor molecules may be formed in both ground and excited states. If the D, A molecules are monomers, then polymerization can occur from certain excited DA complexes (DA)*.

Typical mechanisms for the formation of the excited state DA complex are depicted in Equations 4.3 – 4.5.

Formation of an exiplex type AD*

$$A + D \xrightarrow[h\nu]{h\nu} A^* + D \longrightarrow [A\ \text{- - - -}\ D]^* \qquad (4.3)$$

$$A + D \longrightarrow A + D^* \longrightarrow [A\ \text{- - - -}\ D]^* \qquad (4.4)$$

Formation of an AD* from a ground state CT

hν

$$A + D \longrightarrow [A\ ---\ D] \longrightarrow [A\ ----\ D]^{*} \tag{4.5}$$

When considering the application of these previous photopolymerization concepts to grafting, the acrylamide containing an electron-rich vinyl group as a donor and the maleic anhydride to become maleic acid, on heating and dehydration via irradiation, containing an electron poor vinyl group as an acceptor are interacted to yield CT complexes. Then gamma irradiation may cause a grafting of the CT complex directly. The more energetic ionizing radiation can rupture bonds indiscriminantly in the substrate, solvent, monomer or DA complex to create grafting sites and initiate polymerization [48]. Homopolymer formation may also be observed as a competing reaction during these grafting processes (Equation. 4.6-4.7) where D is the electron rich donor; A is the electron poor acceptor; M is a monomer like acrylamide.

$$D + A \ \hat{}\hat{}\hat{}\!\rightarrow [A\ ----\ D]^{*} \xrightarrow{M} R^{\bullet} \rightarrow RM^{\bullet} \tag{4.6}$$

$$RM^{\bullet} + nM \rightarrow RM^{\bullet}_{n+1} \tag{4.7}$$

The hydrophilic group number of poly(acrylamide-*co*-maleic acid) is more than of the polyacrylamide, so the swelling of starch-*g*-polyacrylamide is obviously lower than that containing the maleic acid moiety. In addition, the lower crosslink density gives the higher water absorption. The water absorbency and the strength of superabsorptive polymers can be expressed by Equation 4.8 (Flory's equation) and Equation 4.9, respectively [48].

$$Q^{5/3} = [(i / 2 * \nu_u S * {}^{1/2})^2 + (1 / 2 - \chi_1) / \nu_1] / (\nu_e / V_0) \tag{4.8}$$

$$G = RT * \nu_e / V_0 \tag{4.9}$$

where G is degree of swelling
i/ν_u is charge density of polymer
S^* is ionic strength of solution
$(1/2 - \chi_1)/\nu_1$ is polymer-solvent affinity
ν_e / V_0 is crosslinking density
G is rigidity

The water absorbency, therefore, increases with increasing numbers of hydrophilic and ionic functional groups, and with decreases in the crosslink density of the polymer network.

However, at the maleic acid content higher than 2% w w^{-1}, the water absorption decreases due to the increases of homopolymer, free copolymer formed, and the decrease in grafting efficiency and percentage add-on. In addition, the formation of insoluble maleic anhydride results in the rigid chain and leads to a photochemically allowed 2+2 cycloaddition formation. This cycloaddition reaction generates a thermodynamically stable cyclobutane ring as a linkage between the two A and D monomers, therefore, the water absorption decreases due to the stiffness of the chain[46].

4.3.4 Effect of Salt Solution on Water Absorption.

Since the starch-*g*-poly(acrylamide-*co*-maleic acid) absorbent is a kind of anionic gel, the surrounding environment, such as temperature, pH, ionic strength of the ions, etc. affects its absorbency. Table 4.7 shows the swelling of starch-*g*-poly(acrylamide-*co*-maleic acid) absorbent in salt solutions. The highest water absorbing copolymer, obtained earlier, having a water absorbency of 2256 ± 25 g g^{-1} was selected to test the salt effect in an isotonic fluid of 0.9% w v^{-1} of NaCl, $MgCl_2$, and $CaCl_2$ solutions.

Table 4.8 Effect of Salt Solution on Water Absorption.

Solution	**Ionic Strength [a] (mole – ion dm^{-3})**	**Water Absorption (g g^{-1})**
Distilled Water		2,256 ± 25
0.9% w v^{-1} NaCl Solution	0.1540	94 ± 11
0.9% w v^{-1} $MgCl_2$ Solution	0.2832	64 ± 7
0.9% w v^{-1} $CaCl_2$ Solution	0.2433	47 ± 5

[a] $I = 1/2\ \Sigma (C_iZ_i^2)$, where I, C_i, and Z_i are the ionic strength, the ionic concentration, and the charge on each individual ion, respectively. [49].

The salt effect is clearly evidenced as a result of the osmotic pressure differential between the internal solution in the gel and the external solution due to the different ion concentrations. When a gel is placed in an ionic solution, an exchange of mobile ions takes place between the gel and the solution, but because of the presence of the bound groups, the mobile ions are unevenly distributed, i.e., the gel contains the higher concentration of mobile ions. The swelling is a result of the entry of water in an attempt to reduce the osmotic pressure differential resulting from the difference in concentration. Swelling continues until the osmotic pressure differential is equal to the resistance to further expansion brought about by the cohesive forces of the molecular network [50].

The decreases in water absorption due to the ionic strength (I) of the salt solution as shown in Table 4.8. At low ionic strength, repulsions are long-range interactions, and the gel expands to minimize the repulsion free energy; as the ionic strength rises, the expansion of the network decreases because of the screening of the ionic charges bound to the network and the decrease of the osmotic pressure difference between the gel and the external solution [51].

The effect of the ionic strength on the swelling has been determined using Flory's equation (Eq. 4.2). According to equation 4.2, the ionic strength of solution increases the water absorbency would then decrease. The ionic strength of the solution depends on both the mobile ion concentration and their valency. Small quantities of divalent or trivalent ions can decrease drastically the swelling values. In addition the divalent Mg^{2+} and Ca^{2+} ions may crosslink the gel by salt formation with the carboxylate groups on adjacent chains or chain segments of the copolymer. Consequently, the crosslink density of the network increases [14, 51].

4.3.5 Effect of pH on Water Absorption.

Table 4.9 and Figure 4.27 show the influence of the water absorbency of the solution pH (3 – 11) on the water absorption capacity of the synthesized graft copolymer, which has the highest water absorption in distilled water (2256 ± 25 g g^{-1}).

Table 4.9 Effect of pH on Water Absorption.

pH of Buffer Solution	**Ionic Strength [a] (mole – ion dm^{-3})**	**Water Absorption g g^{-1}**
pH 3	0.0061	67 ± 7
pH 5	0.0134	115 ± 6
pH 8	0.0212	106 ± 3
pH 11	0.0272	83 ± 5

[a] $I = 1/2\ \Sigma (C_i Z_i^2)$, where I, C_i, and Z_i are the ionic strength, the ionic concentration, and the charge on each individual ion, respectively. [49].

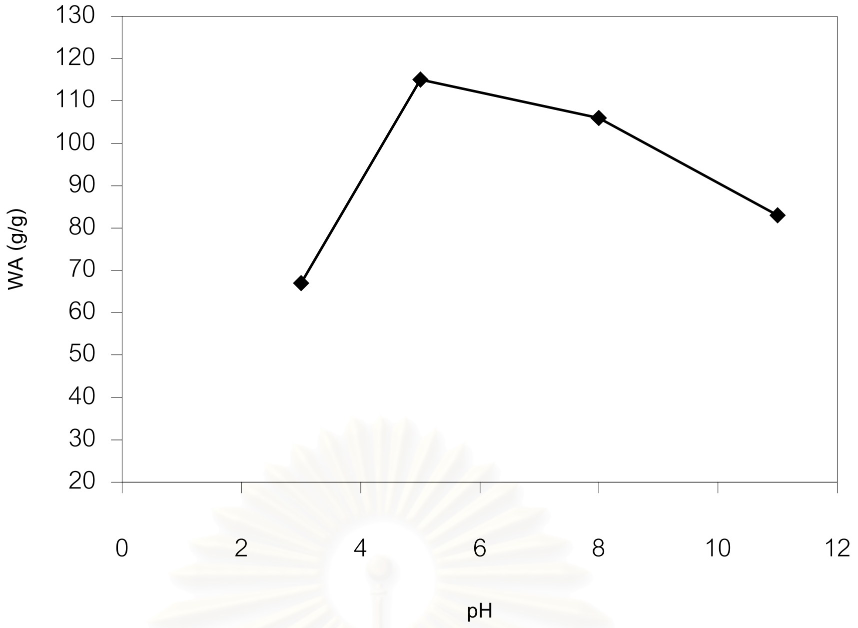

Figure 4.27 Effect of pH on water absorption of the copolymer.

The simplest explanation of the theories attributes the ion swelling pressure to the difference between the osmotic pressure of freely mobile ions in the gel and in the outer solution. The distribution of the ions between the gel and the outer solution is obtained from Donnan equilibrium. Within this theory the ionic forces depend only on the ionic composition of the solvent and on the concentration of fixed ionizable groups in the gel but not on the properties of the neutral network [52].

The swelling of saponified graft copolymer increases significantly from pH 3 to pH 5, and decreases afterwards. As the pH is lowered to the strongly acidic region, the carboxylate side chains of the potassium acrylate become hydrolyzed to be the carboxylic group, thus decreasing the charge density of anions on the network. The concomitant decreases in mobile counterion content of the network sharply decreases the internal osmotic pressure, which retards the observed swelling transitions.

Upon increasing the pH in the weakly acidic and basic solutions, the concentration of the base cations in the outer solution and the concentration of the base cation in the outer solution and the concentration of the base anion inside the network will also increase. These cations will be attracted into the gel to balance the osmotic pressure occurring from the anions of base-hydrolyzed acrylamide and carboxylate groups. Those cations will replace the mobile H^+ ions. The gel acts as an ion exchanger. New H^+ ions will be supplied by water. The concentration of mobile ions in the gel will increase more rapidly than in the outer solution, and the ion swelling pressure will increase. In addition, the maximum extents of swelling is reached at pH 5, this being due to the complete dissociation of acidic groups of maleic acid at this pH value. The first and second dissociation constant of maleic acid are $pK_{a1} = 1.85$ and $pK_{a2} = 6.06$, respectively [30]. With increasing pH, the ion swelling pressure will begin the drop again because the higher ionic strength.

4.3.6 Effect of Particle Size on Water Absorption.

The relation of particle size on the water absorption capacity of the synthesized graft copolymer, which has the highest water absorption in distilled water (2256 ± 25 g g^{-1}) is shown in Table 4.10 and Figure 4.28.

Table 4.10 Effect of Particle Size on Water Absorption.

Particle size (μm)	**Water Absorption (g g^{-1})**
600	1939 ± 10
300	2226 ± 20
180	2527 ± 13
150	2653 ± 25

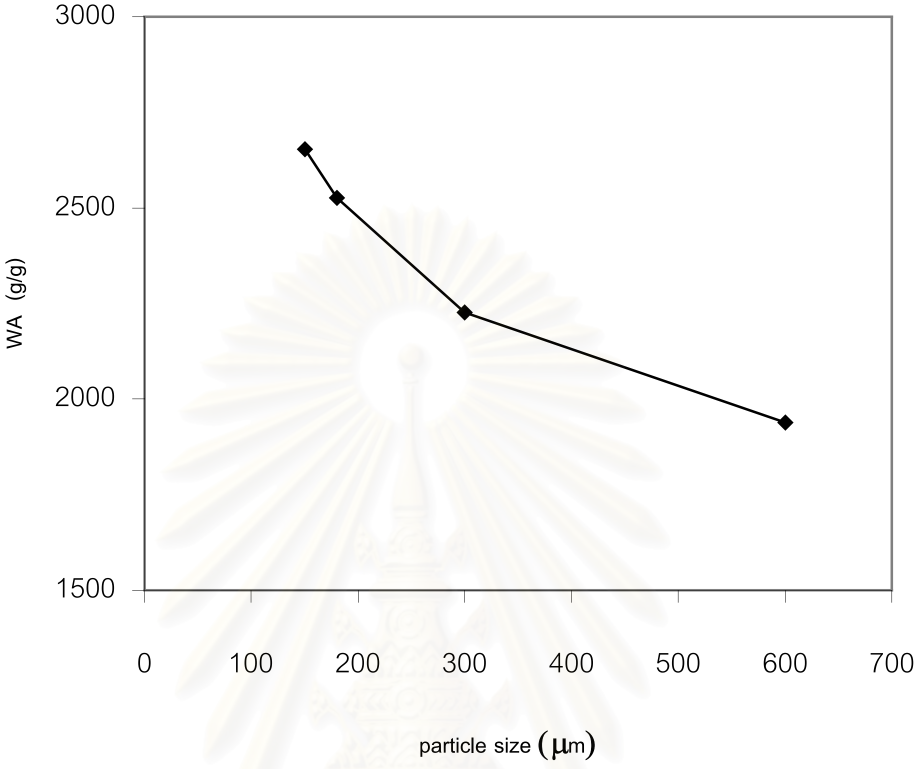

Figure 4.28 Effect of Particle Size on Water Absorption of Copolymer

In this research, we used the gravimetric swelling capacity method for determining the swelling extent of collections of small particles, the additional mass of interparticle, unsorbed liquid was included in the swelling ratios. Water absorption values from this analysis are typically larger than those for methods where interparticle moisture is excluded. The particle size distribution of the sample and the modulus of the swollen polymer affect the way in which the liquid drains from the gel [53]. The absorption increases when the particle size decreases due to the higher interparticle liquid, because the small particle size has higher surface area than the larger particle size at the same quantity.

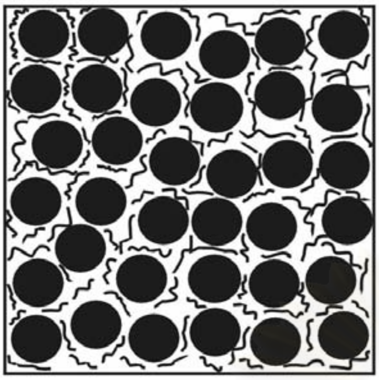

small particle size

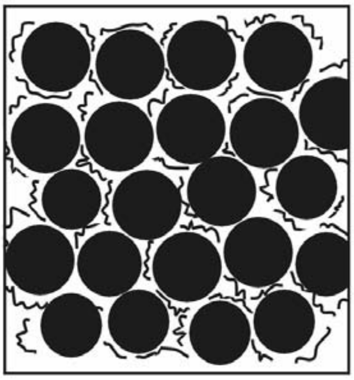

large particle size

4.3.7 Absorption Under Load

An experimental technique that measures the effect of mechanical compression on the swelling process has been used in the study of commercial superabsorbent polymers. This is known as absorbency under load.

Superabsorbents in personal care articles must resist deformation and deswelling under an external load because this ability has been correlated to improved performance in pad analysis and in diapers. When a uniaxial compression is applied to the swelling polymer particle, it is forced to change in shape. The magnitude of the deformation depends on the modulus, which in turn depends on the initial crosslink density and extent of swelling. The change in shape will tend to close off channels in the gel mass that allow the convective flow of free liquids. Thus, the shutting off of liquid flow by compression of the gel mass depends on the elastic modulus and the porosity of the sample bed and on variables that affect them. A real loading of the polymer in the test device and the particle size distribution in the sample are two of these variables.

Swelling under pressure of starch-*g*-poly(acrylamide-*co*-maleic acid) for various maleic acid contents from 0-12% w w^{-1} of acrylamide versus time as a function of the applied load are shown in Tables 4.11-4.17 and Figures 4.29 (a)-4.29 (g). We found that the absorbency under load rises rapidly in the beginning of the test and increases slightly after 10 minutes.

When the applied load increases, the absorbency under load decreases because liquid can be removed from a swollen superabsorbent gel by application of pressure. This deswelling occurs because the application of pressure to the system causes an increase in its free energy and in the chemical potential of any species that can diffuse into or out of the system. The increase in chemical potential serves as a driving force to expel water from the gel into the surroundings when the gel is compressed.

The effect of adding pressure to the gel is similar to adding additional crosslinks to the gel to increase the hydrostatic pressure in the gel phase and to reduce the maximum swelling. The limitation of swelling under pressure and the related deswelling behavior are thus related to the osmotic pressure of the gel, which acts as a polymer solution confined inside a semipermeable membrane [54].

Table 4.11 Water Absorption Under Load of Starch-*g*-Polyacrylamide

Time (min)	Water Absorption Under Pressure (g g^{-1})					
	0 kPa	1 kPa	2 kPa	3 kPa	4 kPa	5 kPa
5	248	23	23	21	17	17
10	266	27	26	23	21	21
15	270	30	29	26	23	24
20	275	33	32	29	25	25
25	277	37	34	31	27	27
30	279	39	36	33	29	28
40	283	42	39	36	32	31
50	287	45	41	38	34	33
60	289	47	43	39	35	34

Table 4.12 Water Absorption Under Load of Starch-*g*-Poly(acrylamide-*co*-maleic acid), 1% MA

Time (min)	Water Absorption Under Pressure (g g^{-1})					
	0 kPa	1 kPa	2 kPa	3 kPa	4 kPa	5 kPa
5	226	24	21	19	21	20
10	238	29	25	23	24	22
15	240	32	28	26	27	25
20	246	34	31	30	30	27
25	248	37	34	32	32	29
30	250	40	35	36	33	31
40	253	44	39	38	35	33
50	255	46	40	41	38	35
60	255	48	42	42	39	36

Table 4.13 Water Absorption Under Load of Starch-*g*-Poly(acrylamide-*co*-maleic acid), 2% MA

Time (min)	Water Absorption Under Pressure (g g^{-1})					
	0 kPa	1 kPa	2 kPa	3 kPa	4 kPa	5 kPa
5	258	19	18	17	15	15
10	260	23	22	20	19	19
15	262	26	24	22	21	22
20	266	28	27	24	24	24
25	270	30	29	26	26	25
30	272	33	30	28	27	27
40	272	34	34	30	30	29
50	274	38	36	33	32	32
60	274	40	38	35	34	33

Table 4.14 Water Absorption Under Load of Starch-*g*-Poly(acrylamide-*co*-maleic acid), 3% MA

Time (min)	Water Absorption Under Pressure (g g^{-1})					
	0 kPa	1 kPa	2 kPa	3 kPa	4 kPa	5 kPa
5	212	23	22	19	18	19
10	232	27	25	23	22	22
15	234	29	27	26	24	24
20	238	33	29	28	26	26
25	242	34	32	29	28	27
30	242	37	34	31	30	29
40	244	42	37	33	33	31
50	246	45	39	35	25	34
60	248	48	42	37	37	35

Table 4.15 Water Absorption Under Load of Starch-*g*-Poly(acrylamide-*co*-maleic acid), 4% MA

Time (min)	Water Absorption Under Pressure (g g^{-1})					
	0 kPa	**1 kPa**	**2 kPa**	**3 kPa**	**4 kPa**	**5 kPa**
5	204	24	19	16	12	15
10	217	27	21	20	16	18
15	223	31	25	23	19	21
20	225	35	29	25	23	23
25	227	37	30	28	25	24
30	229	40	31	29	26	27
40	231	44	35	31	29	30
50	233	46	37	34	33	33
60	235	49	40	36	35	34

Table 4.16 Water Absorption Under Load of Starch-*g*-Poly(acrylamide-*co*-maleic acid), 8% MA

Time (min)	Water Absorption Under Pressure (g g^{-1})					
	0 kPa	**1 kPa**	**2 kPa**	**3 kPa**	**4 kPa**	**5 kPa**
5	231	24	19	17	22	21
10	237	30	23	21	26	26
15	239	31	26	26	31	29
20	239	36	30	30	33	32
25	243	39	34	33	38	36
30	245	41	34	34	40	37
40	247	44	37	37	43	40
50	249	50	40	40	47	43
60	249	53	44	43	47	46

Table 4.17 Water Absorption Under Load of Starch-*g*-Poly(acrylamide-*co*-maleic acid), 12% MA

Time (min)	Water Absorption Under Pressure					
	0 kPa	1 kPa	2 kPa	3 kPa	4 kPa	5 kPa
5	163	34	30	28	28	30
10	187	44	39	34	32	38
15	191	48	43	38	36	42
20	195	52	48	42	40	47
25	197	56	52	46	44	49
30	197	60	54	50	46	51
40	199	66	58	56	50	55
50	201	72	63	60	54	57
60	203	75	65	64	56	59

Figure 4.30 shows the gel swelling versus applied compression for seven different maleic acid contents. It shows that the absorbency under load at the higher loads increases with increasing maleic acid content even through the equilibrium swelling capacity at the zero load decreases. Because more rigid particles of gel at the high maleic acid content maintain their swelling capacity better under load than do the same size distribution of particles of a softer but more deformable gel.

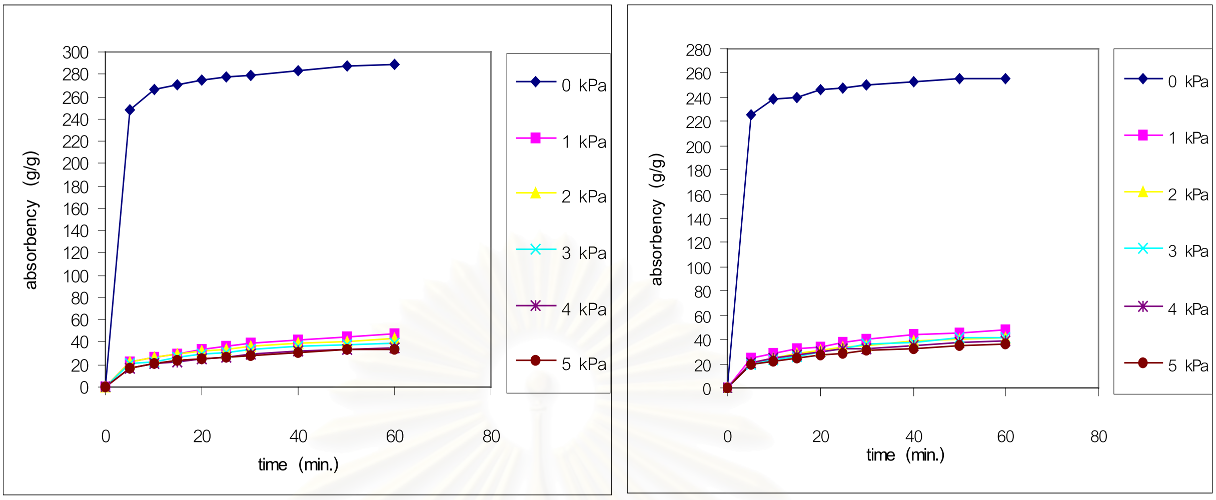

(a) without MA (b) 1% MA

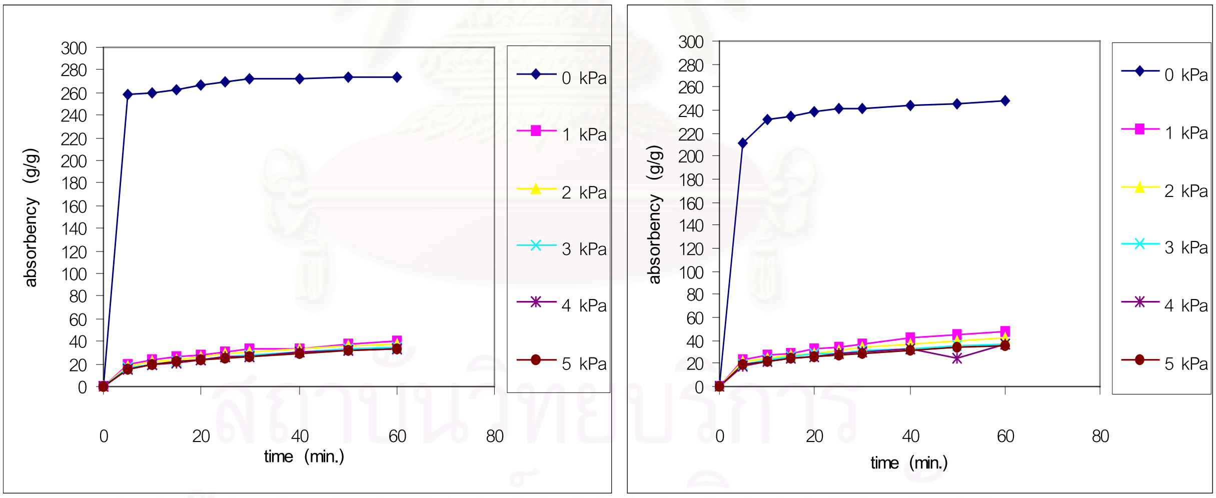

(c) 2% MA (d) 3% MA

Figure 4.29 **Swelling under pressure of starch-*g*-poly(acrylamide-*co*-maleic acid) for various maleic acid contents from 0-12% w w^{-1} of maleic acid versus time as a function of the applied load**

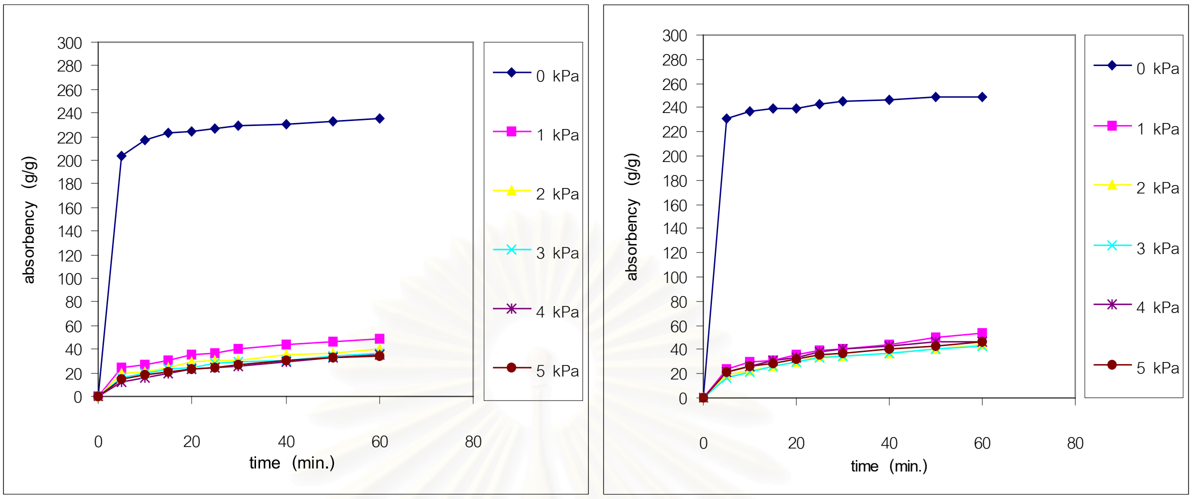

(e) 4% MA

(f) 8% MA

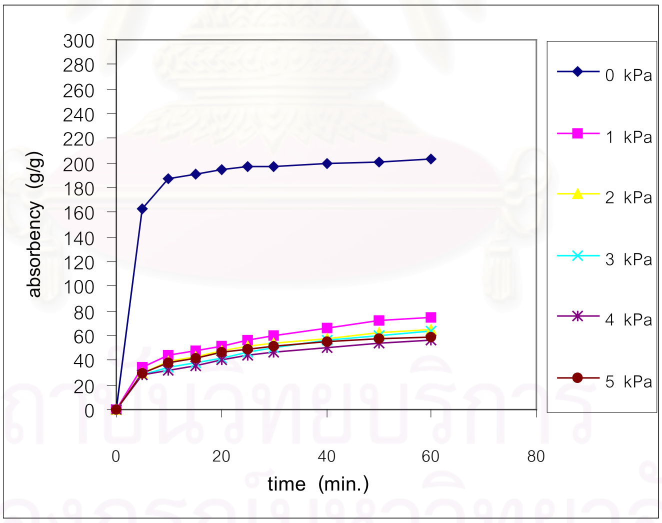

(g) 12% MA

Figure 4.29 Swelling under pressure of starch-*g*-poly(acrylamide-*co*-maleic acid) for various maleic acid contents from 0-12% w w^{-1} of maleic acid versus time as a function of the applied load (continued)

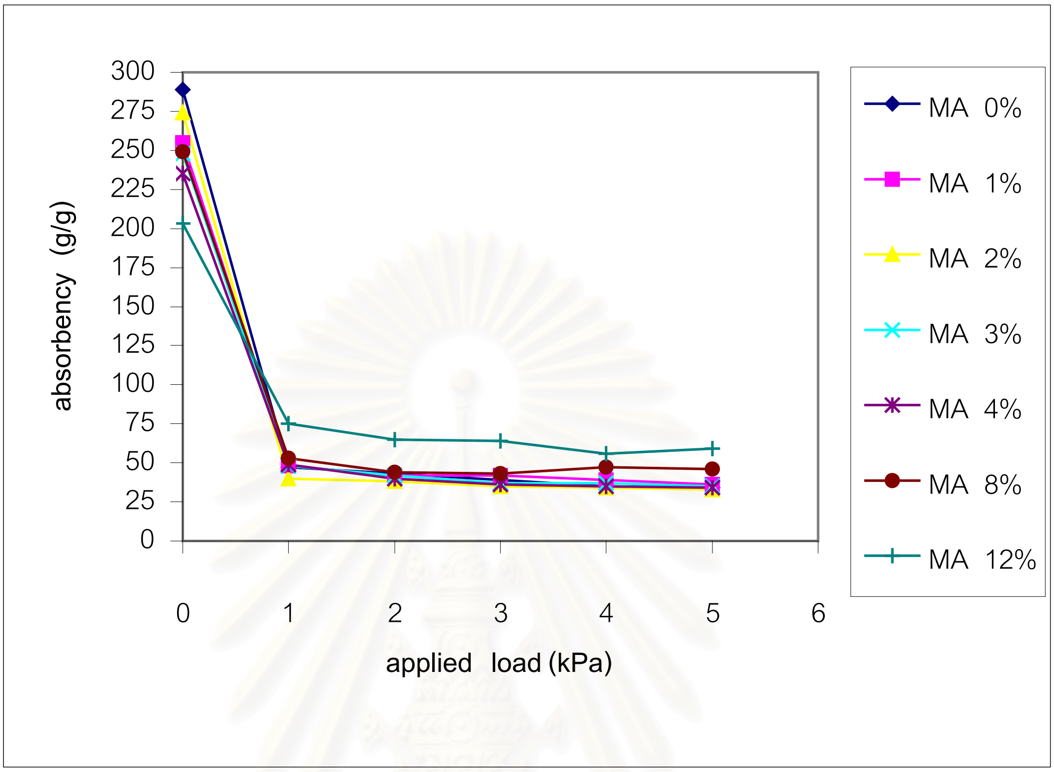

Figure 4.30 Gel swelling versus the applied compression for seven different maleic acid contents.

4.4 Surface Morphology of the Copolymers

The surface appearance and structure of saponified graft copolymer of cassava starch-*g*-AM/MA were observed using the scanning electron microscopy. The photographs taken by the electron microscope of the saponified starch graft copolymers are shown in Figures 4.31-4.37.

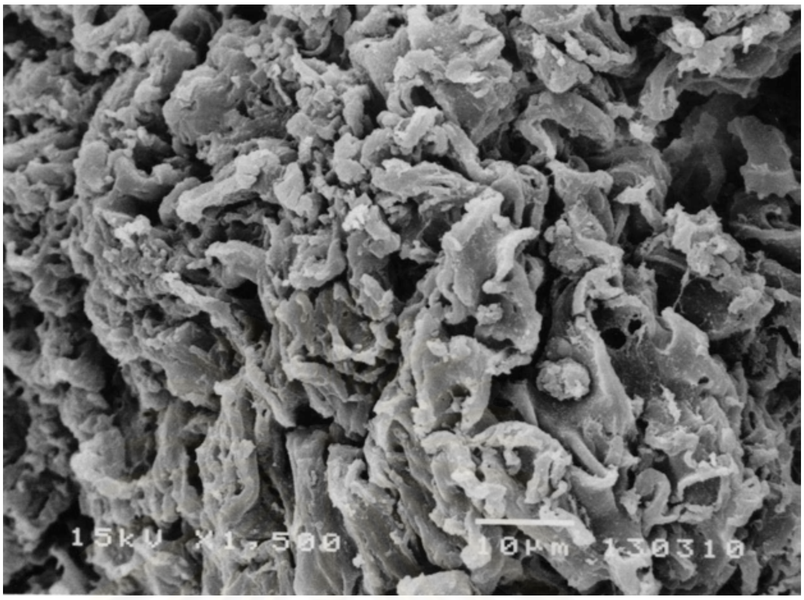

Figure 4.31 SEM photograph of the saponified starch-*g*-polyacrylamide (WA = 1,679 ± 16 g g^{-1})

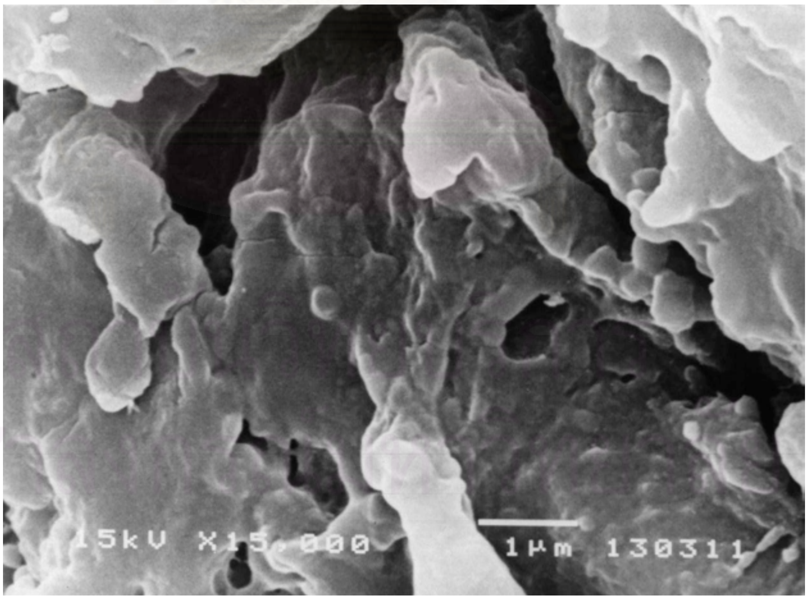

Figure 4.32 SEM photograph showing the non-cellular structure of the saponified starch-*g*-polyacrylamide at 15,000 x magnification (WA = 1,679 ± 16 g g^{-1})

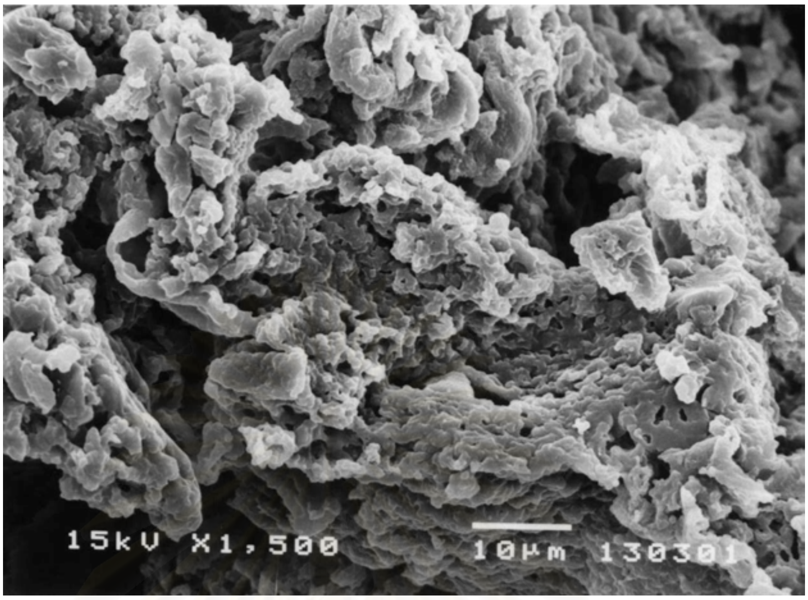

Figure 4.33 **SEM photograph of the saponified starch-*g*-poly(acrylamide-*co*-maleic acid) at DR 11.0 KGy h^{-1} to the TD 0.5 kGy (WA = 608 $\pm$ 7 g g^{-1})**

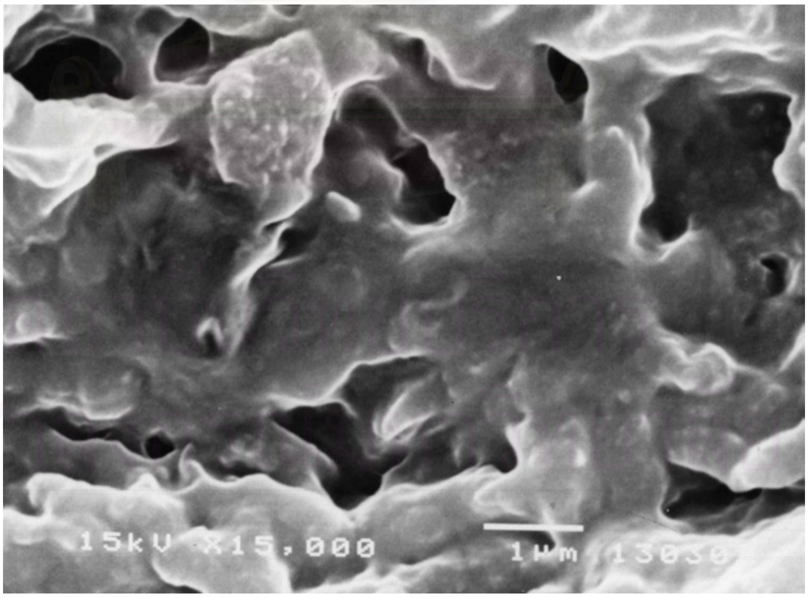

Figure 4.34 **SEM photograph showing the non-cellular structure of the saponified starch-*g*-poly(acrylamide-*co*-maleic acid) at DR 11.0 kGy h^{-1} to the TD 0.5 kGy at 15,000 x magnification (WA = 608 $\pm$ 7 g g^{-1})**

SEM photographs of saponified starch-*g*-polyacrylamide have the water absorption as 1,679 ± 16 g g^{-1} and saponified starch-*g*-poly(acrylamide-*co*-maleic acid) at the dose rate of 11.0 kGy h^{-1} to the total dose 0.5 kGy and the acrylamide-to-starch ratio of 2:1 have the minimum water absorption as 608 ± 7 g g^{-1}, shown in Figures 4.31-4.34. These saponified copolymers as mentioned above figures have less porous, non-cellular structure. On the other hand, the SEM photographs of saponified starch-*g*-poly(acrylamide-*co*-maleic acid) at dose rate of 1.71 kGy h^{-1} to the total dose 4.0 kGy and the acrylamide-to-starch ratio of 2.5:1 have the maximum water absorption as 2,256 ± 25 g g^{-1} shown in Figures 4.35-4.36 have more pores with a structure. It is supposed that these pores are the regions of water permeation in which the interaction of the hydrophilic groups with water makes the saponified copolymer the high water absorption.

Figure 4.37 shows the SEM photograph of starch-*g*-poly(acrylamide-*co*-maleic acid) at dose rate of 1.71 kGy h^{-1} to the total dose of 4.0 kGy at the acrylamide-to-starch ratio of 3:1 has high crosslink density due to the high percentage gel content and increased polyimide from imidization of acrylamide. It appears from the photograph that the starch copolymer is composed of fine network structure. This observation is found to be in a good agreement with its less water absorbency at 2,037 ± 21 g g^{-1}.

Figure 4.35 SEM photograph of the saponified starch-*g*-poly(acrylamide-*co*-maleic acid) at DR 1.71 kGy h^{-1} to the TD 4.0 kGy (WA = 2,256 ± 25 g g^{-1})

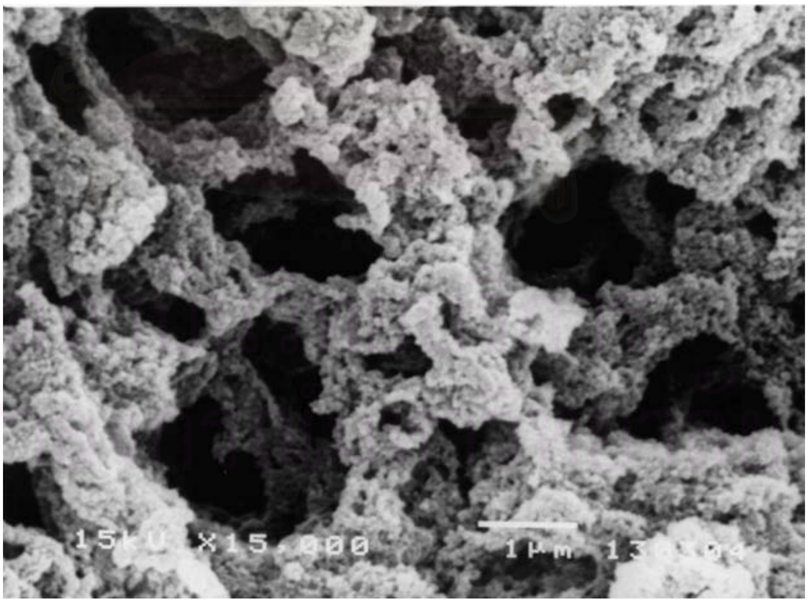

Figure 4.36 SEM photograph showing the cellular structure of the saponified starch-*g*-poly(acrylamide-*co*-maleic acid) at DR 1.71 kGy h^{-1} to the TD 4.0 kGy at 15,000 x magnification (WA = 2,256 ± 25 g g^{-1})

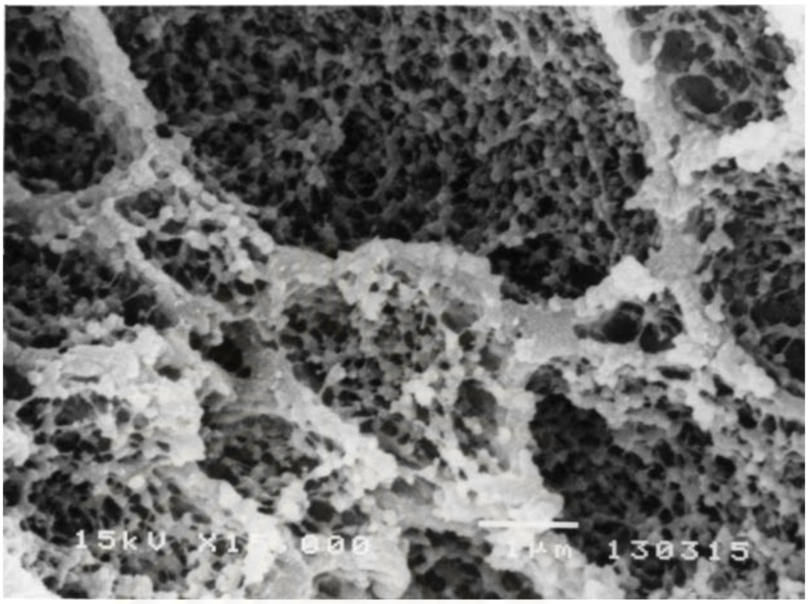

Figure 4.37 SEM photograph showing the cellular structure of the saponified starch-*g*-poly(acrylamide-co-maleic acid) at the acrylamide-to-starch ratio of 3:1 (WA = 2,037 ± 21 g g^{-1})

Part II: **Effect of Acid Additives on Grafting Efficiency and Water Absorption of Cassava Starch–Polyacrylamide/acrylic acid via γ - irradiation.**

4.5 Characterization of the Functional Groups of the Copolymer by FTIR.

The FT – IR spectra of graft copolymer before extraction, after extraction, and after saponification are given in Tables 4.18 – 4.19 and Figures 4.38 – 4.43

The IR spectra of grafting of acrylamide onto the starch backbone before extraction, after extraction and after saponification are similar to the Tables 4.1 and Figure 4.2-4.4 in Part I.

For the acrylic acid graft copolymerization, IR spectra in both before and after extraction (Figures 4.38 – 4.39) give all the absorption peaks of cassava starch and give the additional weak peaks at 2,356 cm^{-1}, strong peak at 1,709 cm^{-1}, weak peak at 1,266 cm^{-1} and 923 cm^{-1} indicating the O – H stretching, C = O stretching, C – O stretching and O – H bending of the - COOH group containing in the acrylic acid, respectively. When starch-*g*-poly(acrylic acid) was saponified, the disappearance of the absorption peaks of - COOH group and the existence of the absorption peaks at 1,407 and 1,572 cm^{-1} of C = O stretching of carboxylate ion indicate that acrylic acid moieties have been converted to acrylate (Figure 4.40).

The IR spectra of starch-*g*-poly(acrylamide-*co*-acrylic acid) in both before and after extraction (Figures 4.41 – 4.42) give all the absorption peaks of cassava starch, acrylamide, and acrylic acid. It is therefore confirmed that both acrylamide and acrylic acid have been grafted onto the cassava starch. After starch-*g*-poly(acrylamide-*co*-acrylic acid) was saponified, we can observe the characteristic absorption peaks of acrylamide and acrylate moieties (Figure 4.43).

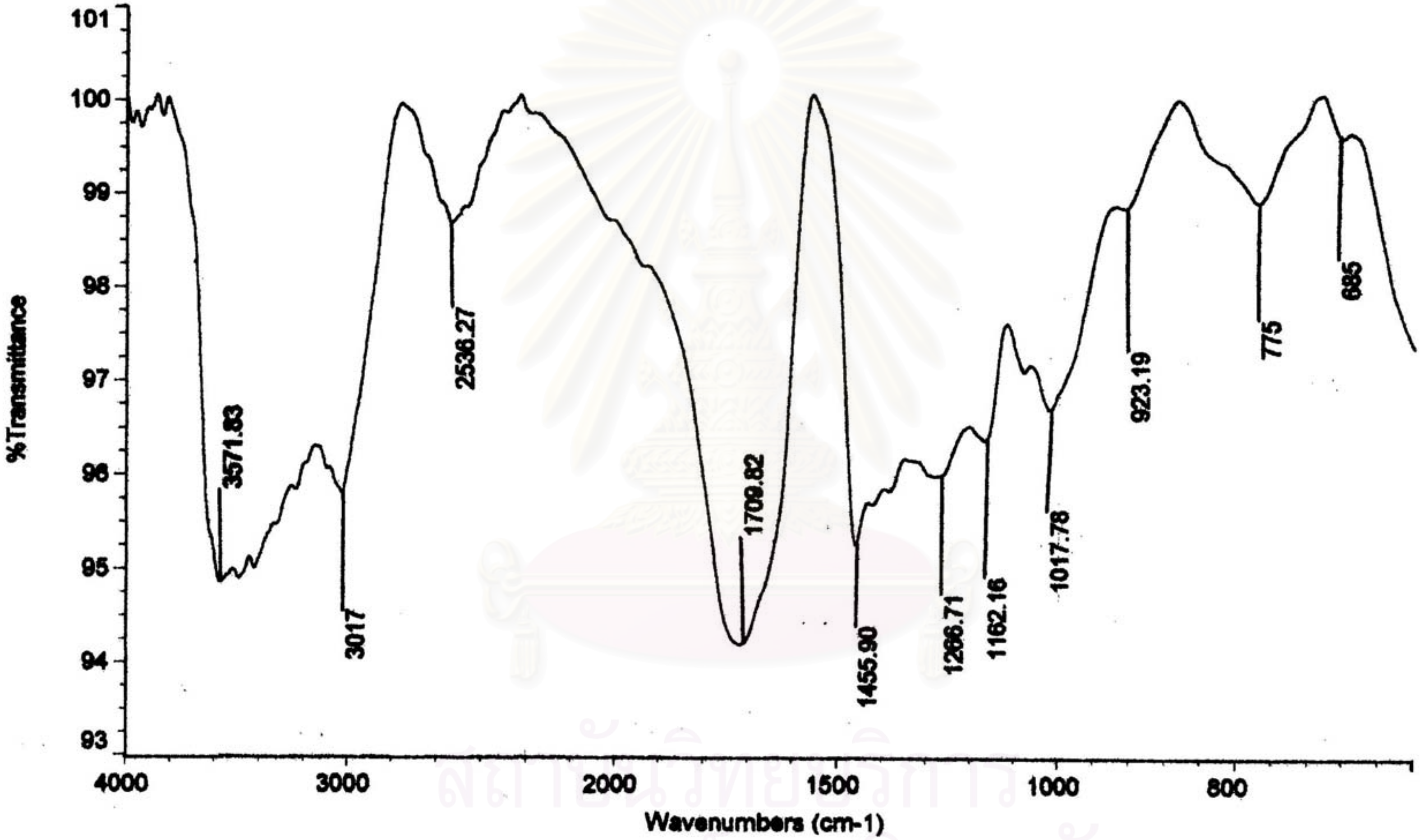

Figure 4.38 Infrared spectrum of starch-g-poly(acrylic acid) before extraction

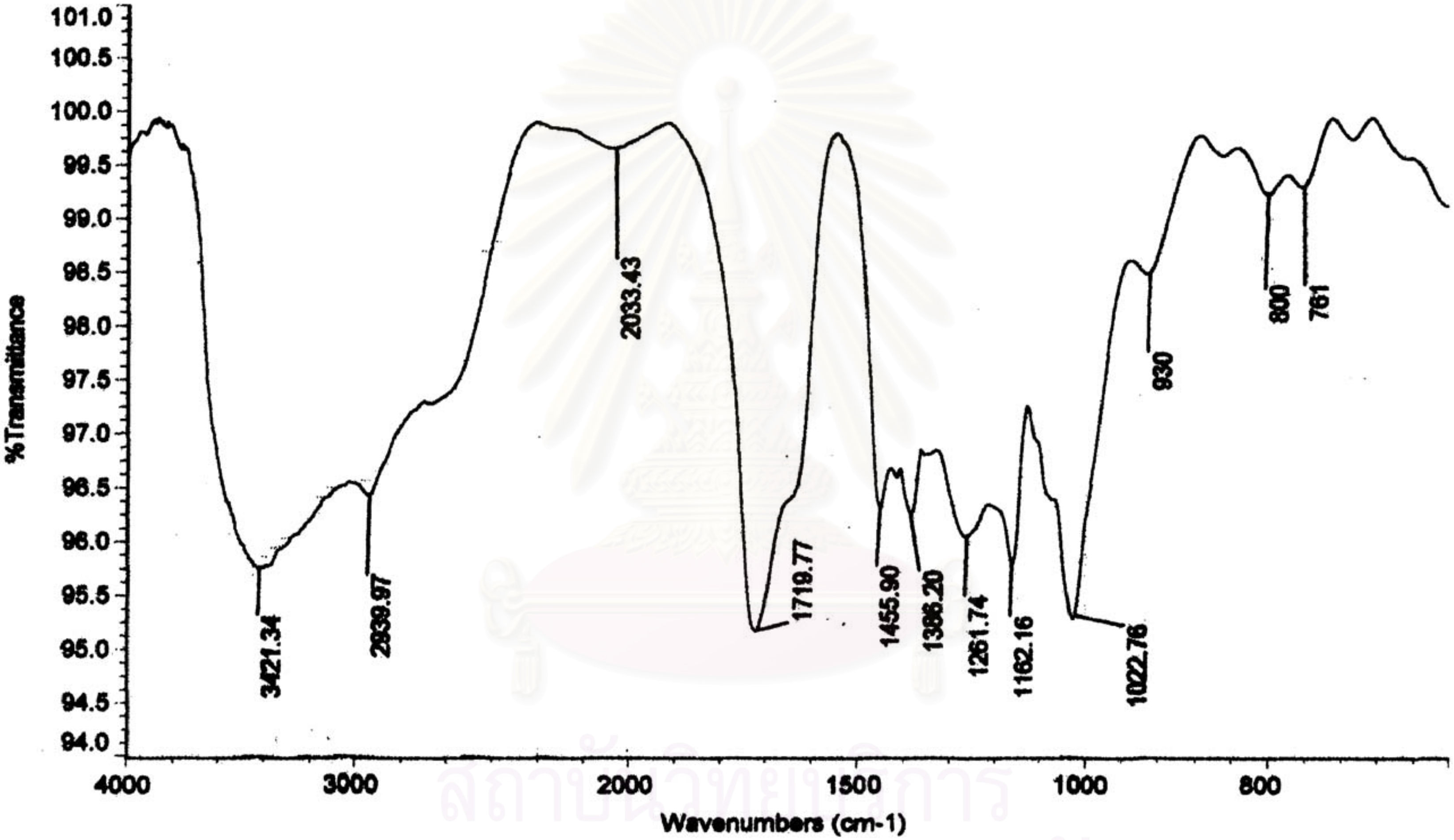

Figure 4.39 Infrared spectrum of starch-g-poly(acrylic acid) after extraction

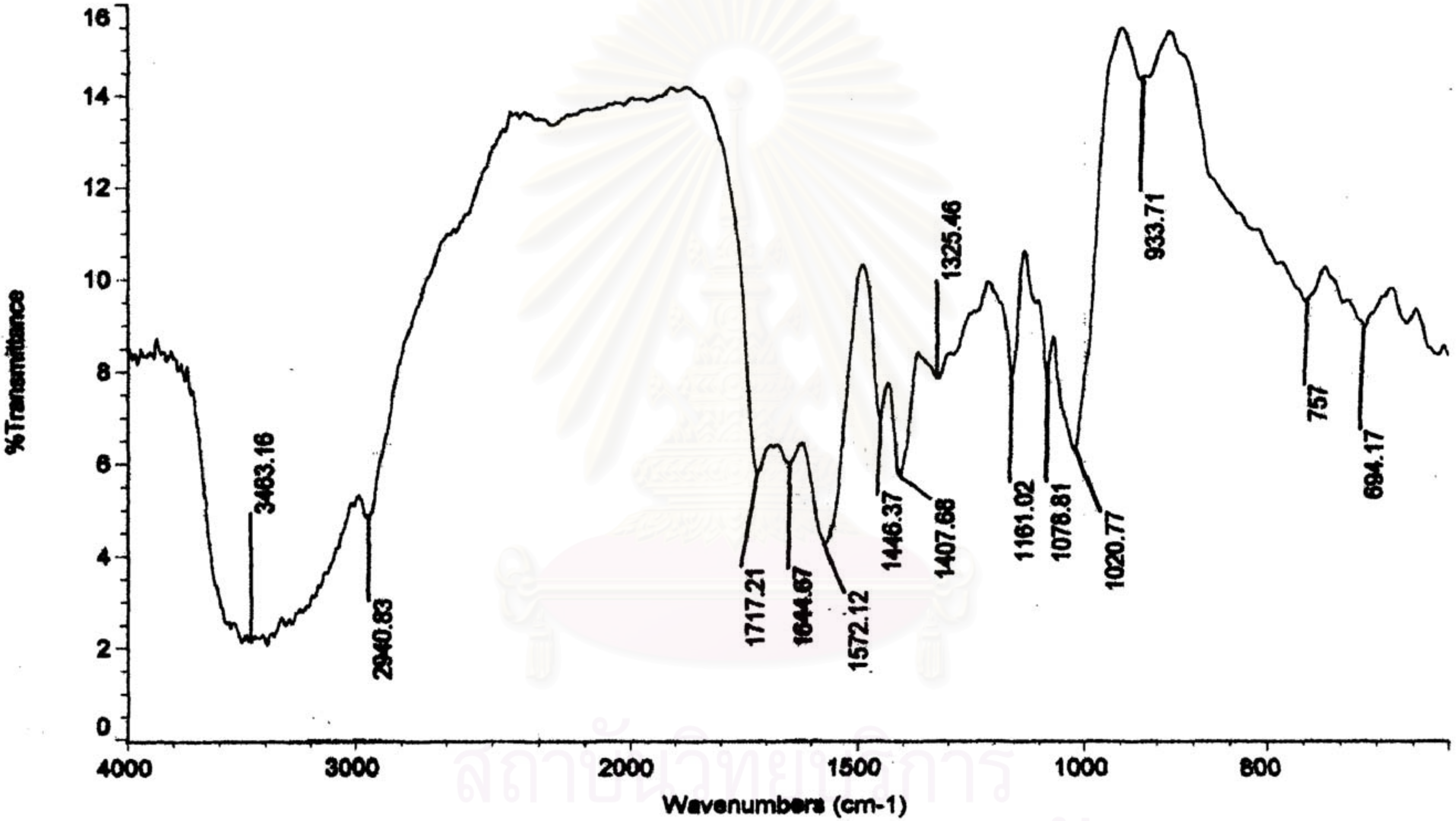

Figure 4.40 Infrared spectrum of starch-g-poly(acrylic acid) after saponification

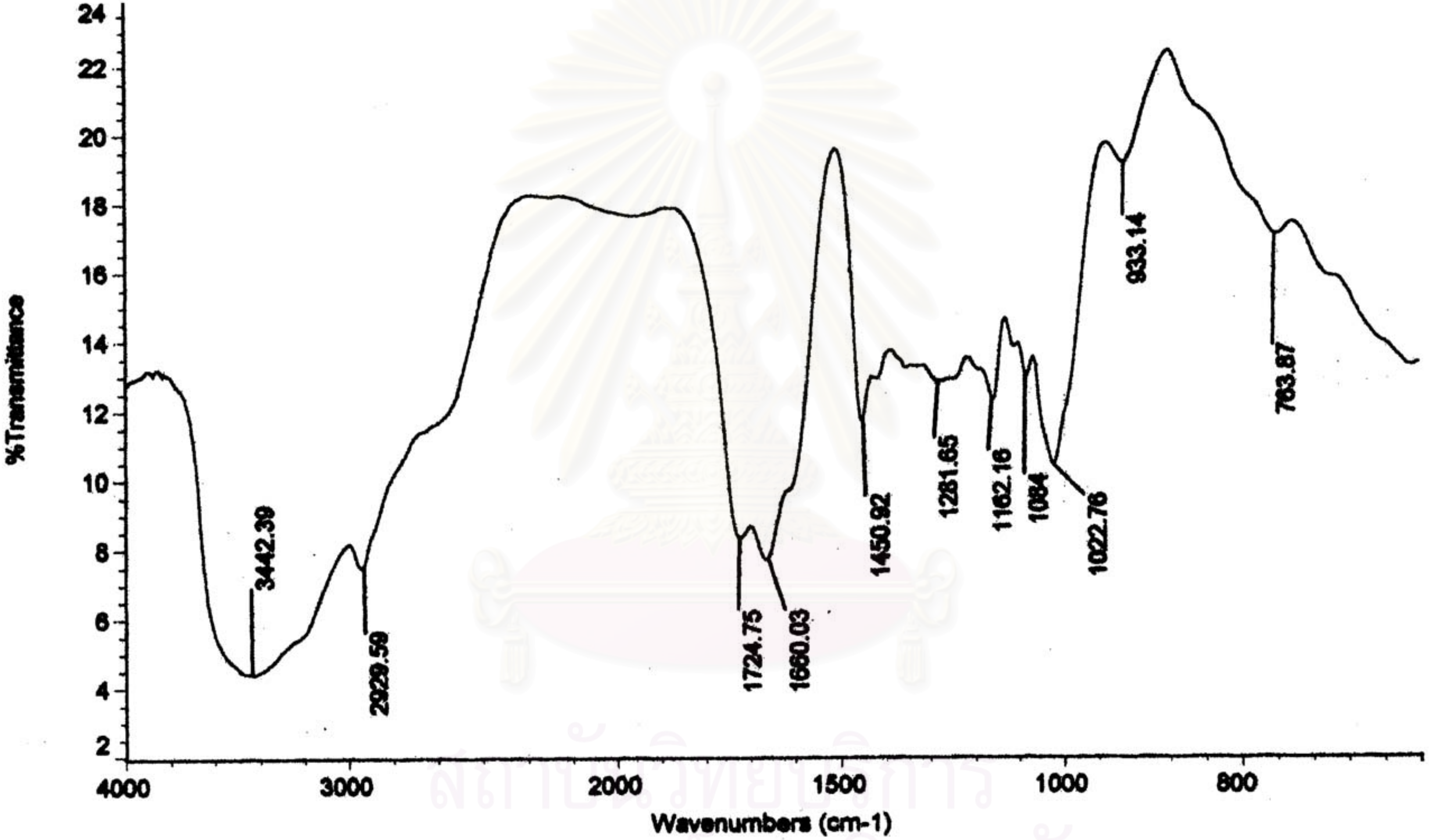

Figure 4.41 Infrared spectrum of starch-g-poly(acrylamide-co-acrylic acid) before extraction

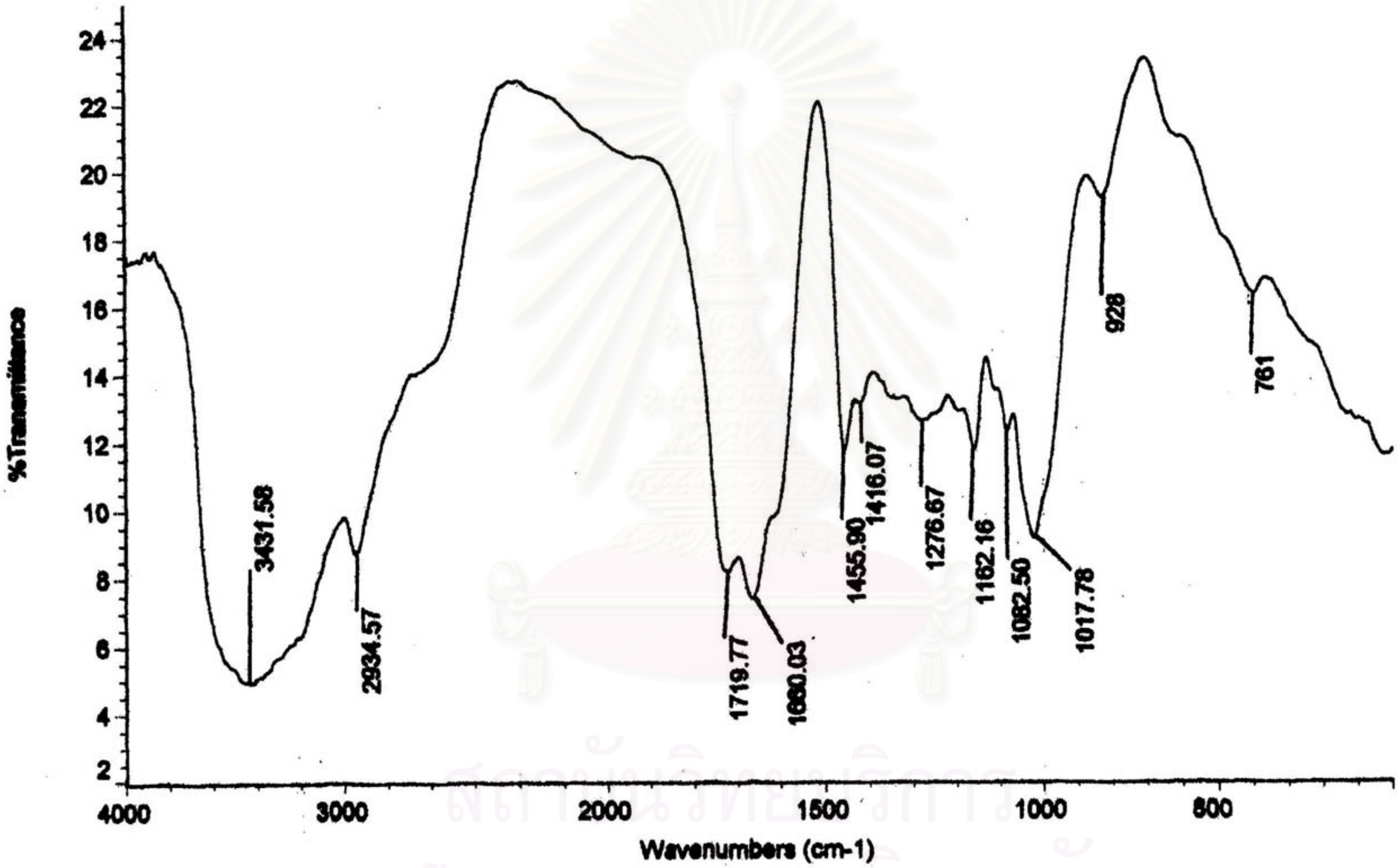

Figure 4.42 Infrared spectrum of starch-g-poly(acrylamide-co-acrylic acid) after extraction

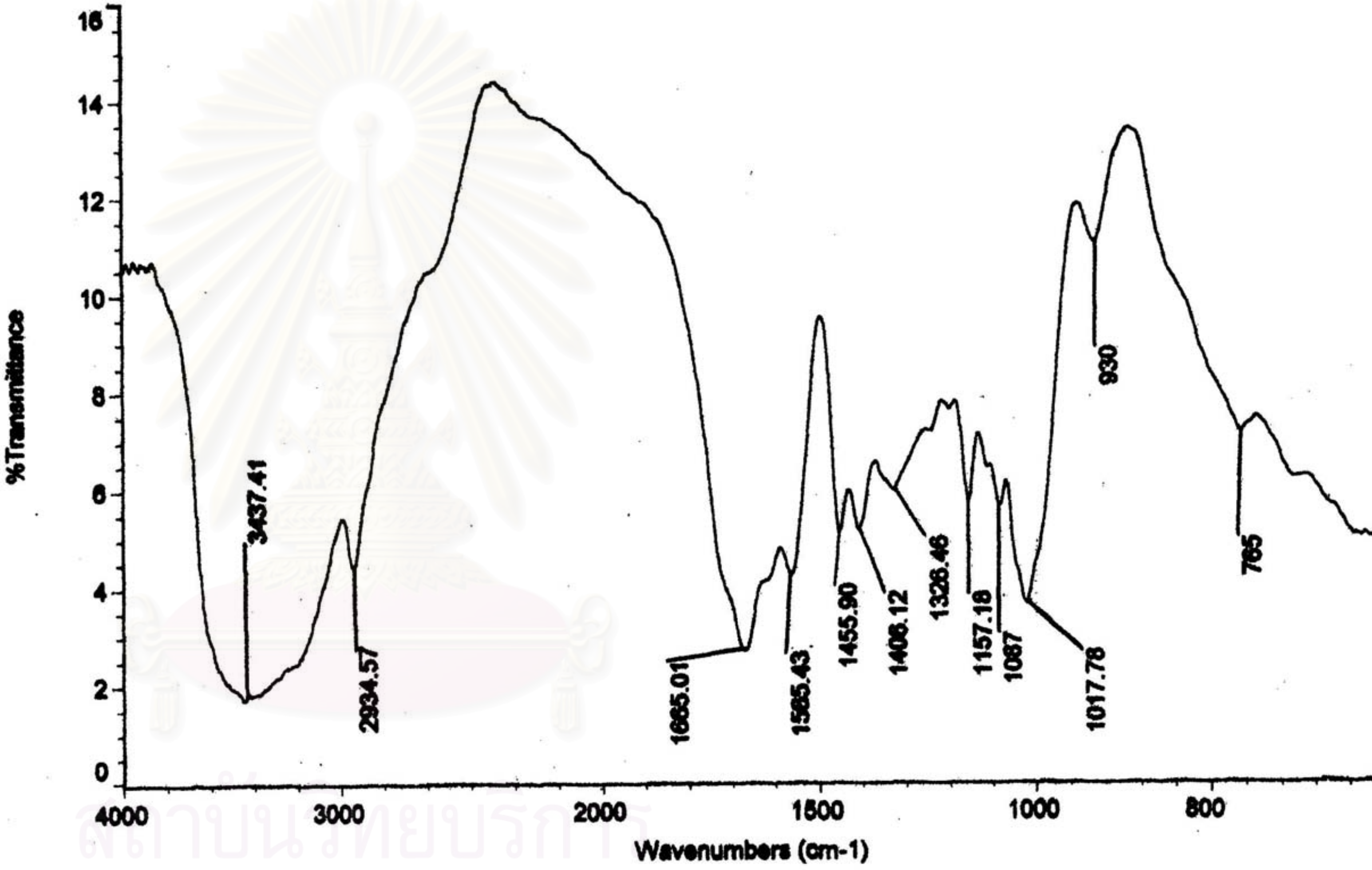

Figure 4.43 Infrared spectrum of starch-g-poly(acrylamide-co-acrylic acid) after saponification

Table 4.18 The Infrared Absorption of Functional Groups in Cassava Starch and Starch-*g*-poly(acrylic acid) Before Extraction, After Extraction, and After Saponification.

Starch		**Starch-*g*-poly(acrylic acid) before extraction**		**Starch-*g*-poly(acrylic acid) after extraction**		**Starch-*g*-poly(acrylic acid) after saponification**	
wave number (cm^{-1})	assignment	wave number (cm^{-1})	assignment	wave number (cm^{-1})	assignment	wave number (cm^{-1})	assignment
3,397	O – H stretching	3,571	O – H stretching	3,421	O – H stretching	3,463	O – H stretching
2,929	C – H stretching of CH_2	3,017	C – H stretching of CH_2	2,939	C – H stretching of CH_2	2,940	C – H stretching of CH_2
1,455	C – H bending of CH_2	1,455	C – H bending of CH_2	1,455	C – H bending of CH_2	1,446	C – H bending of CH_2
1,366 and 1,421	O – H bending	1,386	O – H bending	1,386	O – H bending	1,407	O – H bending
1,017	C – O stretching	1,162	C – O stretching	1,162	C – O stretching	1,161	C – O stretching
		2,536	O – H stretching of carboxylic acid	2,450	O – H stretching of carboxylic acid	2,440	O – H stretching of carboxylic acid
		1,709	C = O stretching of carboxylic acid	1,719	C = O stretching of carboxylic acid	1,717	C = O stretching of carboxylic acid
		1,266	C – O stretching of carboxylic acid	1,261	C – O stretching of carboxylic acid	1,325	C – O stretching of carboxylic acid

Table 4.18 The Infrared Absorption of Functional Groups in Cassava Starch and Starch-*g*-poly(acrylic acid) Before Extraction, After Extraction, and After Saponification (continued).

Starch		**Starch-*g*-poly(acrylic acid) before extraction**		**Starch-*g*-poly(acrylic acid) after extraction**		**Starch-*g*-poly(acrylic acid) after saponification**	
wave number (cm^{-1})	assignment	wave number (cm^{-1})	assignment	wave number (cm^{-1})	assignment	wave number (cm^{-1})	assignment
		923	O – H bending of carboxylic acid	930	O – H bending of carboxylic acid	933	O – H bending of carboxylic acid
						1,572	C = O stretching of carboxylate

Table 4.19 The Infrared Absorption of Functional Groups in Cassava Starch and Starch-*g*-poly(acrylamide-*co*-acrylic acid) Before Extraction, After Extraction, and After Saponification.

Starch		**Starch-*g*-poly(acrylamide-*co*-acrylic acid) before extraction**		**Starch-*g*-poly(acrylamide-*co*-acrylic acid) after extraction**		**Starch-*g*-poly(acrylamide-*co*-acrylic acid) after saponification**	
wave number (cm^{-1})	assignment	wave number (cm^{-1})	assignment	wave number (cm^{-1})	assignment	wave number (cm^{-1})	assignment
3,397	O – H stretching	3,442	O – H stretching	3,431	O – H stretching	3,437	O – H stretching
2,929	C – H stretching of CH_2	2,929	C – H stretching of CH_2	2,934	C – H stretching of CH_2	2,934	C – H stretching of CH_2
1,455	C – H bending of CH_2	1,450	C – H bending of CH_2	1,455	C – H bending of CH_2	1,455	C – H bending of CH_2
1,366 and 1,421	O – H bending	1,281	O – H bending	1,276	O – H bending	1,250	O – H bending
1,017	C – O stretching	1,022	C – O stretching	1,017	C – O stretching	1,017	C – O stretching
		3,110	N – H stretching	3,105	N – H stretching	3,105	N – H stretching
		1,660	C = O stretching of carboxamide	1,660	C = O stretching of carboxamide	1,665	C = O stretching of carboxamide
		1,607	N – H bending	1,607	N – H bending	1,620	N – H bending
		1,245	C – N stretching	1,252	C – N stretching	1,240	C – N stretching

Table 4.19 The Infrared Absorption of Functional Groups in Cassava Starch and Starch-*g*-poly(acrylamide-*co*-acrylic acid) Before Extraction, After Extraction, and After Saponification. (continued)

Starch		**Starch-*g*-poly(acrylamide-*co*-acrylic acid) before extraction**		**Starch-*g*-poly(acrylamide-*co*-acrylic acid) after extraction**		**Starch-*g*-poly(acrylamide-*co*-acrylic acid) after saponification**	
wave number (cm^{-1})	assignment	wave number (cm^{-1})	assignment	wave number (cm^{-1})	assignment	wave number (cm^{-1})	assignment
		2,801	O – H stretching of carboxylic acid	2,805	O – H stretching of carboxylic acid	2,801	O – H stretching of carboxylic acid
		1,724	C = O stretching of carboxylic acid	1,719	C = O stretching of carboxylic acid	1,665	C = O stretching of carboxylic acid
		1,356	C – O stretching of carboxylic acid	1,355	C – O stretching of carboxylic acid	1,326	C – O stretching of carboxylic acid
		933	O – H bending of carboxylic acid	928	O – H bending of carboxylic acid	930	O – H bending of carboxylic acid
						1,585	C = O stretching of carboxylate

4.6 Effect of Acid Additives on Graft Copolymerization.

In a grafting reaction, the presence of additives can influence both the processing conditions and the properties of the finished product.

4.6.1 Effect of Acid Additives on Graft Copolymerization of Acrylamide onto Cassava Starch.

The experimental data for the grafting of AM onto cassava starch with sulfuric acid or maleic acid are shown in Table 4.20.

Table 4.20 Effect of Acid Additives on Graft Copolymerization of Acrylamide onto Cassava Starch.

Additives	**Conv. (%)**	**Homo (%)**	**GE (%)**	**Add-on (%)**	**WA ($g\ g^{-1}$)**
no additive	99.4	7.3	88.2	58.7	593 ± 33
0.01 M H_2SO_4 [a]	96.2	2.5	95.1	50.0	343 ± 42
1% maleic acid [b]	90.6	19.5	71.3	60.2	438 ± 69
2% maleic acid [b]	99.1	22.5	68.4	62.8	482 ± 21
3% maleic acid [b]	96.1	26.9	58.8	52.6	540 ± 58

Conv. = Conversion; Homo = Homopolymer; GE = Grafting Efficiency; WA = Water Absorption; The AM-to-starch ratio = 2:1 with a dose rate of 1.71 kGy h^{-1}, and total dose of 6.0 kGy.

a 10 ml of 0.01 M H_2SO_4

b % by weight of the monomer

4.6.1.1 Effect of Sulfuric Acid on Graft Copolymerization of Acrylamide onto Cassava Starch.

As shown in Table 4.20, the conversion of monomer does not change significantly when the acid was used. At the total dose given, the ionizing radiation can initiate a certain number of free radicals that are used both for homopolymerization and graft copolymerization in a proper ratio.

It is well known that addition of some mineral acids to some grafting solutions could enhance the grafting yield where inclusion of acid in water during irradiation led to an increase in *G*(H2) which was attributed to an enhancement in *G*(H) (Equations 4.11 and 4.12)

$$H_2O + H^+ \rightarrow H_3O^+ \qquad (4.11)$$

$$H_3O^+ + e^-_{aq} \rightarrow H_2O + H^\bullet \qquad (4.12)$$

In grafting systems the H atom produced can initiate the hydrogen abstract reaction with matrix and addition reaction with monomer followed by increasing grafting. Moreover, the acid has a role in partitioning phenomena. The concentration of monomer available at a grafting site in the starch was thus enhanced in the presence of acid. With starch (StOH) as backbone polymer there is an additional mechanism for H atom formation due to the presence of the hydroxyl groups in exchangeable positions (Equations 4.13 and 4.14)

$$StOH + H^+ \rightarrow StOH_2{}^+ \qquad (4.13)$$

$$StOH_2{}^+ + e^- \rightarrow StOH + H^\bullet \qquad (4.14)$$

The process may also lead to the creation of further grafting sites (Equation 4.15) [55].

$$StOH + H^{\bullet} \rightarrow StO^{\bullet} + H_2 \qquad (4.15)$$

These mechanisms of an acid effect in grafting induced by ionizing radiation cause an increase in grafting efficiency and decreasing the homopolymer formation.

The water absorption of saponified starch-*g*-polyacrylamide when the acid was used is lower than that without the acid. More graft copolymer so obtained increase the chain flexibility, though the imidization of the amide pendants in the polymer in the former case restricting its swelling resulting from more rigidity of the chains.

4.6.1.2 Effect of Maleic Acid on Graft Copolymerization of Acrylamide onto Cassava Starch.

The Experimental data of the effect of maleic acid (MA) on the grafting of AM onto starch are given in Table 4.20. As the MA was used, the conversion of monomer is rather constant at the given total dose because the ionizing radiation can initiate a certain number of free radicals.

After the monomers of AM and MA have been irradiated by γ-rays, free radicals are generated. Random reactions of these radicals with the monomers lead to the formation of copolymers of AM and MA. The results show that when maleic acid content increases the homopolymer increases, the grafting efficiency and the percentage add-on decreases. This is due to the formation of the ungrafted, free copolymer of AM and MA.

The water absorption decreases when compared with the copolymers without additive, but it tends to increase when maleic acid content increases. This may be due to the CT complex of AM and MA, because AM as a donor is an electron-rich vinyl monomer while MA as an acceptor is an electron poor vinyl monomer. The CT complex could be an intermediate in the grafting reaction as described in Section 3.3.3.4 in Part I.

4.6.2 Effect of Acid Additives on Graft Copolymerization of Acrylic Acid onto Cassava Starch.

Table 4.21 shows the effect of sulfuric acid on the grafting of AA onto cassava starch in terms of the conversion of monomer, homopolymer formed, grafting efficiency, percentage add-on, and water absorption.

Table 4.21 Effect of Acid Additive on Graft Copolymerization of Acrylic Acid onto Cassava Starch.

Additives	Conv. (%)	Homo (%)	GE (%)	Add – on (%)	WA ($g\ g^{-1}$)
no additive	89.3	2.2	95.9	53.3	237 ± 18
0.01M H_2SO_4[a]	97.5	2.4	95.8	54.7	210 ± 44

Conv. = Conversion; Homo = Homopolymer; GE = Grafting Efficiency; WA = Water Absorption; the AA-to-starch ratio = 2:1 with a dose rate of 1.71 kGy h^{-1} to a total dose of 6.0 kGy

[a] 10 ml of 0.01 M H_2SO_4

As shown in Table 4.21, conversion and homopolymer increases when the sulfuric acid was used because higher radical concentrations increases grafting probability but some homopolymer is always simultaneously formed as a competing reaction to grafting during irradiation. Since acid enhances both processes [56].

The water absorption slightly decreases when sulfuric acid is used. This may be due to the concentration of H_2SO_4 is too high. H_2SO_4 hydrolyzed the starch backbone before the starch can be grafted with acrylic acid so the water absorption decreases.

4.6.3 Effect of Acid Additives on Graft Copolymerization of Acrylamide and Acrylic Acid onto Cassava Starch.

Experimental data for the grafting of AM and AA onto cassava starch with various concentrations of sulfuric acid are shown in Table 4.22

Table 4.22 Effect of Acid Additives on Graft Copolymerization of Acrylamide and Acrylic Acid onto Cassava Starch.

Additive	**Conv. (%)**	**Homo (%)**	**GE (%)**	**Add – on (%)**	**WA (g g-1)**
no additive	98.0	9.8	84.4	58.9	1,230 ± 27
0.001M H_2SO_4	92.8	6.5	88.2	51.6	414 ± 33
0.01M H_2SO_4	97.9	7.9	86.9	56.9	332 ± 50
0.1M H_2SO_4	91.6	15.6	76.3	59.7	277 ± 79

Conv. = Conversion; Homo = Homopolymer; GE = Grafting Efficiency;
WA = Water Absorption; the AM:AA = 50:50 with a dose rate of 1.71 kGy h^{-1} to a total dose of 6.0 kGy

As shown in Table 4.22, the homopolymer decreases when 0.001 *M* H_2SO_4 is used but at the higher acid concentration the homopolymer increases. The grafting efficiency increases at 0.001 *M* H_2SO_4 and tends to decrease at the higher acid concentration and the water absorption decreases with increasing acid concentration. The initiator radicals formed tend to initiate homopolymerization rather than grafting reaction. The higher acidity of sulfuric acid appears to attack and hydrolyse the starch backbone before sufficient protective grafting can occur [57].

Too high an acid concentration causes random cleavage of the $\alpha\ 1 \rightarrow 4$ and $\alpha\ 1 \rightarrow 6$ linkages in the starch molecules. In addition, further hydrolysis causes the outer layer of the starch grain surface to erode away. After complete erosion is accomplished, an inner layer or underlayer is revealed with the smooth surface similar to that of the native starch grain surface. The crystallinity of the starch increases while its amylose content decreases so the grafting efficiency decreases [58]. The graft copolymer with lower grafting efficiency gives the saponified product with a lower water absorption.

4.7 Surface Morphology of the Copolymers of Cassava Starch-g-AA/AM and/or Acrylic Acid.

The surface appearance and structure of saponified graft copolymer of cassava starch-*g*-AA/AM were observed using the scanning electron microscopy. The photographs taken by the electron microscope of the saponified starch graft copolymers are shown in Figures 4.44 – 4.51

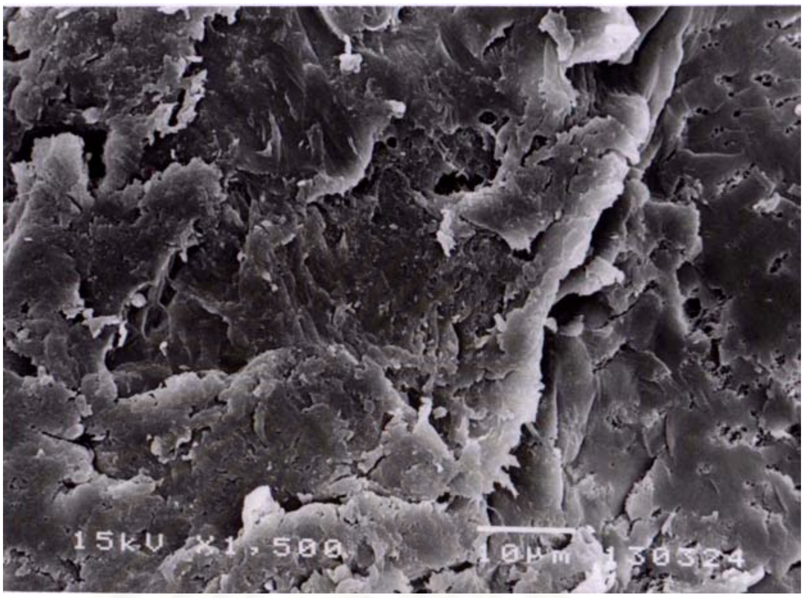

Figure 4.44 SEM photograph of the saponified starch-*g*-polyacrylamide.

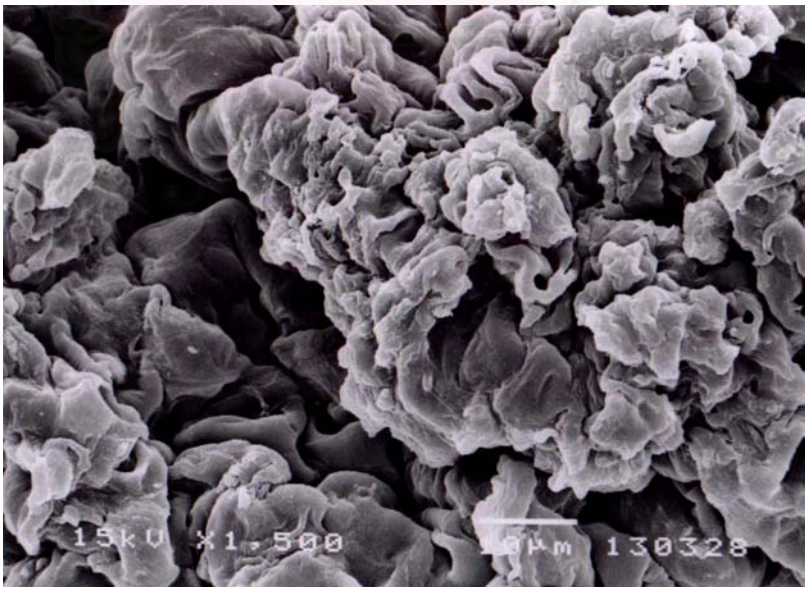

Figure 4.45 SEM photograph of the saponified starch-*g*-poly(acrylamide-*co*-maleic acid), 3% maleic acid.

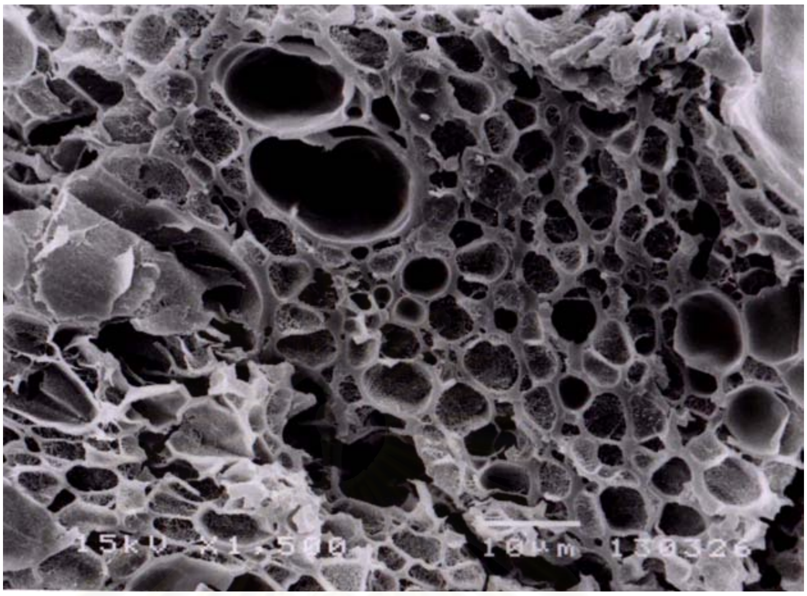

Figure 4.46 SEM photograph of the saponified starch-*g*-polyacrylamide, with 0.01*M* H_2SO_4 as an additive.

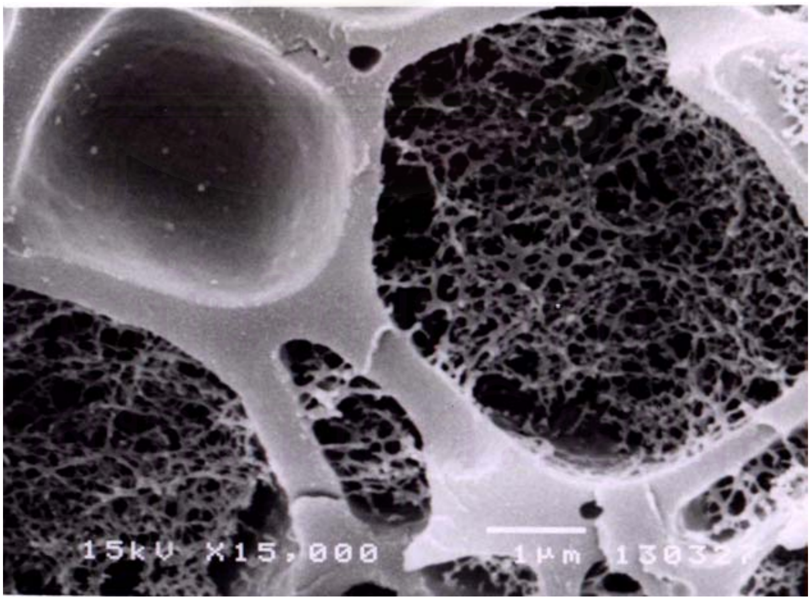

Figure 4.47 SEM photograph showing the cellular structure of the saponified starch-*g*-polyacrylamide, with 0.01*M* H_2SO_4 as an additive at 15,000 x magnification.

SEM photographs of saponified starch-*g*-polyacrylamide and starch-*g*- poly (acrylamide-*co*-maleic acid) (Figures 4.44 - 4.45) show that the saponified graft copolymers have a coarse network with uneven mass and chain entanglement. Figures 4.46 - 4.47 show the porous structure with fine crosslink network of starch-*g*-polyacrylamide in which sulfuric acid is used as an additive. It is supposed that too high the chain entanglement obstructs water absorption.

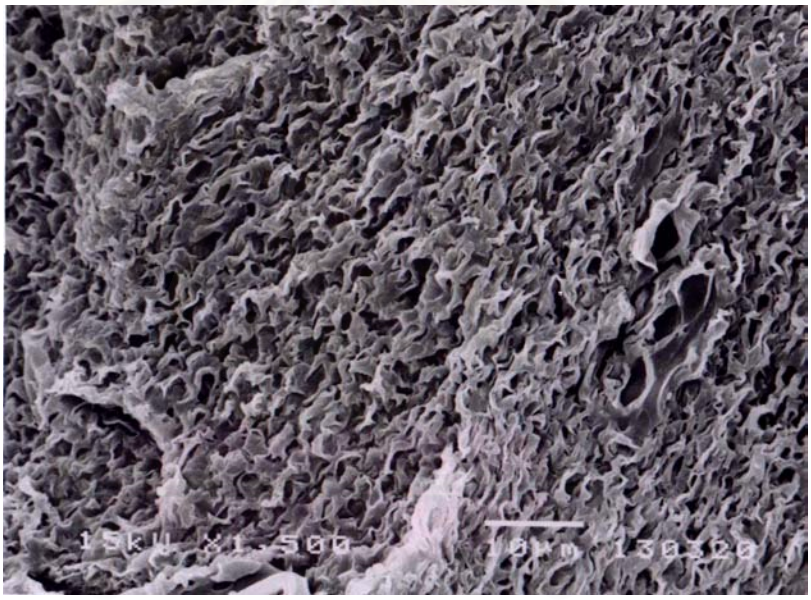

Figure 4.48 SEM photograph of the saponified starch-*g*-poly(acrylic acid).

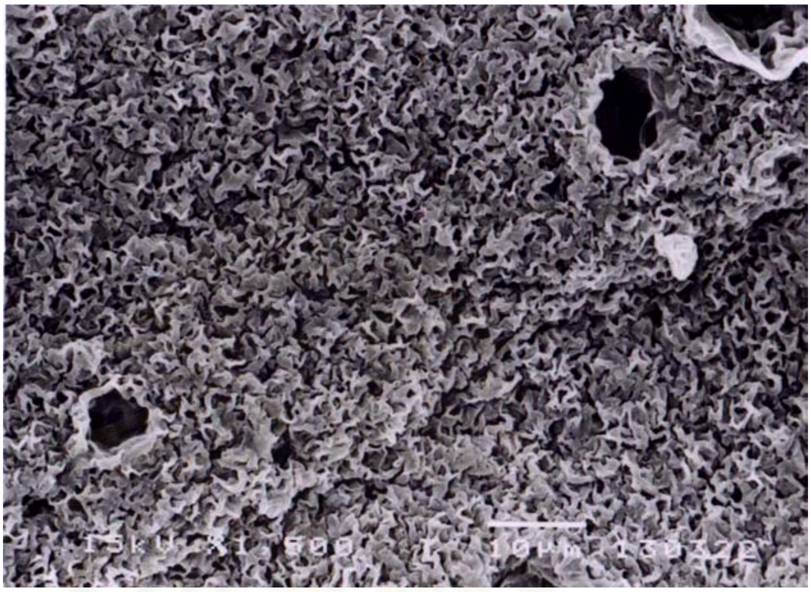

Figure 4.49 SEM photograph of the saponified starch-*g*-poly(acrylic acid), with 0.01*M* H_2SO_4 as an additive.

Figures 4.48 – 4.49 show the SEM photographs of saponified starch-*g*-poly (acrylic acid) and saponified starch-*g*-poly(acrylic acid) with 0.01*M* H_2SO_4, respectively. The photograph shows the porous structures and a broad network of starch-*g*-PAA in Figure 4.48 and a semi-porous structure in Figure 4.49.

SEM photograph of saponified starch-*g*-poly(acrylamide-*co*-acrylic acid), which is polymer of good absorbency, as illustrated in Figure 4.50, shows that the saponified graft copolymer has tiny pores. In the case of saponified starch-*g*-poly(acrylamide-*co*-acrylic acid) with 0.001 *M* H_2SO_4 additive, the SEM photograph (Figure 4.51) shows huge open pores connecting together like a fisherman net.

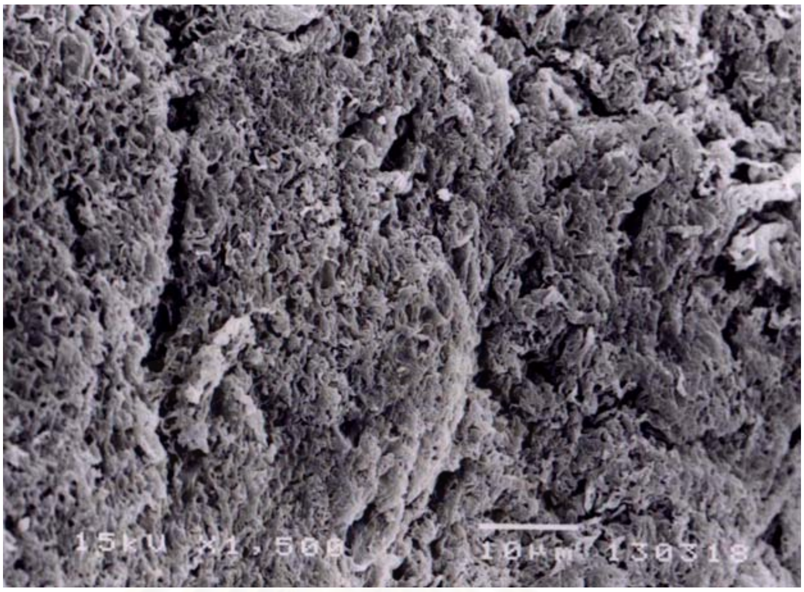

Figure 4.50 SEM photograph of the saponified starch-*g*-poly(acrylamide-*co*-acrylic acid).

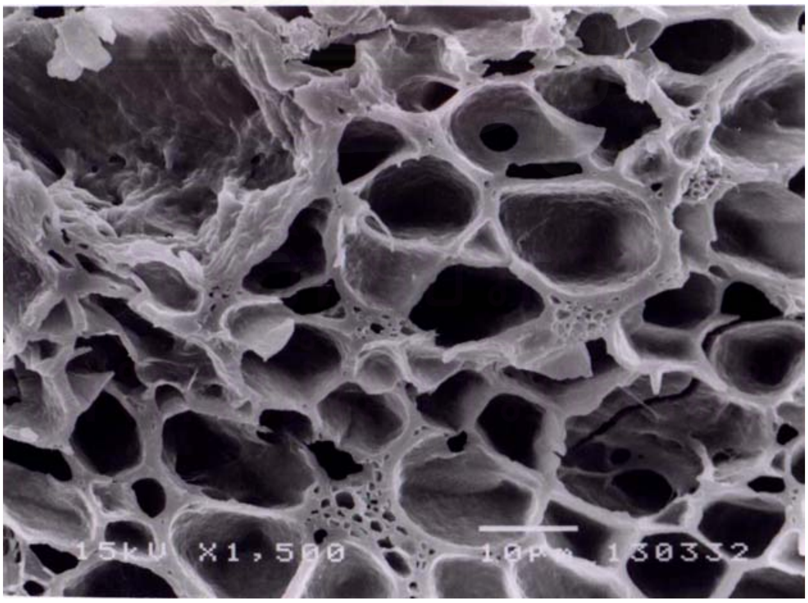

Figure 4.51 SEM photograph of the saponified starch-*g*-poly(acrylamide-*co*-acrylic acid), with 0.001*M* H_2SO_4 as additive.

CHAPTER 5

CONCLUSION and SUGGESTION

5.1 Conclusion

High-water absorption polymers of the saponified starch-*g*-poly (acrylamide-*co*-maleic acid) were synthesized by a simultaneous irradiation technique using gamma rays as an initiator under various conditions followed by alkaline saponification. The effect of acid additive on starch-*g*-polyacrylamide, starch-*g*-poly(acrylic acid), and starch-*g*-poly(acrylamide-*co*-acrylic acid) was determined. The absorption behavior of high-water absorbing polymers is related to their chemical structure, chemical composition, the absorbing environment, and the nature of the solution. Both the positive and negative effects to the above mentioned attributes are found. The positive influences toward enhancement of the grafting reaction and water absorption are, of course, very important. The negative part of the result is the master for future improvement. The results are summarized as follows:

Part I:

1. Starch-*g*-polyacrylamide and starch-*g*-poly(acrylamide-*co*-maleic acid) were synthesized and confirmed by the FT – IR spectroscopy. The infrared absorption spectra of starch-*g*-polyacrylamide give the absorption peaks at 3,397 cm^{-1}, 2,929 cm^{-1}, 1,455 cm^{-1}, at 1,366, 1,421 cm^{-1}, and 1,017 cm^{-1} indicating the O

– H stretching, C – H stretching, C – H bending, O – H bending and C – O stretching of cassava starch, respectively, and the absorption peaks at 3,192 cm^{-1}, 1,664 cm^{-1}, 1,611 cm^{-1}, 1,325 and 1,354 cm^{-1} indicating the N – H stretching, C = O stretching, N – H bending, and C – N stretching of the - $CONH_2$ group containing in the acrylamide, respectively. When the starch-*g*-polyacrylamide was saponified, the addition peak at 1,558 cm^{-1} indicates the C = O stretching of the carboxylate group. In the case of starch-*g*-poly(acrylamide-*co*-maleic acid), its infrared absorption spectra give all absorption peaks of cassava starch and give the additional peaks at 2,786, 1,664, 1,206 and 937 cm^{-1} indicating the O – H stretching, C = O stretching, C – O stretching and O – H bending of the - COOH group containing in maleic acid, respectively. After starch-*g*-poly(acrylamide-*g*-maleic acid) has been saponified, the stronger band at 1,383 cm^{-1} of the C = O stretching of the carboxylate ion indicates that acrylamide and maleic acid moieties have been converted to the carboxylate group.

2. The optimum time and temperature for a saponification of the graft copolymer with 5% potassium hydroxide solution is ninety minutes at room temperature. During this period the acrylamide moieties can be converted to the acrylate salt and give the highest water absorption.

3. Increasing the quantities of total dose to graft copolymerization of acrylamide and maleic acid onto the starch at the fixed three dose rates does not only decrease the homopolymer but also increases the gel content, grafting efficiency, and percentage add-on. However, the total dose higher than 10 kGy at the dose rate of 4.34 kGy h^{-1}, the percentage add-on unfortunately decreases. This is attributed to the formation of small fragments of $OH^{\bullet}$, and e^{-}_{aq} to form homopolymer at the expense of grafting. The highest water absorption is obtained at the total dose of 4.0 kGy and dose rate of 1.71 kGy h^{-1}.

4. An increase in the irradiation dose rate at the fixed total dose increases the homopolymer but decreases conversion of monomer, gel content, grafting efficiency, percentage add-on, and water absorption due to the surplus radicals and short kinetic chains tend to terminate the grafting growing chains before an adequate grafting is reached.

5. Increasing the monomer-to-starch ratio enhances the gel content, the grafting efficiency, the percentage add-on and decreases the homopolymer. The water absorption is highest at the monomer-to-starch ratio of 2.5:1 and decreases with the increasing monomer-to-starch ratio higher than 2.5:1. This may be due to that chain transfer to polymer increases with increasing monomer concentration, which results in increasing amounts of branching and self-crosslinking reactions. Increasing the crosslinking density of the graft copolymer restricts the swelling of the highly water absorbents by elastic retraction forces.

6. An increase in the maleic acid contents decreases the gel content, grafting efficiency, and percentage add-on, but increases the homopolymer and the water absorption is highest at 2% maleic acid. This may be due to the attributes of a charge transfer complex between acrylamide as and electron donor and maleic acid as an electron acceptor. The charge transfer complex could be an intermediate in the grafting reaction so the hydrophilic sites increase. The water absorption decreases with the increasing maleic acid content higher than 2% due to an increase in the ungrafted copolymer of acrylamide and maleic acid at the sacrifice of the grafting acrylamide monomer.

7. The swelling of copolymer which retains distilled water as high as 2,256 g g^{-1} its dried weight, was studied in the isotonic fluid of 0.9% w v^{-1} of NaCl, $MgCl_2$ and $CaCl_2$ solutions. The water absorption in the salt solutions is very much lower than that in distilled water due to the screening of the ionic charge bound to the network, which decreases the osmotic pressure difference between inside of the gel and the external solution. The water absorption in the multivalent saline solution decreases much more strongly in comparison with that in the monovalent saline solution.

8. The water absorbency of the copolymer was found to increase with increasing pHs of the external solution until pH 5, after which it remains relatively uncharged because of the anionic nature of copolymer.

9. The water absorbency of the copolymer was found to increase with decreasing the particle size (μm). Because the additional mass of interparticles, the unsorbed liquid outside was able to penetrate into the mass, which increases the water absorption.

10. The surface morphology of the saponified graft copolymers studied by SEM reveals that saponified graft copolymers having a higher water absorbency are more porous.

Part II:

1. Starch-*g*-polyacrylamide, starch-*g*-poly(acrylic acid), starch-*g*-poly (acrylamide-*co*-acrylic acid) were synthesized and confirmed by the FT – IR spectroscopy. The infrared spectra of starch-*g*-poly(acrylic acid) give all absorption peaks of cassava starch and give the additional peaks at 2,356, 1,709, 1,266, and 923 cm^{-1} indicating O – H stretching, C = O stretching, C – O stretching, and O – H bending of the - COOH group containing in acrylic acid, respectively. After starch-*g*-poly(acrylic acid) has been saponified, the disappearance of the absorption peaks of the - COOH group and the appearance of the absorption peaks at 1,407 and 1,572 cm^{-1} of the C = O stretching of the -COOK group indicates that the carboxylic group of the acrylic acid moiety has been converted to the carboxylate group. The IR spectrum of starch-*g*-poly (acrylamide-*co*- acrylic acid) gives all absorption peaks of cassava starch, acrylamide, and acrylic acid, and after saponification of this graft copolymer, we

can observe absorption peaks of the carboxylate group of the acrylate instead of the carboxylic group of acrylic acid.

2. Adding sulfuric acid into the reaction mixture of starch and acrylamide before irradiation, graft copolymerization increases along with the increasing grafting efficiency; because an increase in hydrogen atom yields [*G* (H)] from secondary electron capture by H^+, which leads to the increasing number of grafting sites, followed by increasing grafting probability caused by the partitioning phenomena. Unfortunately, the water absorption decreases because of the imidization of the amide pendants in the copolymer. The imidized structure of starch grafted acrylamide restricts its swelling due to more rigidity of the chains, which behave like a crosslinking polymer

When the maleic acid was added into the mixture of starch and acrylamide, the homopolymer increases while the grafting efficiency decreases. It indicates that both monomers prefer to copolymerizing as the ungrafted, free copolymer rather than the grafted copolymer onto starch, the water absorption thus decreases.

3. Adding sulfuric acid into the reaction mixture of starch and acrylic acid before irradiation, homopolymer increases while water absorption decrease. Sulfuric acid hydrolyzes the starch backbone before the starch could be grafted with acrylic acid.

4. Adding sulfuric acid into the reaction mixture of starch-g-poly (acrylamide-co-acrylic acid) before irradiation, the grafting efficiency increases and the homopolymer decreases, but at the higher concentration of sulfuric acid the grafting efficiency decreases and the homopolymer increases. At higher acidity of sulfuric acid, it could attack and hydrolyzed the starch backbone before the sufficient grafting occurs and further hydrolysis causes the higher crystallinity of the starch while its amylose content decreases so the grafting efficiency decreases.

5. The surface morphology of the saponified graft copolymers with acid and without acid additive studied by SEM shows that saponified graft copolymers without acid additive having the higher absorbency are more porous with tiny holes widely distributed on its surface.

5.2 Suggestions for Future Work.

The synthesis of saponified cassava starch-acrylamide/maleic acid graft copolymers as superabsorbent polymers by a simultaneous irradiation technique should be further studied as follows:

1. The effect of other kinds of diprotic acid, such as, itaconic acid and cinnamic acid at various concentrations on grafting reaction and water absorption capacity should be carried out.

2. The effect of the other kinds of C-T complex, such as itaconic anhydride and acrylamide at various concentrations on grafting reaction and water absorption should be carried out. Detailed studies of C-T complex formation and mechanism should be elucidated.

3. The effect of particle size and distribution on the water absorption rate is worthwhile to investigate.

4. Investigation of the graft copolymerization of chitosan, acrylamide and acrylic acid should be carried out. We anticipate that the hygiene properties may be improved.

REFERENCES

1. Tanaka, T. Phase transitions of gels. In R.S. Harland and R.K. Prud' homme (eds.), Polyelectrolyte Gels: Properties, Preparation, and Application: ACS Symposium Series # 480. Washington DC: The American Chemical Society, 1992. pp. 1-2.

2. Park, K., and Park, H. Smart hydrogels. In J.C. Salamone (ed.), Polymeric Materials Encyclopedia. Vol. 10. New York: CRC Press, 1996. p. 7785.

3. Ichikawa, T., and Nakajima, T. Superabsorptive Polymers (from natural polysaccharides and polypeptides). In J.C. Salamone (ed.), Polymeric Materials Encyclopedia. Vol. 10, New York: CRC Press, 1996. pp. 8051-8059.

4. Buchholz, F.L., and Burert, J.H. Synthesis and applications of superabsorbent polymers. In C.A. Finch (ed.), Industrial Water Soluble Polymers. London: Hartnolls, 1996. pp. 92-95.

5. Swinkels, J.J.M. Source of starch, its chemistry and physics. In G.M.A. Van Beynum and J.A. Roels (eds.), Starch Conversion Technology. New York: Mercel Dekker, 1985. pp.15-46.

6. Rutenberg, M.W. Starch and its modifications. In R.L. Davidson (ed.), Handbook of Water-Soluble Gums and Resins. New York: McGraw-Hill Book, 1980. pp. 22-1 - 22-21.

7. Wurzburg, O.B., Introduction. In O.B. Wurzburg (ed.), Modified Starches: Properties and Uses. Florida: CRC Press, 1987. p. 9.

8. Kircher, J.F., and Bowman, R.E. Effect of Radiation on Materials and Components. New York: Nostrand Reinhold Publishing, 1964. pp.11-16.

9. Battaerd, H.A.J., and Treear, G.W. Graft Copolymer. New York: Interscience Publishers, 1967. pp. 54-73.

10. Chapiro, A. Radiation Chemistry of Polymeric Systems. New York: Interscience Publisher, 1962. pp. 62-63.

11. Draganic, I.G., and Draganic, Z.D. The Radiation Chemistry of Water. New York: Academic Press, 1971. pp. 38-42.

12. Stannett, V.T., Fanta, G.F., and Doane, W.M. Polymer grafted cellulose and starch. In K. Chatterjee (ed.), Absorbency. New York: Elsevier Science Publishers, 1985. pp. 257-258.

13. Odian, G. Principles of Polymerization 3rd ed. New York: John Wiley & Sons, 1991. pp 715-718.

14. Ranby, B., and Rodehed, C. Water vapor absorption and aqueous retention of hydrolyzed starch polyacrylonitrile graft copolymer “Superabsorbent Starch”. Polymer Bulletin 5(1981): 87-94.

15. Iyer, V., Varadarajan, P.V., Sawakhande, K.H., and Nachane, N.D. Preparation of superabsorbents by gamma-ray radiation. J. Appl. Polym. Sci. 39(1990): 2259-2265.

16. Hongfei, H., Xiaohong, L., and Jilan, W. Effect of acid on radiation grafting of functional monomers onto silicone rubber. Radiat. Phys. Chem. 39,6(1992): 513-516.

17. Kiatkamjornwong, S., Chvajarernpun, J., and Nakason, C. Modification on liquid retention property of cassava starch by radiation grafting with acrylonitrile. I. Effect of γ-irradiation on grafting parameters. Radiat. Phys. Chem. 42,1-3(1993): 47-52.

18. Yao, K. – J., and Zhou, W. – J. Synthesis and water absorbency of the copolymer of acrylamide with anionic monomers, J. Appl. Polym. Sci. 53(1994): 1533-1538.

19. Dung, N.A., Huyen, N.D., Hang, N.D., and Canh, T.T. Immobilization of urease on grafted starch by radiation method. Radiat. Phys. Chem. 46,4 – 6(1995): 1037 – 1042.

20. Saraydin, D., Karadag, E., Cetinkaya, S., and Guven, O. Preparation of acrylamide/maleic acid hydrogels and their biocompatibility with some biochemical parameters of human serum. Radiat. Phys. Chem. 46,4 – 6(1995): 1049 – 1052.

21. Saraydin, D., Karadag, E., Cetinkaya, S., and Guven, O. Acrylamide/maleic acid hydrogels. Polym. Adv. Technol. 6(1995): 719 – 726.

22. Saraydin, D., Karadag, E., Cetinkaya, S., and Guven, O. Adsorption of some basic dyes by acrylamide/maleic acid hydrogels. Sep. Sci. Technol. 31,3(1996): 423 – 434.

23. Saraydin, D., Karadag, E., Cetinkaya, S., and Guven, O. Behaviors of acrylamide/maleic acid hydrogels in uptake of some cationic dyes from aqueous solution. Sep. Sci. Technol. 31,7(1996): 2359 – 2371.

24. Lin, Z.S., and Rempel, G.L. Preparation of superabsorbent polymers by crosslinking acrylic acid and acrylamide copolymers. J. Appl. Polym. Sci. 64,7(1997): 1345 – 1353.

25. Kiatkamjornwong, S., and Suwanmala, P. Partially hydrolyzed polyacrylamide-poly(N-vinylpyrrolidone) copolymers as superabsorbents synthesized by gamma irradiation. J. Appl. Polym. Sci. 68(1998): 191 – 203.

26. Kiatkamjornwong, S., and Meechai, N. Enhancement of the grafting performance and of the water absorption of cassava starch graft copolymer by gamma radiation. Radiat. Phys. Chem. 49,6(1997): 689 – 696.

27. Oztop, H.N., Saraydin, D., Karadag, E., Caldiran, Y., and Guven, O. Influence of some aromatic acids on the swelling behavior of acrylamide/maleic acid hydrogel. Polym. Bull. 40(1998): 575 – 581.

28. Okay, O., Sariisik, S.B., and Zor, S.D. Swelling behavior of anionic acrylamide – based hydrogels in aqueous salt solutions: comparison of experiment with theory. J. Appl. Polym. Sci. 70(1998): 567 – 575.

29. Sen, M., and Guven, O. Prediction of swelling behavior of hydrogels containing diprotic acid moieties. Polymer 39,5(1998): 1165 – 1172.

30. Sen, M., Kantoglu, O., and Guven, O. The effect of external stimuli on the equilibrium swelling properties of poly(N-vinyl-2-pyrrolidone/itaconic) polyelectrolyte hydrogels. Polymer 40(1999): 913 – 917.

31. Sen, M., Yakar, A., and Guven, O. Determination of average molecular weight between cross-links from (Mc) swelling behavior of diprotic acid-containing hydrogels. Polymer 40,11(1999): 2969 – 2974.

32. Tumturk, H., Caykara, T., Sen, M., and Guven, O. Adsorption of α-amylase onto poly(acrylamide/maleic acid) hydrogels. Radiat. Phys. Chem. 55(1999): 713 – 716.

33. Kiatkamjornwong, S., Chomsaksakul, W., and Sonsuk, M. Radiation modification of water absorption of cassava starch by acrylic acid/acrylamide. Radiat. Phys. Chem. 52(2000): 413 – 427.

34. Shugar, G.J., and Dean, J.A. The Chemist' s Ready Reference Handbook. New York: McGraw – Hillny, 1990. pp. 28.22 – 28.25.

35. Kellenberger, S.R. Absorbent products containing hydrogels with ability to swell against pressure. Eur. Patent. Appl. 339, 461(1989).

36. Dennenberg, R.J., and Abbott, T.P. Rapid analysis of starch graft copolymers. J. Polym. Sci., Polym, Lett. Ed. 14(1976): 693 – 696.

37. Kiatkamjornwong, S., and Suwanmala, P. Effect of total dose on water absorption of partially hydrolyzed acrylamide-pyrrolidone copolymers. Radiat. Phys. Chem. 50,6(1997): 617 – 624.

38. Maltesh, C., and Somasundaran, P. Effect of the degree of hydrolysis of polyacrylamide on its interactions with poly(ethylene oxide) and poly(vinylpyrrolidone). Macromolecules 24(1991): 5775 – 5778.

39. Swallow, A.J., Radiation Chemistry of Organic Compounds. London: Pergamon Press, 1960. pp.149 – 154.

40. Odian, G. Principles of Polymerization. 3rd ed. New York: John Wiley & Sons, 1991. pp. 232 – 234, 241 – 243.

41. Kiatkamjornwong, S., and Suwanmala, P. Effect of dose rate on water absorption of partially hydrolyzed polyacrylamide-*co*-poly (vinylpyrrolidone) superabsorbents. Radiat. Phys. Chem. 52,1 – 6 (1998): 217 – 221.

42. Thomas, W.M. Acrylamide polymers. In H.F. Mark and N.G. Gaylord (eds.), Encyclopedia of Polymer Science and Technology. Vol.1. New York: John Wiley & Sons, 1970. pp.181-183.

43. Kiatkamjornwong, S., and Phunchareon, P. Influence of reaction parameters on water absorption of neutralized poly(acrylic acid-*co*-acrylamide) synthesized by inverse suspension polymerization. J. Appl. Polym. Sci. 72(1999): 349 – 1366.

44. Brandrup, J., and Immergut, E.H. (eds.), Polymer Handbook. 2nd ed. New York: John Wiley & Sons, 1975. pp. II – 111 - II – 146.

45. Shimizu, T., and Minakata, A. The dilute solution properties of maleic anhydride and maleic acid copolymers: 1. Light scattering, osmotic pressure and viscosity measurements. Polymer 21(1980): 1427-1432.

46. Jonsson, S., Hultgren, J., Sundell, P.E., Shimose, M., Owens, J., Voughn, K., and Hoyle, C.E. Photocopolymerization initiated by N-substituted maleimides and electron donor olefin combinations “A photoinitiator free UV curable system”. Proc. Rad Tech Asia’ 95, Symposium and Workshop. (n.d.): pp. 283 – 295.

47. Lee, Cherylyn., and Hall, H.K. Photocopolymerizations of electron-rich olefins with electron-poor olefins by irradiation of their EDA complexes. Macromolecules 22(1989): 21 – 25.

48. Garnett, J.L., Ng, L – T., and Viengkhou, V. Grafting of methyl methacrylate to cellulose and polypropylene with UV and ionizing radiation in the presence of additives including CT complexes. Radiat. Phys. Chem. 56(1999): 387 – 403.

49. Christian, G.D. Analytical Chemistry 4th ed. New York: John Wiley & Sons, 1986. pp. 108 – 109.

50. Grignon, J., and Scallan, A.M. Effect of pH and neutral salts upon the swelling of cellulose gels. J. Appl. Polym. Sci. 25(1980): 2829 – 2843.

51. Castel, D., Ricard, A., and Audebert, R. Swelling of anionic and cationic starch – based superabsorbents in water and saline solution. J. Appl. Polym. Sci. 39(1990): 11 – 29.

52. Ricka, J., and Tanaka, T. Swelling of ionic gels: Quantitative performance of the Donnan theory. Macromolecules 17(1984): 2916 – 2921.

53. Cutie, S.S., Smith, P.B., Reim, R.E., and Graham, A.T. Analysis and characterization of superabsorbent polymers. In F.L. Buchholz and A.T. Graham (eds.), Modern Superabsorbent Polymer Technology. New York: John Wiley & Sons, 1998. pp. 149 – 153.

54. Buchholz, F.L. The structure and properties of superabsorbent polyacrylates. In F.L. Buchholz and A.T. Graham (eds.), Modern Superabsorbent Polymer Technology. New York: John Wiley & Sons, 1998. pp. 182 – 190.

55. Viengkhou, V., NG, L – T., and Garnett, J.L. The effect of additives on the enhancement of methyl methacrylate grafting to cellulose in the presence of UV and ionizing radiation. Radiat. Phys. Chem. 49,5 (1997): 595 – 602.

56. Garnett, J.L., Jankiewicz, J.V., and Sangster, D.F. Effect of mineral acid on polymer produced during radiation – induced grafting of styrene monomer. J. Polym. Sci., Polym. Lett. Ed. 20(1982): 171 – 175.

57. Garnett, J.L. Grafting of monomers to cellulose using UV and gamma radiation as initiators. In J.C. Arthur, Jr. (ed.), Cellulose Chemistry and Technology: ACS Symposium Series, No. 48. Washington DC: The American Chemical Society, 1977. pp. 335 – 339.

58. Atichokudomchai, N., Shobsngob, S., and Varavinit, S. Morphological properties of acid-modified tapioca starch. Starch-Starke 52,8-9(2000): 283-289.

APPENDICES

APPENDIX A

DETERMINATION OF COPOLYMER COMPOSITIONS OF CHN METHOD

Compositions of starch-*g*-polyacrylamide after saponification with a 5% potassium hydroxide solution for various periods of time and temperature are shown in Table A – 1.

Table A – 1 Compositions of Starch-*g*-polyacrylamide after Saponification.

Period of Saponification Time and Temperature	Sample NO.	Composition of the Elements (%)		
		Carbon	Hydrogen	Nitrogen
unsaponified sample	1	43.788	5.895	11.973
	2	44.124	5.540	11.871
	Average	43.956	5.718	11.922
room temperature, 30 min.	1	42.763	6.374	10.625
	2	42.947	6.678	10.936
	Average	42.855	6.526	10.780
room temperature, 60 min.	1	41.403	5.976	9.767
	2	41.436	6.134	9.490
	Average	41.420	6.055	9.629
room temperature, 90 min.	1	41.178	6.321	9.384
	2	41.210	6.488	9.117
	Average	41.194	6.405	9.251

Table A – 1 Compositions of Starch-*g*-polyacrylamide after Saponification (continued)

Period of Saponification Time and Temperature	Sample NO.	Composition of the Elements (%)		
		Carbon	**Hydrogen**	**Nitrogen**
50 °C, 30 min.	1	37.156	5.493	6.242
	2	37.261	5.637	6.064
	3	37.200	5.943	6.152
	Average	37.206	5.691	6.153
50 °C, 60 min.	1	37.870	5.612	6.023
	2	37.933	5.722	5.846
	Average	37.902	5.692	5.935
50 °C, 90 min.	1	38.047	5.320	5.911
	2	37.958	5.461	5.888
	Average	38.003	5.391	5.899
75 °C, 30 min.	1	36.251	5.493	4.943
	2	36.617	5.748	4.867
	Average	36.434	5.620	4.905
75 °C, 60 min.	1	36.649	5.462	4.757
	2	36.678	5.751	4.688
	Average	36.664	5.607	4.723
75 °C, 90 min.	1	36.963	5.437	4.588
	2	36.795	5.601	4.570
	Average	36.879	5.519	4.579

These data were analyzed by CHNS/O analyzer (Perkin Elmer PE 2400 Series II, Norwalk Connecticut U.S.A.)

Compositions of starch-*g*-poly(acrylamide-*co*-maleic acid) after saponification with a 5% potassium hydroxide solution at room temperature for 90 minutes for various maleic acid content are shown in Table A – 2.

Table A – 2 Compositions of Starch-*g*-poly(acrylamide-*co*-maleic acid) after Saponification.

Maleic acid content	Sample NO.	Composition of the Elements (%)		
		Carbon	Hydrogen	Nitrogen
non MA	1	44.541	6.613	10.956
	2	44.384	6.576	11.131
	Average	44.463	6.595	11.044
1% MA	1	44.002	6.582	10.646
	2	44.239	6.474	10.925
	3	44.050	6.651	10.785
	Average	44.097	6.569	10.785
2% MA	1	44.100	6.564	10.270
	2	44.042	6.619	10.522
	3	43.992	6.601	10.466
	Average	44.045	6.595	10.419
3% MA	1	43.945	6.449	10.188
	2	44.080	6.288	10.123
	3	43.960	6.362	10.099
	Average	43.995	6.366	10.137

Table A – 2 Compositions of Starch-*g*-poly(acrylamide-*co*-maleic acid) after Saponification (continue)

Maleic acid content	Sample NO.	Composition of the Elements (%)		
		Carbon	Hydrogen	Nitrogen
4% MA	1	43.787	6.198	9.662
	2	43.807	6.156	9.631
	Average	43.797	6.177	9.646
8% MA	1	43.831	6.125	9.488
	2	43.830	6.232	9.199
	Average	43.831	6.178	9.338
12% MA	1	43.825	6.513	8.903
	2	43.801	6.346	9.083
	Average	43.813	6.430	8.993

These data were analyzed by CHNS/O analyzer (Perkin Elmer PE 2400 Series II, Norwalk Connecticut U.S.A.)

APPENDIX B

FREE RADICAL COPOLYMERIZATION REACTIVITY RATIOS

When a vinyl monomer is copolymerized with a second monomer, the relationship between the composition of the initially formed copolymer and the initial monomer mixture is given by

$$\frac{dm_1}{dm_2} = \frac{M_1\ (r_1M_1 + M_2)}{M_2\ (r_2M_2 + M_1)} \qquad \text{(B-1)}$$

where m_1 is the number of moles of monomer 1 entering the copolymer, m_2, the number of moles of monomer 2 entering the copolymer, M_1, the number of moles of monomer 1 in the monomeric mixture, M_2, the number of the moles of monomer 2 in the monomer mixture, and r_1 and r_2 are the monomer reactivity ratios.

The monomer reactivity ratios, r_1 and r_2, for any monomer pair are the ratios of the rate constants of the different propagation reactions:

$$\sim M_1^{\bullet} + M_1 \rightarrow \sim M_1 M_1^{\bullet} \qquad \text{Rate constant } k_{11} \qquad \text{(B-2)}$$

$$\sim M_1^{\bullet} + M_2 \rightarrow \sim M_1 M_1^{\bullet} \qquad \text{Rate constant } k_{12} \qquad \text{(B-3)}$$

$$\sim M_2^{\bullet} + M_2 \rightarrow \sim M_2 M_2^{\bullet} \qquad \text{Rate constant } k_{22} \qquad \text{(B-4)}$$

$$\sim M_2^{\bullet} + M_1 \rightarrow \sim M_2 M_1^{\bullet} \qquad \text{Rate constant } k_{21} \qquad \text{(B-5)}$$

$$r_1 = k_{11}/k_{12} \qquad \text{(B-6)}$$

$$r_2 = k_{22}/k_{21} \qquad \text{(B-7)}$$

$\sim M^\bullet$ represents a polymer chain ending in a radical derived from monomer M.

APPENDIX C

PREPARATION OF BUFFER SOLUTIONS

To prepare 100 mL of any buffer listed in the table, pipet the exact amounts of each solution into a dry container.

Table C-1 Preparation of Buffer Solutions (25^{o}C)

Desired pH	**Solution 1, mL**	**Solution 2, mL**	**Ionic Strength [a] (mole – ion dm^{-3})**
2.0	97.5	2.5	2.51×10^{-3}
2.5	92.0	8.0	4.59×10^{-3}
3.0	88.0	12.0	6.06×10^{-3}
3.5	83.0	17.0	7.86×10^{-3}
4.0	77.5	22.5	9.61×10^{-3}
4.5	72.0	28.0	1.17×10^{-2}
5.0	67.0	33.0	1.34×10^{-2}
5.5	63.0	37.0	1.47×10^{-2}
6.0	59.0	41.0	1.60×10^{-2}
6.5	54.5	45.5	1.74×10^{-2}
7.0	49.5	50.5	1.90×10^{-2}

[a] $I = 1 / 2\ \Sigma\ (C_iZ_i^2)$, where I, C_i, and Z_i are the ionic strength, the ionic concentration, and the charge on each individual ion, respectively. [49].

Table C-1 Preparation of Buffer Solutions (25°C) (continued)

Desired pH	Solution 1, mL	Solution 2, mL	Ionic Strength [a] (mole – ion dm^{-3})
7.5	46.0	54.0	2.01×10^{-2}
8.0	42.5	57.5	2.12×10^{-2}
8.5	39.0	61.0	2.22×10^{-2}
9.0	34.5	65.5	2.36×10^{-2}
9.5	30.0	70.0	2.49×10^{-2}
10.1	27.0	73.0	2.58×10^{-2}
10.5	24.5	75.5	2.65×10^{-2}
11.0	22.0	78.0	2.72×10^{-2}
11.5	16.5	83.5	2.88×10^{-2}
12.0	8.5	91.5	3.10×10^{-2}

[a] $I = 1/2\ \Sigma\,(C_iZ_i^2)$, where I, C_i, and Z_i are the ionic strength, the ionic concentration, and the charge on each individual ion, respectively. [49].

Solution 1. Dissolve 12.37 g of anhydrous boric acid, H_3BO_3, and 10.51 g of citric acid monohydrate in distilled water, and diluted to 1 L in a volumetric flask. This makes a 0.200 M boric acid and a 0.0500 M citric acid solution.

Solution 2. Dissolve 38.01 g of $Na_3PO_4 \cdot 12H_2O$ in distilled water, and dilute to 1 L in a volumetric flask. This makes a 0.100 M tertiary sodium phosphate solution.

VITA

Miss Kanlaya Mongkolsawat was born on December 15, 1975 in Bangkok, Thailand. She received the B.Sc. in Chemistry from Faculty of Science and Technology, Thammasat University in 1998. She began her master study in polymer science, Program of Petrochemistry and Polymer Science, Faculty of Science, Chulalongkorn University in June 1998 and completes the program in April 2001.